REGULATION BY ERK1/2 OF NOVEL SUBSTRATES, KINESINS KIF2A AND KIF2C

APPROVED BY SUPERVISORY COMMITTEE

Melanie H. Cobb, Ph.D. (mentor)
Joseph P. Albanesi, Ph.D. (chair)
Michael A. White, Ph.D.
Beatriz M. Fontoura, Ph.D.

REGULATION BY ERK1/2 OF NOVEL SUBSTRATES, KINESINS KIF2A AND KIF2C

by

ELMA ZAGANJOR

DISSERTATION / THESIS

Presented to the Faculty of the Graduate School of Biomedical Sciences

The University of Texas Southwestern Medical Center at Dallas

In Partial Fulfillment of the Requirements

For the Degree of

DOCTOR OF PHILOSOPHY

The University of Texas Southwestern Medical Center at Dallas

Dallas, Texas

April, 2013

ERK1/2 REGULATION OF NOVEL SUBSTRATES, KINESINS KIF2A AND KIF2C

Elma Zaganjor, Ph.D.

The University of Texas Southwestern Medical Center at Dallas, 2013

Supervising Professor: Melanie H. Cobb, Ph.D.

Abstract: The kinesin-like protein KIF2A is a microtubule-associated motor protein that causes microtubule depolymerization by inducing a conformational change in tubulin. The depolymerase function of KIF2A is utilized in mitotic cells as it is required to establish proper, bipolar spindles. Studies in KIF2A knockout mice revealed KIF2A function in regulation of interphase microtubules as *KIF2A*$^{-/-}$ neurons exhibit abnormal axon branching. Though protein kinases are known to regulate the mitotic function of KIF2A, how KIF2A is regulated in interphase cells has not been studied.

In a yeast-two hybrid screen, designed to preferentially uncover interactors of the active form of ERK2, we identified KIF2A. We find that, human KIF2A can be

phosphorylated *in vitro* by pERK1/2 and that the kinases interact with KIF2A in cells. Through phosphorylation prediction tools and mutagenesis we identified threonine 78 (T78) as a major pERK2 phosphorylation site on KIF2A. Inhibition of ERK1/2 prevents KIF2A from localizing at the leading edge of cells. Additionally, knockdown of KIF2A phenocopies the effect of inhibiting ERK1/2 on microtubules; both treatments result in elongated microtubules. These data suggest that ERK1/2 may regulate KIF2A localization which in turn may be important for KIF2A function in depolymerizing microtubules. The close relative, KIF2C can also bind to and be phosphorylated by pERK1/2 *in vitro*, but the functional significance of this event remains unknown.

In a laboratory generated non-small cell lung cancer (NSCLC) in which oncogenic K-Ras^{G12V} has been overexpressed and the tumor suppressor p53 has been knocked down, we found an increase in expression of KIF2A and KIF2C. This increase could be suppressed by inhibiton of the effector pathway RAS-RAF-MEK1 but not the PI3K pathway. As it is accepted that cancer cells have more dynamic microtubules that give them a migratory advantage, we hypothesized that upregulation of KIF2A and KIF2C also promote migration. Indeed, knockdown of KIF2A and KIF2C resulted in reduced migration in cancer cell lines. Microarray studies that had been performed on lung cancer lines revealed upregulation of KIF2A and KIF2C in cancers, suggesting that these proteins may be significant factors in the development of lung cancer.

Finally, KIF2A and KIF2C regulate lysosomal dynamics. This regulation has an impact on signaling, particularly for mTORC1 which requires lysosomal localization for its activity.

TABLE OF CONTENTS

PRIOR PUBLICATIONS

Elma Zaganjor, Jihan K. Osborne , Lauren M. Weil , Laura A. Diaz-Martinez , Joshua X. Gonzales , Stina M. Singel , Jill E. Larsen , Luc Girard , John D. Minna and Melanie H. Cobb. Ras regulates kinesin 13 family members to control cell migration pathways in cancer. In revision, Oncogene.

Aileen M. Klein, **Elma Zaganjor** and Melanie H. Cobb. Chromatin-tethered MAPKs. Current Opinion in Cell Biology. 2013 March. S0955-0674 epub

Eric M. Wauson, **Elma Zaganjor** and Melanie H. Cobb. Amino acid regulation of autophagy through the GPCR TAS1R1-TAS1R3. Autophagy. 2012 Dec; Volume 9 (3):418-9.

Eric M. Wauson, **Elma Zaganjor**, A-Young Lee, Marcy L. Guerra, Anwesha B. Ghosh, Angie L. Bookout, Chris P. Chambers, Arif Jivan, Kathleen McGlynn, Michele R. Hutchison, Ralph J. Deberardinis, Melanie H. Cobb. (2012). The G Protein-Coupled Taste Receptor T1R1/T1R3 Regulates mTORC1 and Autophagy. *Molecular Cell* 47(6):851-62.

Jihan K. Osborne, **Elma Zaganjor**, Melanie H. Cobb. (2012). Signal control through Raf: in sickness and in health. *Cell Research* 22(1): 14-22

Michael C. Lawrence, Arif Jivan, Chunli Shao, Lingling Duan, Daryl Goad, **Elma Zaganjor**, Jihan Osborne, Kathleen McGlynn, Steve Stippec, Svetlana Earnest, Wei Chen, and Melanie H. Cobb. (2008). The roles of MAPKs in disease. *Cell Research* **18**: 436-442.

Nicholas Yagoda, Moritz von Rechenberg, **Elma Zaganjor**, Andras J. Bauer, Wan Seok Yang, Daniel J. Fridman, Adam J. Wolpaw, Inese Smukste, John M. Peltier, J. Jay Boniface, Richard Smith, Stephen L. Lessnick, Sudhir Sahasrabudhe, Brent R. Stockwell. (2007). RAS-RAF-MEK-dependent oxidative cell death involving voltage-dependent anion channels. *Nature* 447(7146): 864-8.

LIST OF FIGURES

LIST OF TABLES

ABBREVIATION

AICAR	5-aminoimidazole-4-carboxamide-1-β-D-ribofuranoside
ADP	adenosine diphosphate
AMP	adenosine monophosphate
AMPK	AMP-activated protein kinase
APC	adenomatous polyposis coli
ATP	adenosine-5'-triphosphate
aPK	atypical protein kinase
CDK	cyclin-dependent kinase
DAPI	4',6-diamidino-2-phenylindole
Dlg1	disc large 1
EBSS	Earl's Balanced Salt Solution
EGFR	epidermal growth factor receptor
EMT	epithelial to mesenchymal transition
ePK	eukaryotic protein kinase
ERK	extracellular signal-regulated protein kinase
FGFR	fibroblast growth factor receptor
GPCR	G-protein coupled receptor
GRB2	growth factor receptor bound 2
GSK	glycogen synthase kinase
GTP	guanosine triphosphate
HBEC	human bronchial epithelial cell
JNK	c-Jun-N-terminal kinase

KSFM	keratinocyte serum free medium
MAP-2	microtubule-associated protein 2
MAPK	mitogen-activated protein kinase
MAP3K	MAP kinase kinase kinase
MAP2K	MAP kinase kinase
MBP	myelin basic protein
MCAK	mitotic centromere-associated kinesin
MEK	MAP kinase/ERK kinase
MTOC	microtubule organizing center
mTOR	mechanistic target of rapamycin
NES	nuclear export signal
NLS	nuclear localization signal
NSCLC	non-small cell lung cancer
OPA1	optic atrophy 1
PI3K	phosphatidylinositol 3-kinase
PKA	protein kinase A
PKC	protein kinase C
RSK	ribosomal S6 kinase
SAPK	stress-activated protein kinase
SH2	src homology 2
SOS	son of sevenless
qPCR	quantitative polymerase chain reaction

TSC2	tuberous sclerosis complex protein 2
WRC	WAVE2 regulatory complex
WAVE2	WASP family Verprolin-homologous protein
WASP	Wiskott-Aldrich syndrome protein (WASP)-family protein

CHAPTER ONE
Introduction

I. MAP Kinases

A. Kinase Discovery

Nearly all aspects of cellular life involve a reversible phosphorylation event. Phosphorylation can enhance or inhibit protein function by altering its interactions, localization, stability and so on. Protein kinases are enzymes that perform a transfer of the γ phosphoryl group from ATP to serine, threonine or tyrosine residues on substrates; this process is reversed by another set of catalytic enzymes, the phosphoprotein phosphatases. One of the first studies that came across the process of phosphorylation, though it took many years to finally understand it, was performed in the late 1930s by Gerty and Carl Cori. The Coris identified an enzyme glycogen phoshporylase, which catalyzes the first step in glycogen breakdown pathway, to exist in two forms phosphorylase a (active) and phosphorylase b (inactive) that can be interconverted *in vivo* (Cori & Cori, 1945; Cori & Green, 1943). The Coris observed that 5' AMP was required for phosphorylase b activation; however, the chemical mechanism of switching between active and inactive state was not understood. Protein kinase activity was not observed until 1954 when Eugene Kennedy using rat liver mitochondria showed that an enzyme can phosphorylate casein in the presence of ATP (Burnett & Kennedy, 1954) . Expanding on the Coris' findings, Fischer and Krebs presented evidence that phosphorylase b can be converted to phosphorylase a in the presence of cell-free muscle extract, ATP and a divalent metal ion *in vitro* (Fischer & Krebs, 1955; Krebs & Fischer, 1955, 1956).

Sutherland and Wosilait further concluded that a release of phosphate from purified liver phosphorylase results in enzyme inactivation and is related to a physiological mechanism (Sutherland & Wosilait, 1955). This was also the first demonstration that hormones, adrenaline or glucagon could stimulate glycogenolysis.

B. The Kinome and MAPK

The early studies on kinases could not have predicted the importance of this family of enzymes that transfer phosphate onto substrates to activate or inactivate them. Indeed, eukaryotic protein kinases (ePKs), defined by conservation of their catalytic domain in both sequence and structure, constitute one of the largest protein families; the 532 known members account for more than 2% of all eukaryotic protein coding genes (Manning, Plowman, Hunter, & Sudarsanam, 2002). ; Additional protein kinases have been found that are grouped as atypical protein kinases (aPK) because they generally share structure but not sequence similarity to ePK. By several twenty-year-old estimates, protein kinases were expected to phosphorylate ~30% of the total proteome. The fraction of the proteome that is phosphorylated is apparently much larger (70% or more), based on data accumulated from proteomic studies (e.g., see www.phosphosite.org).

An early study by Hunter's group aligned the sequences of the 65 protein kinase sequences known at the time (Hanks, Quinn, and Hunter, 1988). Although no mitogen-activated protein kinase (MAPK) sequences had yet been determined, the analysis of the known sequences demonstrated some important conserved relationships. For example, the similarity between sequences of two kinases from different fungi was recognized; these kinases were later identified as MAPK kinases (also known as MAP2Ks, MAPKKs, MEKs, or MKKs), representing the first identified components of MAPK cascades.

Analysis of the similarities among sequences of all protein kinases in *Saccharomyces cerevisiae* and later human by use of genomic, complementary DNA, and expressed sequence tag (EST) sequences led to the assignment of the ePKs in a dendrogram tree sorted into seven major groups with a few outliers (Figure 1.1) (Manning et al, 2002a, 2002b).The major branches are: (1) AGC kinases named after protein kinase A (PKA and PKG) and protein kinase C (PKC); (2) CMGC kinases, including cyclin-dependent kinases (CDK), mitogen activated protein kinases (MAPK), glycogen synthase kinases (GSK), the casein kinase II family and the Cdk-like (Clk) family, serine/arginine-rich protein kinases, and others; ; (3) CaMK which includes calcium/calmodulin-dependent protein kinases and relatives (4) STE, which includes kinases related to those identified in the yeast mating pathway (e.g., MAP2Ks, MAPK kinase kinases (MAP3Ks or MAPKKK), and p21-activated kinases (PAKs)); (5) CKI, the casein kinase I group; (6) TK group which includes all conventional tyrosine kinases; and (7) TKL, the tyrosine kinase-like enzymes, e.g., Raf and receptor guanylate cyclases (Manning et al, 2002a,2002b). From this effort Hunter and collaborators coined the term the kinome..

The prototypic MAPK signaling cascade comprises of three core kinases: the MAPK kinase kinase (MAP3K), which phosphorylates and activates the MAPK kinase (MAP2K), which in turn phosphorylates and activates the MAPKs (Figure 1.2). The research of this thesis focuses on the exemplary three-kinase signaling cascade that includes Rafs (MAP3K), MEKs 1 and 2 (MAP2K) and ERKs 1 and 2 (MAPK). Other well studied MAPKs are p38 (four genes: $\langle\alpha,\beta,\gamma,\delta$), c-Jun-N-terminal kinase/stress-activated protein kinase (JNK/SAPK) (three genes), and ERK5 (Figure 1.2). MAPK signaling is generally activated through stimulation of cell surface receptors by growth

factors, cytokines and ligands that bind G-protein coupled receptors (GPCR). Describing the receptor tyrosine kinase pathway, once bound to ligand, the receptors are phosphorylated on tyrosine residues on the cytoplasmic side of the plasma membrane, which allows for recruitment of adapter molecules such as GRB2 (growth factor receptor bound 2) via SH2 (Src homology 2) domains. The adapter molecules via SH3 domains bind the guanine nucleotide exchange factor, SOS (son of sevenless) for example, which can then activate a small GTPase of the Ras family at the membrane. Once activated, Ras, bound to guanosine triphosphate (GTP), recruits Raf to the membrane, where it is subsequently further activated by phosphorylation and propagates signaling to MEK and ERK.

C. ERK1/2 Discovery And Characteristics

Because the early work on phosphorylation identified a link between a hormonal stimulus and a kinase-regulated function, the search was ongoing for kinases that were involved in growth regulation. At the time when MAPKs were being characterized, insulin-stimulated phosphorylation of ribosomal protein S6 in 3T3-L1 adipocytes was used as a context to define the enzymes involved in the process (Cobb & Rosen, 1983). Ray and Sturgill therefore, identified a serine/threonine kinase activity, later identified as ERK1/2, that phosphorylated a microtubule-associated protein 2 (MAP-2) in response to insulin treatment (Ray & Sturgill, 1987). Using Xenopus oocytes, Erikson and Maller, identified RSK, a kinase that phosphorylated S6 during growth stimulation (Erikson & Maller, 1986; Stefanovic, Erikson, Pike, & Maller, 1986). Soon after their identification, individual studies by Sturgill and Ahn revealed placement of ERK upstream of RSK in what was starting to look like a signaling cascade (Ahn & Krebs, 1990; Sturgill, Ray,

Erikson, & Maller, 1988). Progress in cDNA technology allowed for cloning of ERK1 and realization of its homology to yeast FUS3 and KSS1 which were already known to be involved in cell cycle regulation in response to mating factors, providing further clues into MAPK function (Boulton et al., 1990).

ERK1 and ERK2 are 43 and 41 kDa proteins, respectively and they share 85 % sequence identity (Boulton, Nye, et al., 1991; Boulton et al., 1990). ERK1 and ERK2 are often used interchangeably in the literature and are thought to have overlapping substrate specificities. However, the knockout mouse studies suggest functional differences between ERK1 and ERK2. *erk2* $^{-/-}$ mice die during embryonic development and they fail to form mesoderm, while *erk1*$^{-/-}$ mice are viable, normal in size and fertile but have defects in thymocyte maturation (Nekrasova et al., 2005; Pages et al., 1999; Yao et al., 2003). ERK1 and ERK2 were found to have similar specific activities, approximately 2 micromol/min/mg (Boulton, Gregory, & Cobb, 1991; Robbins et al., 1993). Lefloch and colleagues confirmed that *in vitro* ERK1 and ERK2 have equal activity toward a substrate Elk and it is the amount of total expression of ERK1/2 rather than individual gene property that is important for proliferation (Lefloch, Pouyssegur, & Lenormand, 2008). Based on these combined findings it is possible that difference in ERK1 and ERK2 expression profiles lead to differences in phenotypes in the knockout mouse studies.

As all other kinases, ERK1/2 have two globular domains: a small upper N-terminal domain that has five β-strands and a lower and larger C-terminal domain that is composed of α-helices (F. Zhang, Strand, Robbins, Cobb, & Goldsmith, 1994). ERK1 and ERK2 share almost complete sequence identity in the activation loop where they are

phosphorylated on phosphoacceptor residues spaced one residue apart. on ERK2 tyrosine (185, rat sequence) and threonine (183) are phosphorylated and on , ERK1, the comparable residues (Payne et al., 1991). These sites are separated by glutamate yielding the motif TEY. These phosphorylations cause major rearrangements of the activation loop and enhance substrate binding, therefore phosphorylation of both residues is required for full kinase activity (Canagarajah, Khokhlatchev, Cobb, & Goldsmith, 1997; J. Zhang, Zhang, Ebert, Cobb, & Goldsmith, 1995). MEK1/2 interact with ERK1/2 through a 50-residue region, termed the MAP kinase insert, also found in CDKs and GSK3 (Kannan & Neuwald, 2004; Robinson, Whitehurst, Raman, & Cobb, 2002). The catalytic residues characteristic of ePKs are conserved in ERK2 including the phosphate-binding (often called catalytic) lysine, K52, and the catalytic base, D147. Conformation transitions upon phosphorylation include movement of αC-helix, which contains as conserved glutamate residue, E69, which is able to form a salt-bridge with K52 in the activee site. The phosphate anchor ribbon, also known as the glycine-rich region (GxGxxG), or the P-loop, located between the β1- and β2-strands, interacts with adenine of ATP.

ERK1/2 often phosphorylate serine and threonine residues that are followed by proline (S/T-P). Proline in the P+1 position allows substrates to bind on a surface depression in the ERK1/2 active site that accommodates this residue. Substrate specificity is also influenced by interactions with regions of MAPKs outside of their active sites. Segments on the C-terminal domain of MAPKs have been identified as domains important for binding to substrates (Tanoue, Adachi, Moriguchi, & Nishida, 2000) Lee, Hoofnagle, et al, 2004. The first such region is an acidic docking groove,

evolutionarily conserved and termed the common docking (CD) domain. The CD site binds to basic/hydrophobic docking sequences (D motifs) in substrates and regulators of the form (R/K)2-3-X1-6-Φ- X-Φ (Φ, hydrophobic residue) (Barsyte-Lovejoy, Galanis, & Sharrocks, 2002; Ho, Bardwell, Abdollahi, & Bardwell, 2003). Because about 30% of human proteins in the Swiss-Prot data base contain one or more typical MAPK phosphorylation site sequences (PX(S/T)P), the occurrence of docking sites may limit inappropriate phosphorylation events (Sheridan, Kong, Parker, Dalby, & Turk, 2008).. (. The D domain is found in both upstream regulators of MAPK, such as MAP2K family members, phosphatases (e.g. MKP3 (Brunner, Hafen 1994)), and many downstream effectors such as Elk1 and JIP1 (Bardwell, Abdollahi, & Bardwell, 2003; Barsyte-Lovejoy et al., 2002). The second MAPK docking motif, FXFP, also known as DEF (docking site for ERK, FXFP), was identified by Kornfeld and coworkers (Jacobs et al 1999) and later found to interact on the kinase surface around a structural element known as the MAPK insert (Lee et al 2004). These docking interactions assist in defining specificity of kinase-substrate binding and also affect the structures of the kinases themselves (Chang, Goldsmith and others, 2002). FXFP motifs are found on many transcription factors such as Elk1, nuclear pore proteins such as Nup153 and Nup214, and many other ERK binders (Fantz, Jacobs, Glossip, & Kornfeld, 2001; Jacobs, Glossip, Xing, Muslin, & Kornfeld, 1999; Kosako et al., 2009; Porter, Brown, & Palmenberg, 2010). A number of MAPK substrates, for example Elk1, contain multiple docking sites of one or both types, which are thought to function additively for a high-affinity interaction (Jacobs et al., 1999).

D. ERK1/2 in Disease

Cancer

The possibility of ERK1/2 involvement in cancer biology was first recognized from studies implicating the upstream, activating regulators, the small GTPase Ras family of proteins, as oncogenes with transforming potential, once it was realized that Ras regulated the ERK1/2 cascade (Thomas, Brugge et al., 1992; Wood, Blenis et al, 1992; Leevers and Marshall, 1992; Robbins et al, 1992). Mutations in Ras are observed in 30% of all cancers including 90% of all pancreatic, 50% of thyroid and colon and about 25% of all lung and melanoma cancers. A high frequency of somatic mutations in Raf proteins has also been observed, with as high as 60% occurrence in melanoma. Initially it was believed that these upstream mutations contribute to constitutive activation of the ERK1/2 pathway without mutations in ERKs or MEKs. Nevertheless, mutations in ERK2 have been observed, though it is not clear if and how they contribute to tumorigenicity (Table 1.1).

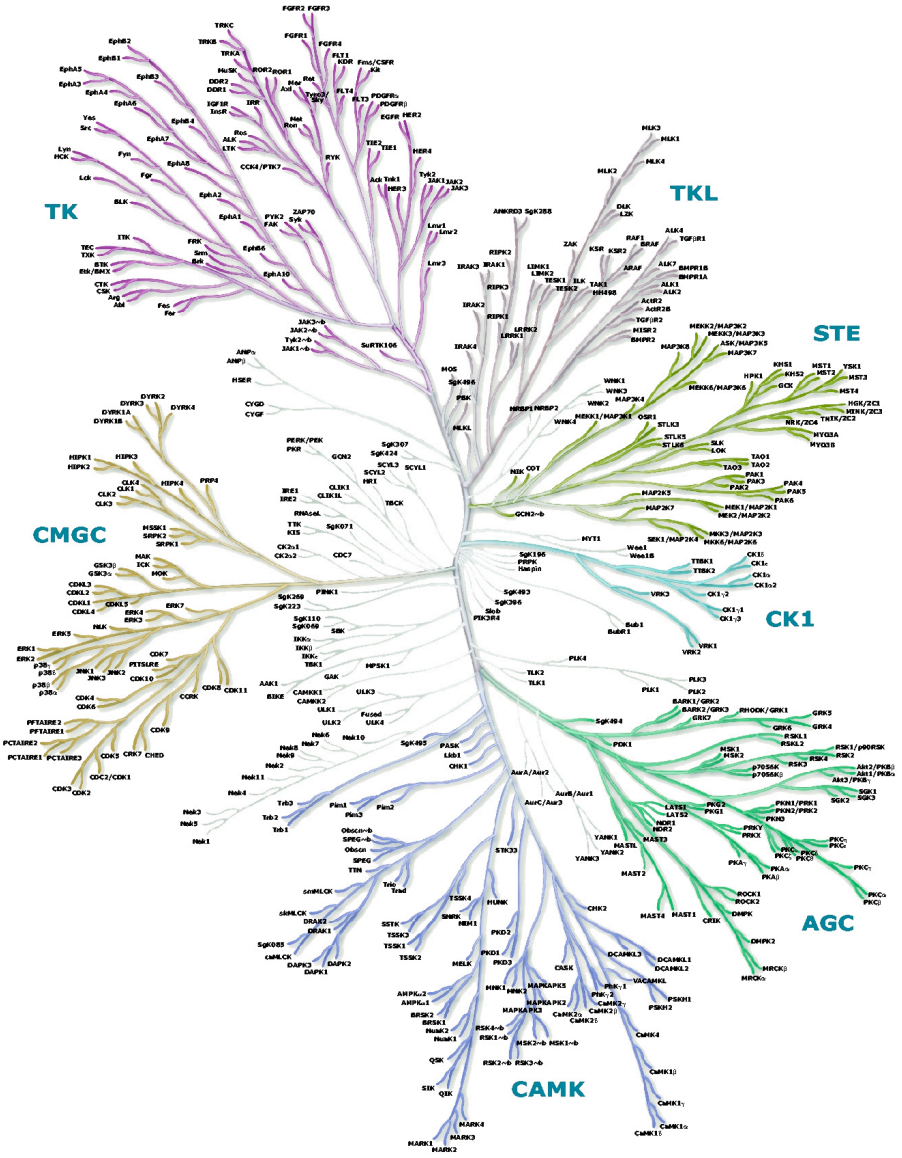

Figure 1.1. Dendogram of major groups of protein kinases. Dendogram is based on sequence similarity of catalytic domain; the shorter the distance along the branches between two kinases, the less divergent their sequences. Reprinted with permission from G. Manning et al., 2002.

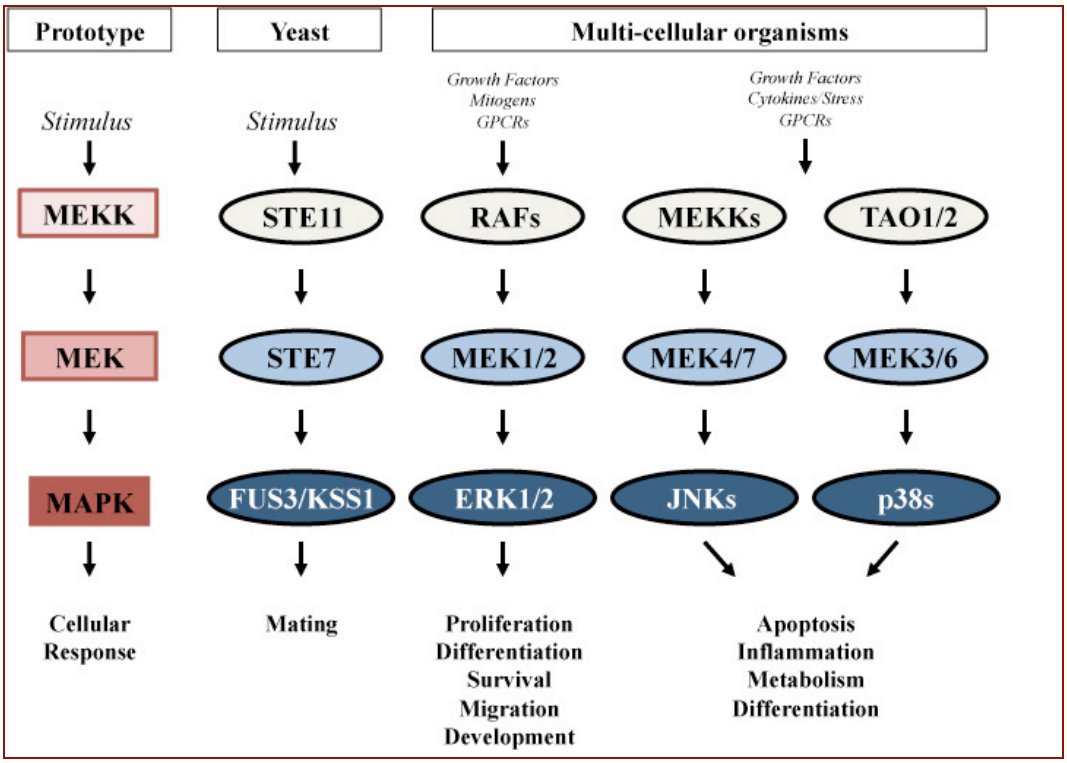

Figure 1.2. A MAPK signaling cascade. Simplified model of organization of kinase activation.

Mutation (CDS)	Mutation (Amino Acid)	Mutation ID (COSM)	Count	Mutation Type
c.868T>C	p.L290L	COSM219388	1	Substitution synonymous
c.781A>G	p.R261G	COSM478771	1	Substitution missense
c.964G>A	p.E322K	COSM461148	1	Substitution missense
c.892C>A	p.P298T	COSM1032481	1	Substitution missense
c.285C>T	p.I95I	COSM419632	1	Substitution synonymous
c.485A>G	p.D162G	COSM726222	1	Substitution missense
c.548T>C	p.F183S	COSM1032483	1	Substitution missense
c.471C>A	p.L157L	COSM726221	1	Substitution synonymous
c.961G>A	p.D321N	COSM98175	1	Substitution missense
c.785A>C	p.N262T	COSM282659	1	Substitution missense
c.188C>T	p.T63I	COSM110008	1	Substitution missense
c.154G>T	p.A52S	COSM296310	1	Substitution missense
c.572G>A	p.R191H	COSM215856	1	Substitution missense
c.515G>A	p.R172H	COSM166663	1	Substitution missense
c.429T>A	p.A143A	COSM82238	1	Substitution synonymous
c.685C>T	p.P229S	COSM135912	1	Substitution missense
c.600G>T	p.L200F	COSM216556	2	Substitution missense

Table 1.1. Observed ERK2 mutations. The mutation data were obtained from the Sanger Institute Catalogue Of Somatic Mutations In Cancer website, http://www.sanger.ac.uk/cosmic (Bamford et al., 2004).

II. Overview of kinesins

The first hint at the existence of kinesins came from a 1985 study that utilized then novel technology, video-enhanced light microscopy. This improvement in technology allowed for an observation that a nonhydrolyzable analog of ATP, 5'adenylylimidodiiphosphate (AMP-PNP), inhibited vesicle transport on microtubules of the axoplasm extruded from the squid giant axon (Lasek & Brady, 1985). The authors speculated that AMP-PNP must be binding to an ATP-binding site on the transport machinery, subsequently stabilizing the complex between an ATPase, a microtubule and a vesicle. Following on this observation, Vale and colleagues purified protein from squid giant axons and optic lobes that induced microtubule-based movements and formed a high affinity complex with microtubules in the presence of AMP-PNP. Distinct from myosin, which moves along actin and dynein to drive retrograde transport along microtubules, this newly identified, force-generating protein was named kinesin. This first identified kinesin was found to have a molecular weight of 600 kilodaltons consisting of 110-120 and 60-70 polypeptides (Vale, Reese, & Sheetz, 1985).

To date, 45 kinesins have been identified in humans and all have murine orthologs (Miki, Setou, Kaneshiro, & Hirokawa, 2001). Based on the results from phylogenetic analysis, kinesins have been grouped into 15 families, termed from kinesin 1 to kinesin 14B (Lawrence et al., 2004; Miki et al., 2001). Further, kinesins can be sorted into 3 categories based on the placement of the motor domain in the molecule: amino-terminal motor domain represents the N-kinesin family, carboxy-terminal motor domains are found on C-kinesins, and motor domain located in the middle of the primary sequence constitute M-kinesins. The position of the motor domain within the kinesin

molecule does have functional relevance. N-kinesins transport cargo in a plus-end direction, whereas C-kinesins transport cargo in a minus-end direction. M-kinesins are believed to only have a microtubule depolymerase activity, rather than a cargo transporting function (Figure 2.1). Whether, they transport cargo or regulate microtubule dynamics, kinesin function is important for processes that include chromosomal movement and spindle formation in mitosis, as well as signaling events and vesicular traffic in interphase cells. The need for a great number of cargo-carrying kinesins is thought to have emerged to accommodate diversity of cargo and provide specificity to kinesin-cargo binding, though there is some overlap and redundancy. Kinesins can either use adapter and scaffold proteins or bind directly to cargo.

Two defining properties of kinesins are that they have a globular, motor domain, consisting of a catalytic region, which hydrolyzes ATP, and a microtubule binding region. This motor domain containing ~320 residues is significantly smaller than those in dynein or myosin. The directionality of transport along microtubules is provided by microtubules themselves. Microtubules are polar polymers composed of α and β tubulin. They start with slow-growing α-tubulin at the minus end and terminate with β-tubulin at the fast-growing plus-end. Structural comparison and biochemical, chimeric studies using the conventional N class kinesin (KHC) which moves in a plus end direction and *Drosophila* ncd motor which moves in the minus end direction were used to determine the defining properties that lead to directionality along the microtubules. The findings were surprising because these two motors had similar sequence, structure and enzymatic activity. Rather, it is a short sequence outside of the motor domain, in the neck region of a kinesin that is important for directionality (Endow & Waligora, 1998). The motor

domain including the catalytic and neck region is highly conserved; the stalk and the tail regions of kinesins provide diverse functions by allowing for unique interactions with other cargo molecule containing proteins, lipids and nucleic acids.

In this review, I will particularly focus on kinesins that we found misregulated in lung cancer lines. In a microarray study comparing 148 lung cancer lines to 59 normal lung cells, we identified a number of kinesins that were upregulated: KIF1A, KIFC1, KIF4A, KIF5C, KIF11, KIF14, KIF15, KIF20A, KIF23, KIF2A and KIF2C; we also found tow downregulated: KIF1C and KIF16B (Figure 2.2, 2.3, 2.4, 2.5).

KIF1A

KIF1A, a monomeric N-type kinesin binds to synaptic vesicle precursors and transports them (Okada, Yamazaki, Sekine-Aizawa, & Hirokawa, 1995). These synaptic vesicle precursors that KIF1A associates with in mature peripheral nerves contain synaptophysin, synaptotagmin and Rab3a. Mice that have the KIF1A gene disrupted die within a day of birth and exhibit motor and sensory dysfunction. Further, neurons of these mice also show a decrease in transport of synaptic vesicle precursors (Yonekawa et al., 1998).

KIFC1

KIFC1, a C-type kinesin, directs microtubule-based traffic in the minus-end direction. KIFC1 co-localizes on the population of the same early endocytic vesicles along with a plus-end directed kinesin, KIF5B where they are thought to act antagonistically (Nath et al., 2007).

KIF4A

A kinesin 4 family protein, KIF4A is best characterized as a kinesin important in regulation of midzone microtubule length during cytokinesis (Hu, Coughlin, Field, & Mitchison, 2011). The mechanism of KIF4A regulation of microtubules at the end of mitosis is believed to occur through its direct interaction with a microtubule-bundling protein, protein regulator of cytokinesis 1 (PRC1) (Kurasawa, Earnshaw, Mochizuki, Dohmae, & Todokoro, 2004). KIF4 concentrates PRC1 at the midline, and, when depleted, PRC1 is dispersed along the central spindle (Zhu & Jiang, 2005).

KIF5C

KIF5C is a family 1 member that also includes KIF5A and KIF5B. This N-terminal kinesin is also known as a conventional kinesin heavy chain (KHC) kinesin. Unlike KIF5B, which is ubiquitously expressed, KIF5C is specifically expressed in neurons and positively affects brain size (Kanai et al., 2000). Nevertheless, KIF5A/B/C may be functionally redundant and have originated out of gene duplication. KIF5 proteins bind cargo with and without interaction with the kinesin light chain (KLC). Cargo type transported by KIF5 is diverse and includes mitochondria, lysosomes, vesicles, mRNP complex, etc (Hirokawa, Noda, Tanaka, & Niwa, 2009).

KIF11

KIF11, also known as Eg5, is one of the more studied kinesins that is emerging as a potential target for cancer therapy. KIF11 is the sole member of the N-terminal, kinesin 5 family that is involved in the formation of the bipolar spindle in mitosis (Blangy et al., 1995). Depletion of KIF11 by siRNA or its inhibition with a small molecule inhibitor monastrol results in monopolar spindles and cell cycle arrest in prometaphase (Kapoor, Mayer, Coughlin, & Mitchison, 2000; Whitehead & Rattner,

1998). As with a number of other kinesins that regulate spindle formation, KIF11 mitotic function is regulated by phosphorylation by Polo-like kinase (Plk1) that targets KIF11 to spindle poles and cyclin-dependent kinase (CDK1) (Smith et al., 2011).

KIF14

A small siRNA screen was designed to dissect functions of kinesins and dyneins. One of the molecules found was KIF14, identified as one of the motors required for chromosome congregation and alignment in mitosis (Zhu et al., 2005).

KIF20A

KIF20A, also known as Rab 6 kinesin and mitotic kinesin-like protein 2 (MKLP2), is a kinesin 6 family protein that contributes to central spindle assembly. Aside from the mitotic function, KIF20A along with cytoplasmic dynein and KIFC3 (both minus directed motors) contributes to Golgi positioning and integrity (Echard et al., 1998). The studies showing KIF20A regulation of Golgi trafficking are controversial. Hill et al. found that KIF20A is regulated during the cell cycle reaching highest expression in mitosis and being degraded thereafter. Additionally, no co-staining of KIF20A with Golgi was observed by this group (Hill, Clarke, & Barr, 2000).

KIF23

KIF23, also known as a mitotic kinesin-like protein 1 (MKLP1), is another N-terminal kinesin motor in the kinesin 6 family. KIF23 is required for cytokinesis, a function which is regulated by a number of phosphorylation events (Guse, Mishima, & Glotzer, 2005; Liu, Zhou, Kuriyama, & Erikson, 2004). CDK1 phosphorylates and negatively regulates KIF23 in metaphase, but Aurora B phosphorylation at the end of anaphase promotes KIF23 activity (Neef, Klein, Kopajtich, & Barr, 2006). Recent

findings suggest that KIF23 can also recruit a small GTPase Arf6 to the cleavage furrow and this complex connects microtubule bundles to membranes providing for completion of cytokinesis (Makyio et al., 2012).

KIF2A

KIF2A, along with a related family 13 kinesin protein KIF2C, was first identified as a microtubule destabilizing kinesin (Desai, Verma, Mitchison, & Walczak, 1999). Using in vitro assays the authors were able to determine that these two kinesins target to microtubule ends where they induce conformational changes and catastrophy of microtuble polymers. ATP hydrolysis helps dissociate kinesins from tubulin. Further functional information on KIF2A emerged from a study with KIF2A$^{-/-}$ mice. These knockout mice died one day after birth, unable to suck milk with a number of brain phenotypes. The neuronal phenotypes observed included abnormal axonal branching and elongated collateral branches suggesting a function for KIF2A in suppression of collateral branch extension (Homma et al., 2003). More recently, Noda et al. found that KIF2A's function as a neuronal microtubule depolymerase is enhanced through phosphorylation by phosphatidylinositol 4-phosphate 5-kinase alpha (PIPKα) (Noda et al., 2012). Studies using a KIF2A *Drosophila* orthologue KLP10A, show an interphase function in S2 cells, namely the ability to induce catastrophe of microtubules, promoting shrinkage rather than growth (Mennella et al., 2005). End binding (EB1) protein, a plus-end tracking protein is required to deposit KLP10A on microtubules. Aside from regulating interphase microtubule function, KIF2A also has mitotic functions. KIF2A is required for proper bipolar spindle formation and chromosome segregation (Ganem & Compton, 2004). These functions are also regulated by phosphorylation. For example

Aurora B inhibits KIF2A depolymerase activity through phosphorylation on serine 132 (Knowlton, Vorozhko, Lan, Gorbsky, & Stukenberg, 2009). KIF2A interaction with the inner centromere Kin-I stimulator (ICIS) can reactivate KIF2A after it has been inhibited by Aurora B. Plk1 also interacts with and phosphorylates KIF2A. This phosphorylation event enhances KIF2A depolymerase activity affecting spindle microtubule intensity in cells (Jang, Coppinger, Seki, Yates, & Fang, 2009). KIF2A localization on spindle poles is regulated through its association with DDA3, also known as proline/serine-rich coiled-coil 1 (PSRC1), in a microtubule-dependent mechanism (Jang et al., 2008).

KIF2C

KIF2C, also known as the mitotic centromere-associated kinesin (MCAK), is the best studied kinesin 13 family protein. It regulates microtubule turnover at the kinetochores (Ganem & Compton, 2004; Ganem, Upton, & Compton, 2005; Wordeman & Mitchison, 1995). The mitotic function of KIF2C is regulated by a number of phosphorylation events. Aurora B phosphorylates *Xenopus* KIF2C on S196 and inhibits its ability to destabilize microtubules but inhibition of Aurora B enhances KIF2C accumulation at centromeres suggesting that Aurora B is important for KIF2C activity and localization (Andrews et al., 2004; Lan et al., 2004; Ohi, Sapra, Howard, & Mitchison, 2004). Aurora A is believed to regulate KIF2C localization to spindle poles through phosphorylation on S719, and activity through a phosphorylation on S196 (Zhang, Ems-McClung, & Walczak, 2008). Unlike Aurora A, CDK1 only phosphorylates one residue on KIF2C, T537 which is located in the core domain of KIF2C. Potentially this negative charge interferes with the ability of KIF2C to interact with microtubules (Sanhaji et al., 2010). Aside from the mitotic function, KIF2C is also believed to regulate

microtubules in interphase. For example, a study with a Drosophila orthologue KLP59C shows that it represses rescue/growth of microtubules at the plus end (Mennella et al., 2005).

KIF1C

KIF1C was first described as a Golgi-localized motor that may regulate Golgi-to-endoplasmic reticulum transport (Dorner et al., 1998). Though partial Golgi co-localization of KIF1C was confirmed by a Nakajima et al. study, no defect in Golgi-to-ER transport were identified in KIF1C$^{-/-}$ mice (Nakajima et al., 2002). It is possible that compensatory changes from kinesins with redundant functions were able to correct for retrograde transport defect observed in a cell-based system, but further studies are required to examine the involvement of KIF1C in microtubule-propagated transport.

KIF16B

Like KIF1C, KIF16B is also a kinesin 3 family protein that is thought to be an early endosome carrier. Binding to endosomes occurs through a PX domain that is located in the C-terminal region of the KIF16B and can bind PtdIns(3,4,5)P (Blatner et al., 2007). The small GTPase Rab5 and its interactor the phosphatidylinositol 3-kinase (PI3K) VPS34 appear to be required for the transport of early endosomes to the plus end of microtubules by KIF16B but the mechanism is not entirely understood (Hoepfner et al., 2005). The regulation of endosomal traffic by KIF16B affects the epidermal growth factor receptor (EGFR) recycling and degradation. Therefore, it will be important to examine if the downregulation of KIF16B function in tumorigenicity is linked to receptor availability in the cells. The endosomal trafficking function of KIF16B is of pivotal importance in mouse development. KIF16B$^{-/-}$ mice failed at the peri-implantation stage,

unable to form epiblast and primitive endoderm lineages. Because of the similarity of this phenotype to the fibroblast growth factor receptor (FGFR2) knockout embryos, the authors investigated the connection between KIF16B and FGFR2 and found that KIF16B interacts directly with Rab14 and promotes Golgi-to-endosome trafficking of FGFR (Ueno, Huang, Tanaka, & Hirokawa, 2011).

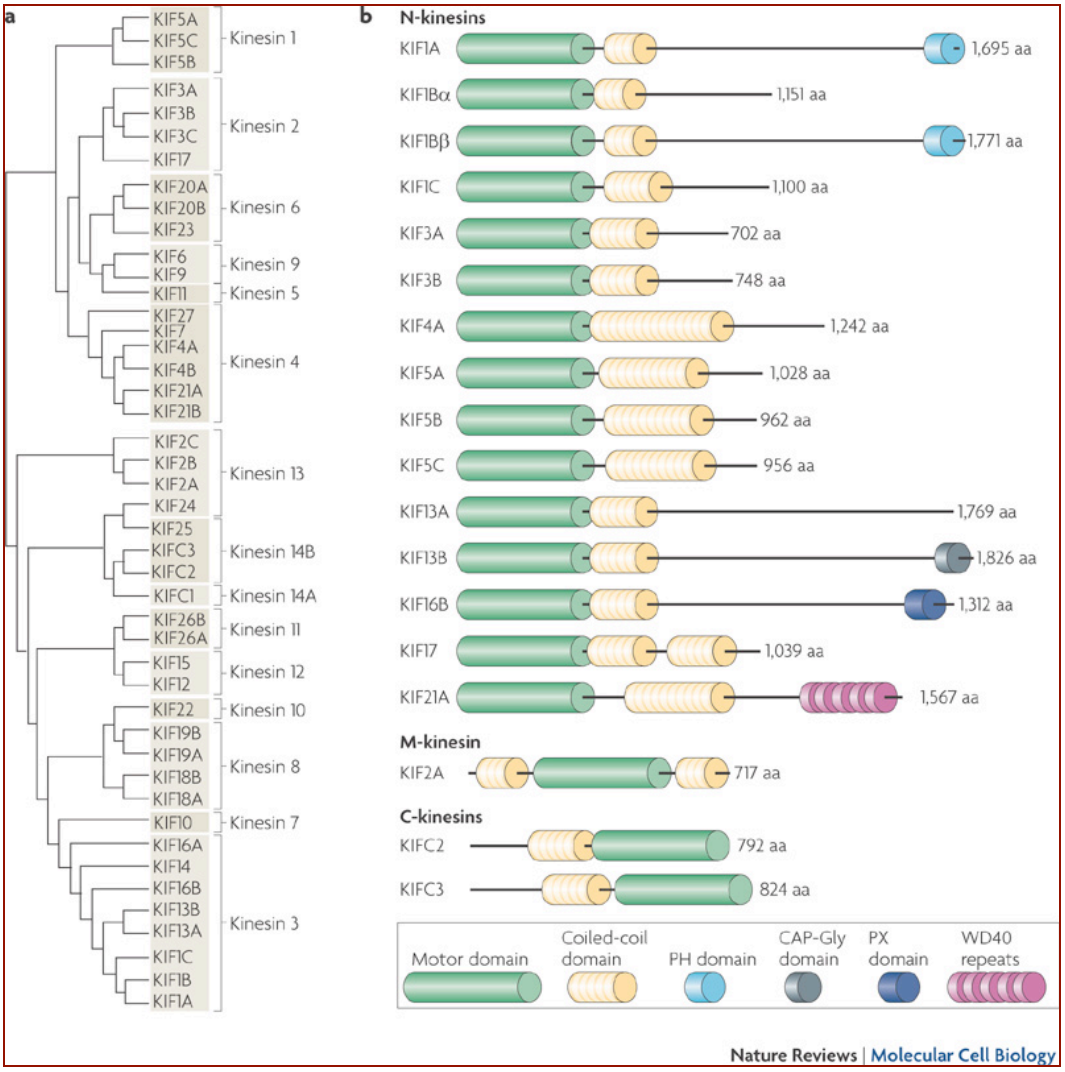

Figure 1.3. A phylogenetic tree of all 45 kinesin superfamily members. Kinesins are sorted into 15 families, 1 to 14B, based on sequence similarity or in 3 families (N, C and M family) based on the location of the motor domain in their primary sequence. Reprinted with permission from Hirokawa N et al, 2009.

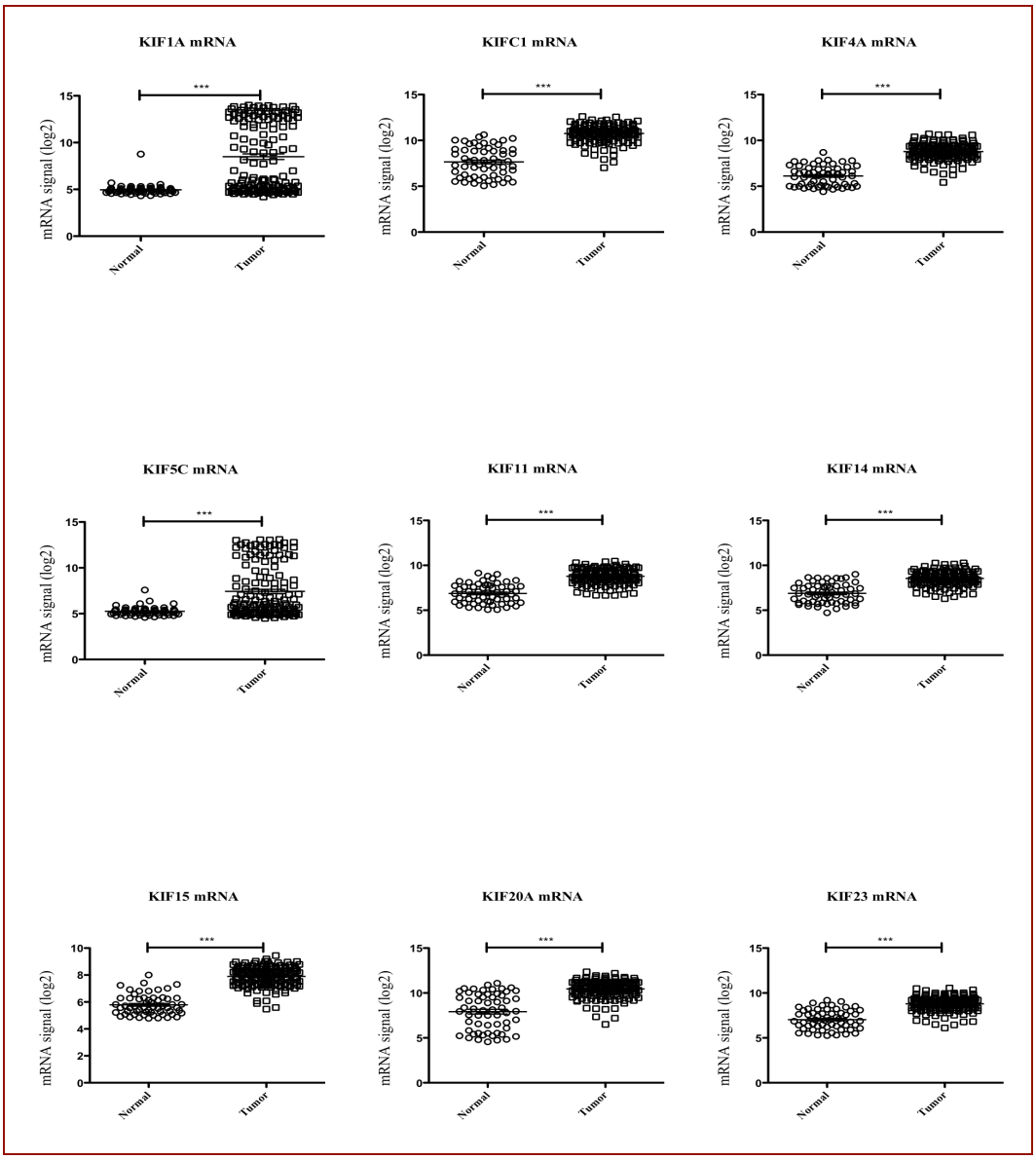
KIF1A mRNA
KIFC1 mRNA
KIF4A mRNA
KIF5C mRNA
KIF11 mRNA
KIF14 mRNA
KIF15 mRNA
KIF20A mRNA
KIF23 mRNA
mRNA signal (log2)
***
Normal
Tumor

Figure 1.4. Nine kinesins that are significantly upregulated in lung cancer cell lines. The microarray study was performed using the Minna laboratory cell line panel consisting of 118 NSCLCs, 29 SCLCs, 30 HBECs (immortalized human bronchial epithelial cells), and 29 HSAECs (immortalized human small airway epithelial cells). Amplified and labeled cRNA probes (1.5 μg) were hybridized to Illumina HumanWG-6 V3 Expression BeadChip (BD-101-0203). All array data are deposited in GEO (GSE32036).

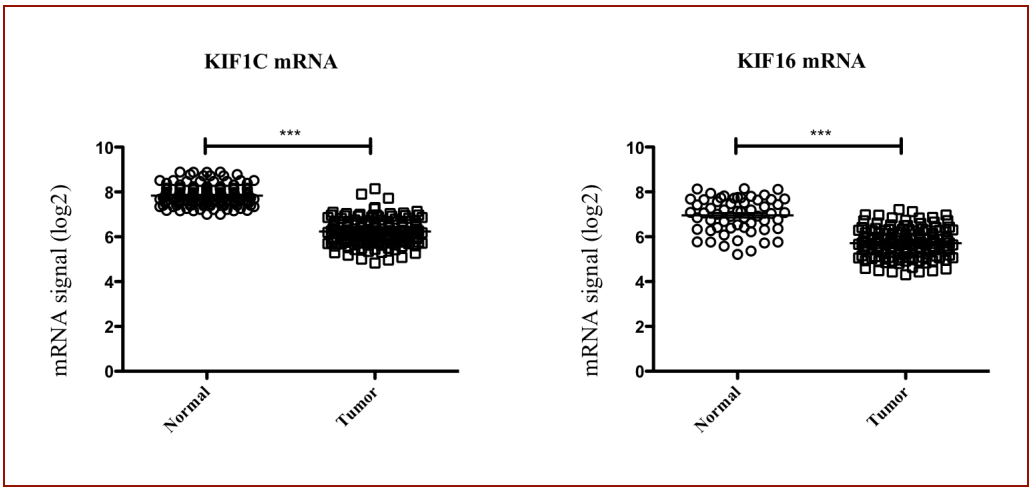

Figure 1.5. Two kinesins that are significantly downregulated in lung cancer cell lines. The microarray was performed as in Figure 2.2.

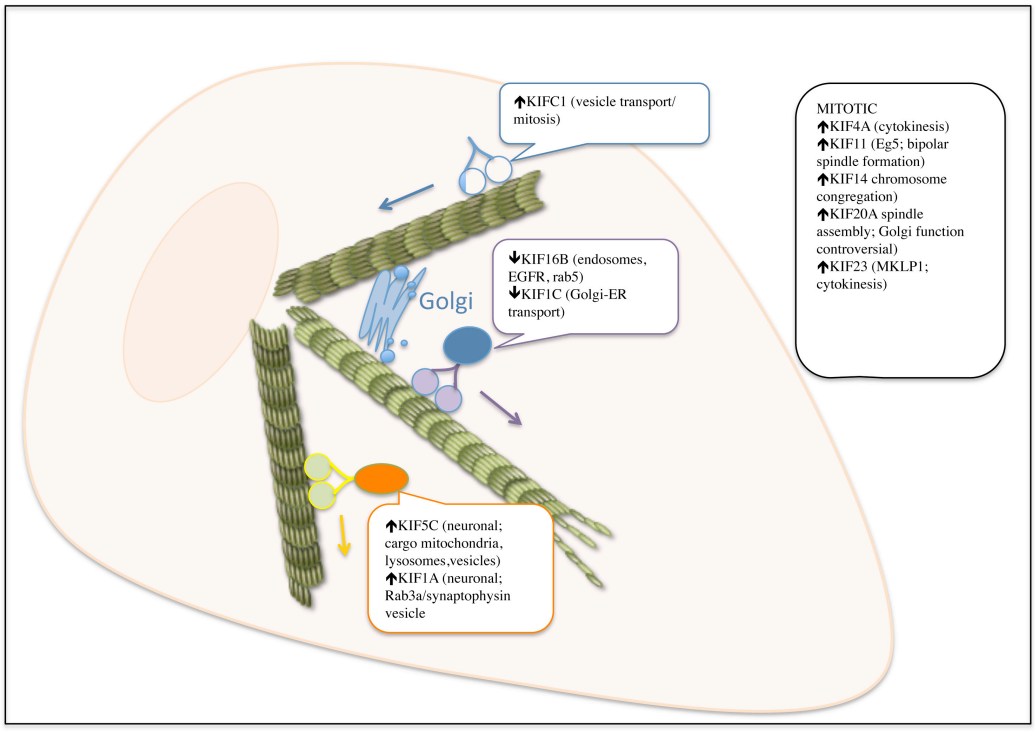

Figure 1.6. Summary of kinesin function that were upregulated or downregulated in cancer cells based on our microarray data. The illustration depicts kinesin directionality as they move along microtubules as well as current, published functional information.

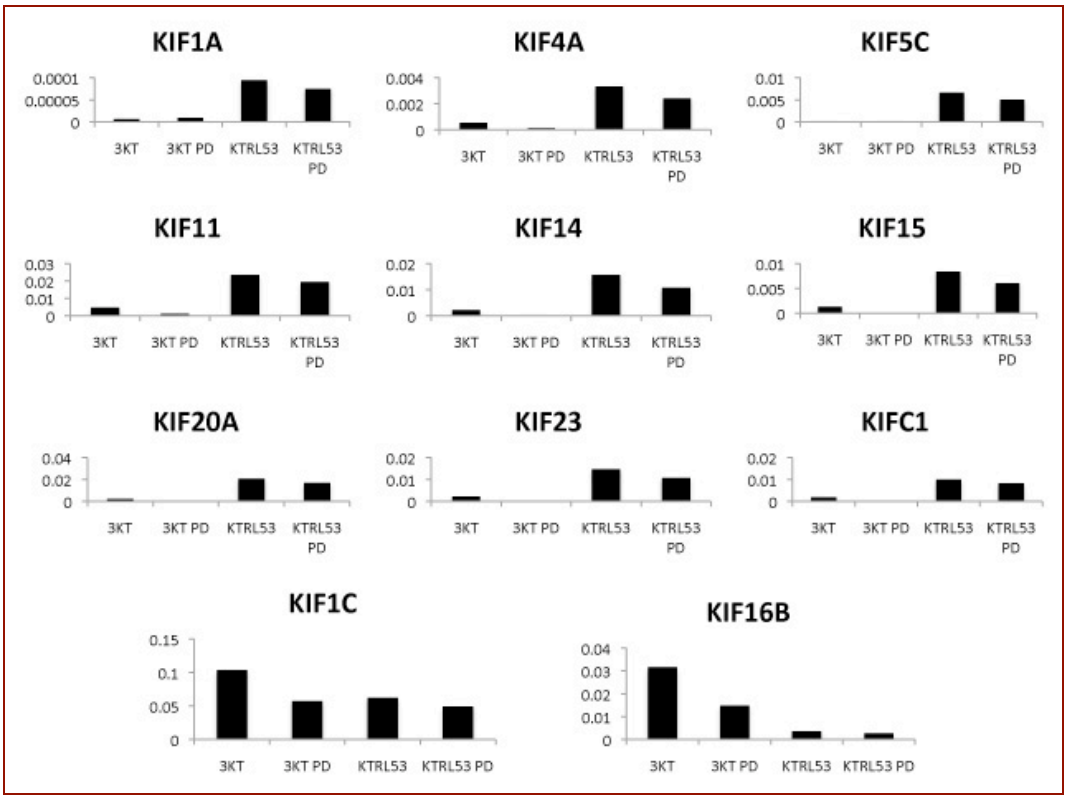

Figure 1.7. Confirmation of microarray data by qPCR. Y-axis represents mRNA signal (log2) normalized to beta actin. HBEC3KT (3KT) or HBEC3KTRL53 (KTRL53) cells were treated for 2 days with DMSO or 100 nM PD0325901. qPCR is further described in later chapters. The following primers were used: KIF1A (Forward 5'è3': GTCCGCCCCTTCAATTCCC; Reverse 5'è3':GAGGTGTGCGACCAGTAGG), KIFC1(F:GGTGCAACGACCAAAATTACC;R:GGGTCCTGTCTTCTTGGAAAC), KIF4A (F:TACTGCGGTGGAGCAAGAAG; R:CATCTGCGCTTGACGGAGAG), KIF5C(F:ATGTCTTCGACAGAGTGCTACC;R:ACGCAAAAATCGTCCCGTTAT), KIF11(F:TCCCTTGGCTGGTATAATTCCA;R:GTTACGGGGATCATCAAACATCT), KIF14(F:CCTCACCCACAGTAGCCGA; R:AAGTGCCAATCTACCTACAGGA), KIF15(F:AAAACTGAGTTACGCAGCGTG;R:AGTTGCGAATACAGATTCCTGAG),

KIF20A(F: TGCTGTCCGATGACGATGTC; R: AGGTTCTTGCGTACCACAGAC), KIF23 (F: AGTCAGCGAGAGCTAAGACAC; R: GGTTGAGTCTGTAGCCCTCAG), KIF1C (F: AGGGTTCGGCCCTTTAACG; R: GTCCCGATACACTTGCTGCT), KIF16B F:TCGGCACAGATGTCGTGAAG; R: CCGAGGTATTAAGCCAGAATCTC)

CHAPTER TWO

ERK1/2 regulate the microtubule depolymerase KIF2A

Abstract

The kinesin-like protein KIF2A is a microtubule-associated motor protein that causes microtubule depolymerization by inducing a conformational change in tubulin. The depolymerase function of KIF2A is utilized in mitotic cells to establish proper bipolar spindles. Studies in KIF2A knockout mice revealed KIF2A function in regulation of interphase microtubules, as $KIF2A^{-/-}$ neurons exhibit abnormal axon branching, but little is known about KIF2A regulation during interphase. Here, we show that ERK1/2 regulate KIF2A function by directing it to the leading edge in interphase cells. Phosphorylation by ERK1/2 may also be required to suppress apoptosis induced by KIF2A overexpression.

Introduction

Extracellular signal-regulated kinase 1/2 (ERK1/2) extend the impact of the Ras/mitogen-activated protein kinase (MAPK) signaling cascade in multiple directions through diverse substrates. ERK1/2 were first identified as insulin-stimulated enzymes that phosphorylated the microtubule-associated protein MAP2 (Ray, L. B. & Sturgill, T. W., 1987) and associate with microtubules in both stimulated and unstimulated states (Olsen, M. K., Reszka, A. A., & Abraham, I., 1998; Leinweber, B. D., Leavis, P. C.,

Grabarek, Z., Wang, C. L., & Morgan, K. G., 1999). Addition of purified ERK2 to *Xenopus* interphase extracts induced rearrangement of microtubule arrays and altered microtubule dynamics in reconstituted systems (Gotoh, Y. et al., 1991b). ERK1/2 inhibit microtubule polymerization in part through MAPs. MAP2, MAP4, and tau, once phosphorylated by ERK1/2, are less effective in inducing tubulin polymerization or inhibiting catastrophe (Sanchez, C., az-Nido, J., & Avila, J., 2000; Hoshi, M. et al., 1992; Drechsel, D. N., Hyman, A. A., Cobb, M. H., & Kirschner, M. W., 1992). ERK1/2 can also enhance polymerization of the microtubule network through phosphorylation of the stathmin Op18, which, in the unphosphorylated state, sequesters free tubulin preventing polymerization (Di, Paolo G., Antonsson, B., Kassel, D., Riederer, B. M., & Grenningloh, G., 1997; Gotoh, Y. et al., 1991a; Marklund, U., Brattsand, G., Shingler, V., & Gullberg, M., 1993). Colchicine and vinblastine, drugs that disrupt microtubules, lead to increased ERK1/2 activity (Shinohara-Gotoh, Y., Nishida, E., Hoshi, M., & Sakai, H., 1991); thus, ERK1/2 association with cytoskeletal components affects both its own activity and functional changes in the cytoskeleton (Olsen, M. K., Reszka, A. A., & Abraham, I., 1998; Pullikuth, A. K. & Catling, A. D., 2007).

Kinesins are motor proteins originally identified by the capacity to move cargo along microtubules in an anterograde direction towards the periphery (Kardon, J. R. & Vale, R. D., 2009). More than forty kinesins have now been identified in mammals with a diversity of functions (Miki, H., Setou, M., Kaneshiro, K., & Hirokawa, N., 2001; Lawrence, C. J. et al., 2004). The kinesin motor domain may be located at the amino-terminus (N-kinesins), carboxy-terminus (C-kinesins), or in the middle (M-kinesins). The position of the motor domain within the kinesin molecule specifies function; N-

kinesins transport cargo in a plus-end direction towards the periphery, C-kinesins transport cargo in a minus-end or retrograde direction towards the nucleus, and M-kinesins depolymerize microtubules (Miki, H., Okada, Y., & Hirokawa, N., 2005).

KIF2A, an M-kinesin, regulates the cytoskeleton by depolymerizing microtubules, as do related members of the kinesin 13 family (Desai, A., Verma, S., Mitchison, T. J., & Walczak, C. E., 1999). The most thoroughly studied, KIF2C, is also known as the *m*itotic *c*entromere-*a*ssociated *k*inesin (MCAK), and localizes to centromeres to regulate microtubule turnover at the kinetochore (Rogers, G. C. et al., 2004; Ganem, N. J. & Compton, D. A., 2004). KIF2B is mostly centromeric and is required for many processes, including spindle formation and cytokinesis (Manning, A. L. et al., 2007). KIF24 has only recently been defined functionally as a centriolar kinesin that regulates ciliogenesis but does not significantly alter cytoplasmic microtubules (Kobayashi, T., Tsang, W. Y., Li, J., Lane, W., & Dynlacht, B. D., 2011). KIF2A is phosphorylated and required for mitosis due to its regulation of spindle formation (Ganem, N. J. & Compton, D. A., 2004)(Knowlton, A. L., Vorozhko, V. V., Lan, W., Gorbsky, G. J., & Stukenberg, P. T., 2009). Klp10, the Drosophila KIF2A ortholog, depolymerizes microtubules during interphase, indicating that this kinesin has multiple functions during the cell cycle (Mennella, V. et al., 2005). Most studies of KIF2A have focused on its function in mitosis; little is known, however, about how KIF2A is regulated in interphase cells.

In this study, we describe the interaction between ERK1/2 and KIF2A. The connection between ERK1/2 and KIF2A provides an additional input from this kinase pathway to regulate the microtubule cytoskeleton.

Materials and Methods

Antibodies - The following antibodies were used: KIF2A (Abcam, 37005; Novus Biologicals, NB500), α-tubulin (Sigma,T6199), GAPDH (Santa Cruz, sc-25778), actin (Millipore, MAB1501MI), FLAG (Sigma, F3165), pS6 (Cell Signaling Technology, 5364), pERK (Sigma, M8159; Cell Signaling, 9106), and ERK1/2 (Boulton, T. G. & Cobb, M. H., 1991).

Plasmids- Human KIF2A in pCMV-SPORT6 vector was obtained from Open Biosystems (Accession number: BC031828).

Cell Culture- Immortalized HBEC3KT and HBEC3KT53 cells were cultured in Keratinocyte serum free medium (KSFM) (Invitrogen) supplemented with 5 ng/mL epidermal growth factor and 50 μg/mL bovine pituitary extract according to manufacturers recommendations. HeLa were cultured in Dubelcco's modified Eagles medium (DMEM) containing 10% heat-inactivated fetal bovine serum (vol/vol) and 2 mM L-glutamine. HBEC3KTRL53 were cultured in RPMI-1640 medium supplemented with 5% heat-inactivated fetal bovine serum (vol/vol) and 2mM L-glutamine. Cells were grown at 37°C in a humidified atmosphere of 5% CO_2.

RNAi - Cells were transfected with dsRNA oligonucleotides using Lipofectamine RNAiMax according to manufacturer's protocol (Invitrogen). After 96 hr, cells were processed. The following target sequences for KIF2A were used: GAATTGACTGTAGATCCAA (Ambion) and GACCCTCCTTCAAGAGATA (Thermo Scientific); ERK1 siRNA (Applied Biosystems #11141, sequence GGACCGGATGTTAACCTTT), ERK2 siRNA (Applied Biosystems #11137, sequence CAGGGTTCCTGACAGAATA).

Cell harvest and immunoprecipitation- Cells were lysed as previously described except 1% Triton X-100 was used (Jivan, A., Earnest, S., Juang, Y. C., & Cobb, M. H., 2009). For immunoprecipitation, cells were washed twice with phosphate-buffered saline and resuspended in 10 mM HEPES, pH 7.5, 0.25 M sucrose, 1 mM $MgCl_2$, phenylmethylsulfonyl fluoride, 1.6 μg/ml aprotinin, and 10 μg/ml each of N^{α}-p-tosyl-L-lysine chloromethyl ketone, N^{α}-p-tosyl-L-arginine methyl ester, pepstatin A, and leupeptin. Cells were passed through a 30 gauge needle four times, followed by centrifugation for 5 min at 16,000 × g in a microcentrifuge at 4 °C. Cytosol was collected from the supernatant fraction and the pellet was resuspended in the above mentioned lysis buffer containing 0.1% Triton X-100. Both cytosolic and pellet fraction were used for immunoprecipitation with KIF2A antibody (1:100 dilution) at 4°C overnight. Then 30 μl of protein A-Sepharose beads was incubated with the lysate for 1 hr at 4 °C. Following washing of beads in lysis buffer with no detergent, beads were resuspended and subsequently boiled in Laemmli sample buffer (2% sodium dodecyl sulfate, 10% glycerol, 5% β-mercaptoethanol, 0.01% bromophenol blue, 50 mM Tris-HCl) and subjected to electrophoresis as previously described (Jivan, A., Earnest, S., Juang, Y. C., & Cobb, M. H., 2009).

Protein purification and kinase assays- His_6-ERK1 and ERK2 were purified as described (Robbins, D. J. et al., 1993). GST-KIF2A was expressed in bacterial strain BL21(DE3) by induction for 4 hr at 16°C with 0.5 mM Isopropyl β-D-1-thiogalactopyranoside (IPTG). Proteins were purified from bacterial lysates with glutathione Sepharose (GE Amersham) and eluted with 10 mM glutathione. FLAG-KIF2A was expressed in bacterial strain BL21(DE3) by induction for 4 hr at 30°C with 1 mM isopropyl β-D-1-

thiogalactopyranoside (IPTG). Bacteria were lysed in 80 mM PIPES buffer, pH6.8, 20% glycerol, 1 mM $MgCl_2$, 1 mM EGTA, 0.2 mM EDTA, 0.5M NaCl, 0.5 mM ATP, 1% NP-40 and protease inhibitors using sonication. Protein was purified from bacterial lysate with anti-FLAG M2 Affinity Gel (Sigma-Aldrich, A2220) and eluted with FLAG peptide (Sigma, F3290). Kinase assays were in 30 µl reactions containing 10 mM $MgCl_2$, 5 µM ATP (15 cpm/fmol [γ-^{32}P]ATP), 1 mM dithiothreitol, and 10 mM HEPES (pH 7.5), and 1 µg recombinant substrates or 5 mg of myelin basic protein (MBP). Reactions were incubated at 30°C for 30 min and terminated with 5x sample buffer. Samples were boiled and resolved by electrophoresis under denaturing conditions, and processed for autoradiography.

Immunofluorescence - Immunofluorescence was performed exactly as described (Tu, S., Bugde, A., Luby-Phelps, K., & Cobb, M. H., 2011).

qRT-PCR - Cells were harvested and RNA was extracted using QuickRNA™ (Zymo Research) according to the manufacturer's protocol. RNA was reverse transcribed using the iScript cDNA synthesis kit (BioRad). PCR reactions were performed with IQ SYBR Green Supermix (BioRad), and fluorescence was measured using a quantitative real-time thermocycler (ABI 7500). The following primer sets were used: KIF2A (sense 5'-TGCAAATAGGGTCAAAGAATTG-3'and antisense 5'-TTGTTCACAAAGAAGTTTTAGATCAT-3'); beta actin(5'-CATGTACGTTGCTATCCAGGC-3' and antisense 5'-CTCCTTAATGTCACGCACGAT-3'). Relative changes in gene expression were calculated by $2^{-\Delta Ct}$, where ΔCt= Ct(KIF2A)-Ct(ActinB).

Supplementary Methods

Plasmid construction -KIF2A was subcloned into pET11d-FLAG vector for bacterial expression using a forward NotI site-containing upstream primer 5'-CTTGCGGCCGCGATGGTAACATCTTTAAATG-3' and a BamHI site-containing reverse primer 5'-CCGGGATCCTCTAGATTAAAGGGCACGGGG-3'. Human KIF2A was subcloned into pFLAG-CMV vector using the following forward and reverse primers: GACAAGCTTGCGGCCGCG ATGGTAACATCTTTAAATG and GGATCCTCTAGAGTCGACTGGTTAAAGGGCACGGGG. PCR products were digested with SalI and NotI and ligated into pFLAG-CMV vector. Human KIF2A T78A was generated using QuikChange mutagenesis with forward and reverse primers: GAACCCAGTCCAGAAGCACCTCCACCTCCAGCA and TGCTGGAGGTGGAGGTGCTTCTGGACTGGGTTC. Human KIF2A T78E was generated using QuikChange mutagenesis with forward and reverse primers: GAACCCAGTCCAGAAGAACCTCCACCTCCAGCA and TGCTGGAGGTGGAGGTTCTTCTGGACTGGGTTC. Human KIF2A and KIF2A T78A was subcloned into pGEX-GST vector using the following forward and reverse primers: CGTGGATCCCCGATGGTAACATCTTTAAATG and GTCTAGAATTCCACCTTAAAGGGCACGGGG. PCR product were digested with BamHI and EcoRI and ligated into pGEX-GST vector. *Proteomics* - Bands from gels were excised and the proteins within them digested overnight with trypsin (Promega, Madison, WI) after reduction and alkylation with dithiothreitol and iodoacetamide (Sigma-Aldrich, St Louis, MO). The resulting samples were analyzed by tandem mass-spectrometry (MS) using an LTQ-Orbitrap Velos mass-spectrometer (Thermo Electron,

Bremen, Germany) coupled to an Ultimate 3000 RSLC-Nano liquid chromatography system (Dionex, Sunnyvale, CA). Peptides were loaded onto a 75 μm ID, 40 cm self-packed column containing 1.9 μm C18 resin (Dr. Maisch, Ammerbuch, Germany), and eluted with a gradient of 0-28% buffer B in 100 min, followed by 28%-40% buffer B in 20 min: Buffer A, 2% acetonitrile and 0.1% formic acid in water; Buffer B, 80% acetonitrile, 10% trifluoroethanol and 0.08% formic acid in water. The LTQ-Orbitrap acquired up to 10 collision induced dissociation (CID) fragment spectra in the ion-trap for each full spectrum acquired in the Orbitrap.

Raw MS data were converted to peak list format using ProteoWizard msconvert (version 3.0.3535) (1). The resulting files were analyzed using the Central Proteomics Facilities Pipeline (CPFP) (2). Peptide identification was performed using the X!Tandem (3) and OMSSA (4) search engines against the UniProtKB human whole proteome sequence database (release 2012_02) (5), with reversed decoy sequences appended (6). Fragment and precursor tolerances of 20 ppm and 0.5 Da were specified and two missed cleavages were allowed. Carbamidomethylation of Cys was specified as a fixed modification. Oxidation of Met and phosphorylation of Ser, Thr, Tyr were specified as variable modifications. Validation and combination of results is performed within CPFP using the Trans-Proteomic Pipeline tools (7). Identifications were filtered to <1% false discovery rate. Initial assessment of localization ambiguity for phosphorylations assigned by the search engines was performed using the ModLS tool within CPFP, which is based on the PTMScore method (8,9).

Results

ERK1/2 interact with KIF2A and have overlapping localizations. We identified KIF2A as an ERK2 binding protein through a yeast-two hybrid screen constructed to uncover proteins that bind with high affinity to phosphorylated ERK2 (pERK2) as described previously (Jivan, A., Earnest, S., Juang, Y. C., & Cobb, M. H., 2009). In this screen yeast were transformed with a bait vector that contained ERK2 and active MEK1 (MEK1R4F), to phosphorylate and activate ERK2 in yeast. Binding of KIF2A to ERK2 co-expressed with MEK1R4F was nearly 3-fold stronger than to ERK2 alone, based on β-galactosidase activity (Fig. 2.1A). Recombinant His_6-ERK2 or His_6-pERK2 both bound GST-KIF2A, as did His_6-pERK1 (Fig. 2.1C). Addition of a non-hydrolyzable analog of ATP, adenylyl-imidodiphosphate (AMP-PNP), which stabilizes ATP binding proteins, enhanced ERK2-KIF2A binding (Fig. 2.1B).

For the majority of these studies we examined KIF2A in human bronchial epithelial cells (e.g., HBEC3, HBEC30, number designating different patients) immortalized by expression of CDK4 and telomerase (hTERT), yielding HBEC3KT, and in a derivative of these cells further manipulated by stable suppression of p53 alone (HBEC3KT53) or together with stable expression of active K-Ras^{G12V} (HBEC3KTRL53). The nomenclature and properties of these cells have been described in detail (Ramirez, R. D. et al., 2004; Sato, M. et al., 2006). To determine if pERK1/2-KIF2A binding can be detected in cells, we immunoprecipitated endogenous KIF2A from HBEC3KTRL53. ERK2 and to a lesser extent ERK1 were detected in KIF2A immunoprecipitates from the cytosol fraction (Fig. 2.1E). To determine if KIF2A and pERK1/2 display any

overlapping cellular localization, we stained for endogenous KIF2A and endogenous pERK1/2 in HBEC3KTRL53. The specificity of the KIF2A antibody for immunofluorescence was first validated by KIF2A knockdown with siRNA (Fig. 2.S1) and the specificity of pERK1/2 staining was validated through use of the small molecule inhibitor PD0325901 which, by inhibiting MEK1, blocks phosphorylation and activation of ERK1/2 (Fig. 2.5A, 2.5B, 2.6B). KIF2A and pERK1/2 were both observed on the leading edges of HBEC3KTRL53 with a Pearson coefficient of 0.36 (Fig. 2.1D), reflecting a substantial extent of co-localization. The co-localization also reflects the fact that both proteins are microtubule-associated.

Changes in KIF2A expression influence interphase microtubules. KIF2A depolymerase activity and its regulation in interphase cells has not been studied in depth. *KIF2A*$^{-/-}$ mice display abnormally long collateral branches, suggesting that KIF2A may also be a developmentally important neuronal microtubule depolymerase (Jang, C. Y., Coppinger, J. A., Seki, A., Yates, J. R., III, & Fang, G., 2009). The fly ortholog, Klp10, depolymerizes microtubules in interphase cells in association with KLP59C, the KIF2C ortholog (Ems-McClung, S. C. & Walczak, C. E., 2010). To determine the actions of KIF2A on interphase microtubules, we expressed human KIF2A in HeLa cells and observed that staining of α-tubulin was diminished in cells (Fig. 2.4A). Similarly, in HBEC3KT cells overexpression of KIF2A destabilized microtubules, particularly depleting the microtubule polymers at the microtubule organizing center (MTOC) (Fig. 2.4A). Conversely, knockdown of KIF2A in HBEC3KT and HBEC3KTRL53 by siRNA resulted in elongated microtubule polymers and cellular spreading, suggesting that KIF2A is required for microtubule retraction during interphase (Figure 2.4B).

ERK activity regulates cellular morphology and KIF2A localization. The ability of ERK1/2 to regulate microtubule dynamics is believed to contribute to the invasive phenotype in cancer. For example, previously it was shown that microtubules become less stable in fibroblasts expressing mutant active H-Ras, an effect blocked with the MEK1 inhibitor PD98059 (Harrison, R. E. & Turley, E. A., 2001). To evaluate the idea the morphological effects of ERK1/2 may be mediated in part through KIF2A, we inhibited ERK1/2 in both HBEC3KT and HBEC3KTRL53 by treatment with PD0325901. We observed a change in morphology of both cell types, but a more drastic change in HBEC3KTRL53 that resulted in flattening of these cells (Fig. 2.5). The more obvious phenotypic difference in HBEC3KTRL53 is most likely due to the aberrant activation of the ERK pathway that has initially transformed their morphology and is highly dependent on the constitutive activation of the pathway (Zaganjor, E, et al., in preparation). Along with flattening of the cells, we observed elongated microtubules reminiscent of KIF2A knockdown cells (Fig. 2.5A, 2.5B, 2.6A). Inhibition of pERK1/2 activity resulted in relocalization of KIF2A, from perinuclear, nuclear, and plasma membrane staining, to a more uniform distribution. Inhibiting ERK1/2 only affected KIF2A localization during interphase; we did not observe any change in KIF2A localization in metaphase cells upon inhibition of pERK1/2 activity in HeLa cells, suggesting that prolonged suppression of pERK1/2 does not interfere with functions of KIF2A during cell division (Fig. 2.6B).

We also observed that KIF2A localized to lamellipodial protrusions, with enhanced enrichment in HBEC3KTRL53 as compared to HBEC3KT (Fig. 2.5A, 2.5B). ERK is known to regulate actin cytoskeleton dynamics at leading edges to promote

migration (Mendoza, M. C. et al., 2011). We hypothesized that continuous ERK1/2 activation may be responsible for KIF2A localization at leading edges where it may regulate microtubule dynamics. To test this hypothesis we treated HeLa cells with PD0325901 or vehicle for a shorter time (6 hr) and counted cells that exhibited KIF2A localization at leading edges. KIF2A localized to leading edges in 66% of vehicle-treated cells and in only 18% of PD0325901-treated cells (Fig 2.S4). We observed a similar KIF2A distribution pattern in a HBEC30KT after treatment with the PD compound for only 4 hr (Fig. 2.6C). Furthermore, in cells treated with PD for only 4-6 hr, microtubules are not elongated, indicating that KIF2A is relocalized prior to major cytoskeletal rearrangements.

Inhibition of ERK activity causes a decrease in KIF2A amounts in cells. To examine possible mechanisms by which ERK1/2 affect KIF2A, we determined whether or not prolonged MAPK pathway activation had any effect on KIF2A expression, we compared its behavior in HBEC3KT to that in HBEC3KTRL53. Immunoblotting analysis revealed increased KIF2A expression in cells with oncogenic K-Ras^{G12V} compared to HBECs (Fig 2.3A). Inhibition of ERK1/2 by exposure of cells to the MEK1/2-selective inhibitor PD0325901 for 72 hr, or knockdown of ERK1/2 both with and without addition of 10 nM PD0325901 for 48 hr decreased KIF2A expression by approximately 30% (Fig 2.3A, 2.3C). To determine if inhibition of pERK1/2 has an effect on KIF2A mRNA we treated HBEC3KTRL53 for 2 days with PD0325901. KIF2A mRNA as determined by quantitative polymerase chain reaction (qRT-PCR) also decreased with reduced ERK1/2 activity (Fig. 2.3D, 2,S3). On the other hand, there was less KIF2A mRNA present in HBEC3KT and HBEC3KT53; the reduction upon treatment with PD0325901, however,

did not reach statistical significance (Fig. 2.S3). To test whether inhibition of other important growth-regulatory pathways affected KIF2A expression, cells were treated with rapamycin to inhibit mTOR or wortmannin to inhibit PI3K and compared to effects of PD0325901. These inhibitors caused small to insignificant changes in KIF2A expression (Fig. 2.3B).

KIF2A is an ERK1/2 substrate. An *in vitro* kinase assay showed that KIF2A was indeed a substrate of both pERK2 and pERK1 (Fig. 2.2A,B). *In silico* prediction of consensus ERK1/2 phosphorylation motifs on KIF2A suggested T78 as the major site (Obenauer, J. C., Cantley, L. C., & Yaffe, M. B., 2003). Phosphorylation of this residue was also found through proteomic studies (Hornbeck, P. V. et al., 2012). T78 lies in a portion of KIF2A that is thought to be important for its localization, distant from segments of the protein involved in microtubule binding or depolymerization. This region is also not highly conserved among the related kinesin 13 family members. Mutation of T78A reduced phosphorylation by pERK2 by 50% (Fig. 2.2C), suggesting that T78 is a major site of phosphorylation. Three additional in vitro sites were also identified by mass spectrometry (Fig. 2.S2); however, these sites were not found in KIF2A immunoprecipitated from cells.

We tested potential effects of ERK1/2 phosphorylation on KIF2A microtubule depolymerizing activity by expressing KIF2A wild type, T78A and the potential phosphomimetic mutant KIF2A T78E in cells. Both mutants induced microtubule depolymerization comparable to that caused by wild type KIF2A (Fig. 2.4C), consistent with the idea that ERK1/2 phosphorylation does not affect KIF2A depolymerizing

activity. On the other hand, heterologously expressed KIF2A did not localize like the endogenous protein; thus, effects of mutants on localization could not be evaluated.

Because active Ras and ERK1/2 promote survival of transformed cells, we examined the effect of wild type KIF2A and T78 mutants on cleavage of poly-ADPribose polymerase (PARP). Expression of wild type KIF2A and KIF2A T78A resulted in PARP cleavage (Fig. 2.4D). On the other hand, expression of KIF2A T78E even at higher levels than wild type KIF2A did not result in detectable cleavage of PARP, revealing a functional effect of ERK2 phosphorylation.

Discussion

Our studies suggest that KIF2A may be important in morphological changes that may facilitate cell migration by drawing the cell towards leading edge through its depolymerase activity or by promoting local cytoskeletal rearrangements. Enhancing the localization of KIF2A to the leading edge of cells appears the most significant effect of ERK1/2 on this kinesin. The fraction of KIF2A at the leading edge of cells during interphase is substantially reduced following treatment with the MEK inhibitor, which has no effect on the localization of KIF2A during mitosis. Prolonged inhibition of ERK1/2 causes morphological changes in cells that are reminiscent of those resulting from KIF2A knockdown. Of course, some of the morphological alteration may also be due to loss of effects of ERK1/2 on MAPs and other microtubule regulatory elements. However, relatively brief ERK inhibition, is sufficient to remove much of the KIF2A from the leading edge prior to causing substantial morphological changes, consistent with

an appropriate temporal relationship for a contribution of KIF2A to actions of ERK1/2 on cell morphology.

The control of KIF2A function and cellular activity is intertwined on many levels with the MAPK cascade. Multiple lines of evidence, some direct and some indirect, support the conclusion that the proteins are linked functionally. Co-immunoprecipitation and co-localization can be detected in cells. The ability of both proteins to bind microtubules suggests they will be in proximity, enhancing the likelihood of potential regulatory events. KIF2A is phosphorylated on a site that has been identified through proteomic analysis of human mitotic spindle proteins. This site is not conserved in KIF2C, the most closely related family member and lies outside microtubule binding and depolymerizing regions. A phosphomimetic substitution of the major ERK1/2 site did not induce apoptosis which is usually associated with KIF2A overexpression, demonstrating a functional consequence of ERK1/2 phosphorylation of KIF2A. The amount of KIF2A protein in cells increases and decreases by approximately 30% with ERK1/2 activity and is paralleled by changes in KIF2A mRNA, suggesting that ERK1/2 have a modest effect on KIF2A transcription or stability of its mRNA.

KIF2A $^{-/-}$ mice display abnormally long collateral branches, suggesting that KIF2A is a developmentally important neuronal depolymerase that acts as cells extend processes (Homma, N. et al., 2003). During the preparation of this manuscript, Noda et al. published work showing interphase regulation of KIF2A in neuronal cells by phosphatidylinositol 4-phosphate 5-kinase alpha, PIP5 kinase α (Noda, Y. et al., 2012). The *in vitro* microtubule depolymerase activity of KIF2A was enhanced in the presence of the lipid kinase and the kinase was shown to interact with neck region of KIF2A. It

will be important to understand the physiological contexts under which distinct kinases regulate KIF2A and to characterize how interactions, phosphorylations, and localization are integrated into proper KIF2A function during interphase.

F1

A.

Clone	pERK2	ERK2
KIF2A	0.140	0.049
Synapsin II	0.075	0.005
RSP3	0.025	0.010

B.

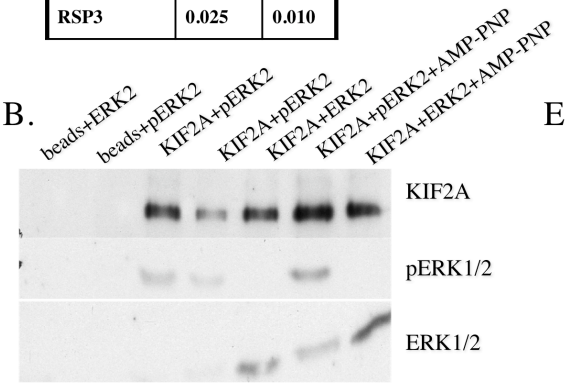

C.

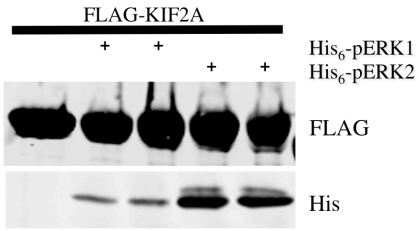

D.

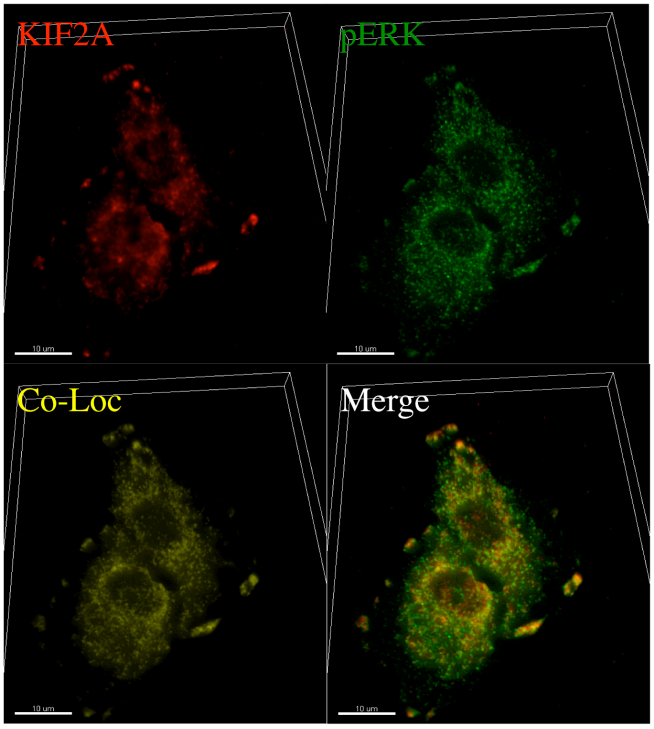

E.

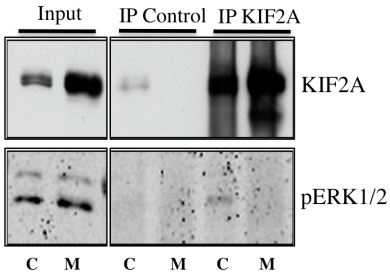

Figure 2.1. ERK1/2 interacts with KIF2A. (A) Top interactors from a β-galactosidase activity assay for a yeast two-hybrid screen that utilized pERK2 (active MEK1 (MEK1R4F) and ERK2) or ERK2 as bait vectors and fetal mouse brain cDNA library as prey. Other proteins identified in the screen were radial spoke protein 2 and synapsin 2 (Jivan, A., Earnest, S., Juang, Y. C., & Cobb, M. H., 2009). (B) GST or GST-KIF2A were immobilized on glutathione-agarose beads and incubated with His_6-ERK2 or His_6-pERK2 in the presence or absence of AMP-PNP. The associated ERK2 and pERK2 proteins were resolved by electrophoresis and detected by immunoblotting with pERK1/2 and ERK1/2 antibodies. (C) FLAG-KIF2A associates with both His_6-ERK1 and His_6-ERK2 in an *in vitro* pulldown assay. (D) Immunostaining of endogenous KIF2A (red) and pERK1/2 (green) HBEC3KTRL53. The colocalization channel was generated by Imaris software and Pearson's coefficient in co-localized volume was determined to be 0.36. (E) KIF2A was immunoprecipitated from HBEC3KTRL53 and co-precipitating pERK1/2 proteins were detected by immunoblotting. Immunoprecipitation with normal rabbit IgG was used as a negative control.

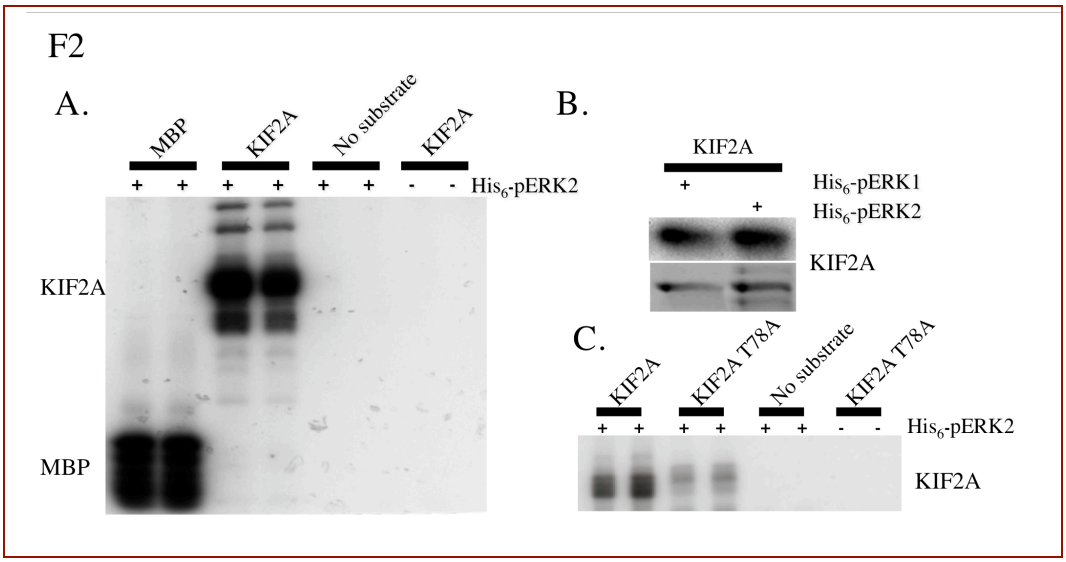

Figure 2.2. ERK2 phosphorylates KIF2A. (A) Purified recombinant His_6-pERK2 was used in an *in vitro* kinase assay with GST-KIF2A as a substrate. A representative autoradiogram is shown. (B) Bacterially expressed and purified FLAG-KIF2A was used in an *in vitro* kinase assay with His_6-pERK1 and His_6-pERK2. Autoradiogram (top) and coommassie stained gel (bottom) show KIF2A phosphorylation and expression. (C) GST-KIF2A or GST-KIF2A T78A were used as substrates in an *in vitro* kinase reaction with purified, recombinant His_6-pERK2. Mutating T78 significantly reduced ^{32}P incorporation.

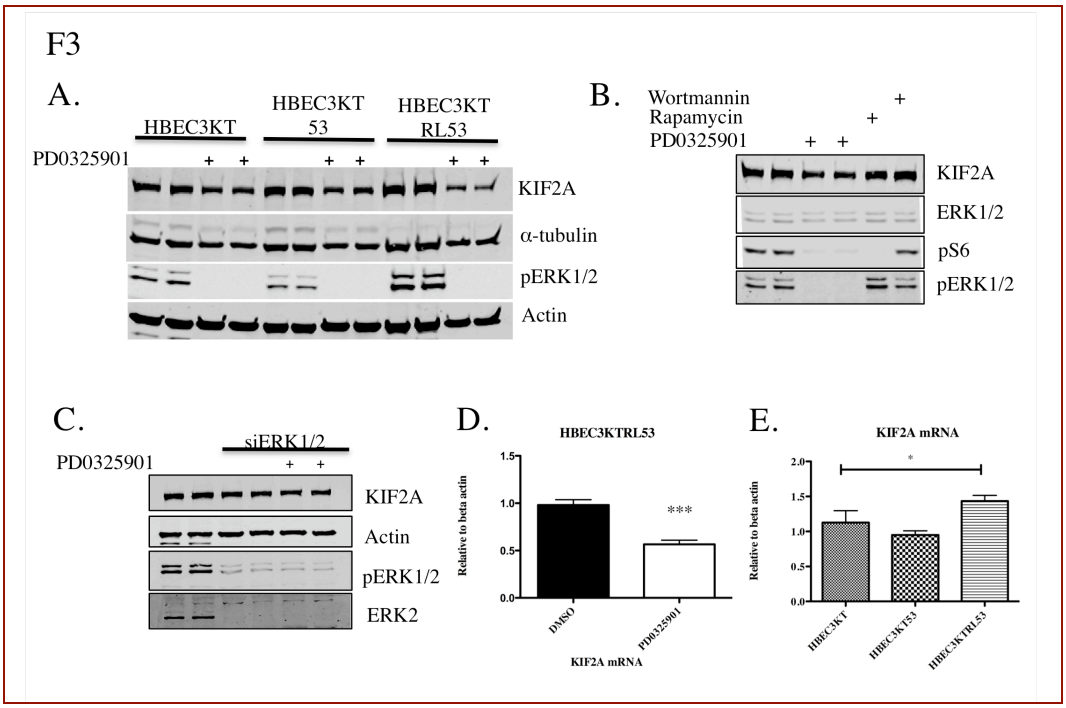

Figure 2.3. ERK activity positively regulates KIF2A expression. (A) HBEC3KT, HBEC3KT53 and HBEC3KTRL53 cells were treated for 72 hr with 1 μM PD0325901. 35 μg whole cell lysates resolved on gels and immunoblotted with designated antibodies, detected by Licor Odyssey infrared system. (B) HBEC3KT were treated with 100 nM rapamycin, 50 nM wortmannin or 1 μM PD0325901 for 72 hr. (C) HBEC3KTRL53 transiently transfected with siControl or siERK1/2 were treated with 10 nM PD0325901 or DMSO for 48 hr. (D) RNA was isolated from HBEC3KTRL53 cells and Kif2A gene expression by measured by qPCR after treatment with 1 μM PD0325901 for 48 hr; data from three independent experiments. Statistical analysis was performed by t-test of control versus treatment; p-value 0.0301 in an unpaired t test. (E). RNA was isolated from HBEC3KT, HBEC3KT53 and HBEC3KTRL53. Kif2A gene expression was

measured by qPCR. P value for this experiment was 0.045 in an ANOVA (one-way analysis of variance) analysis.

F4

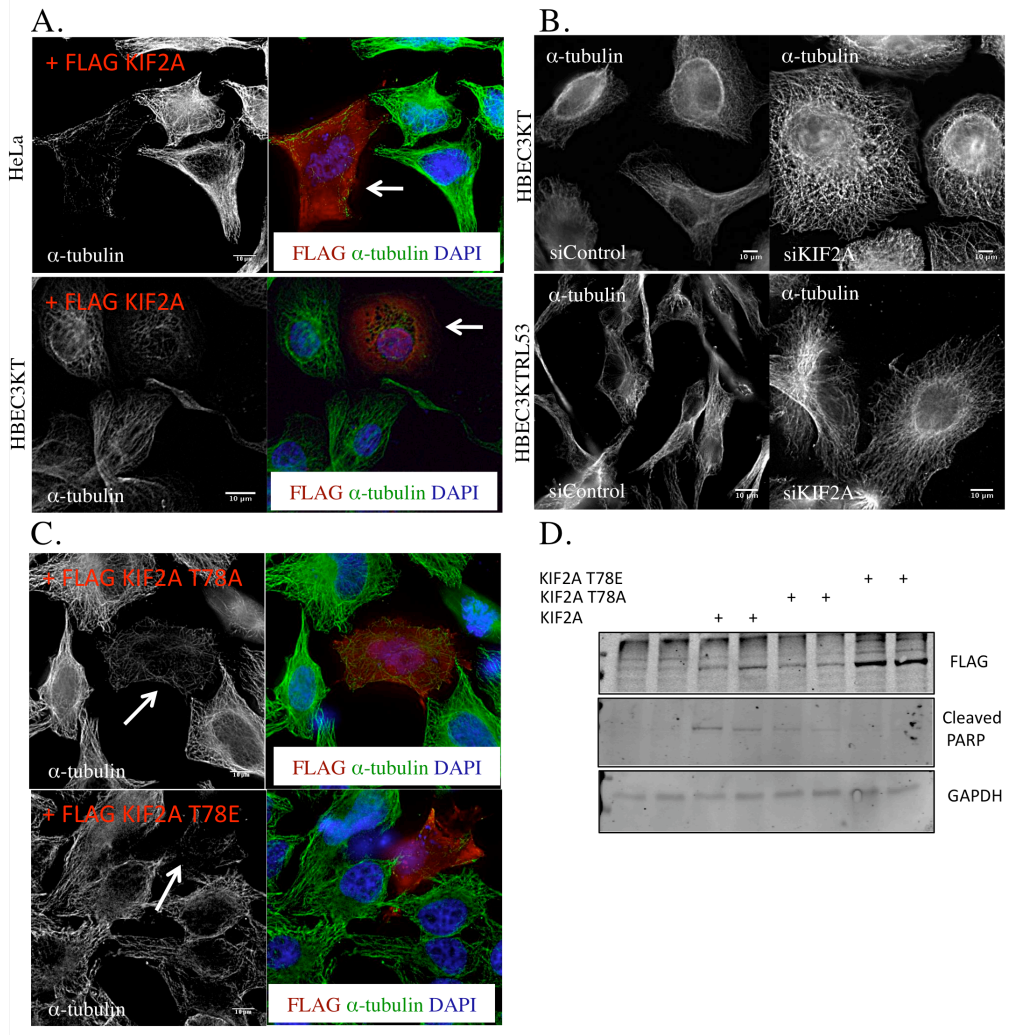
A.
HeLa
+ FLAG KIF2A
α-tubulin
FLAG α-tubulin DAPI
HBEC3KT
+ FLAG KIF2A
α-tubulin
FLAG α-tubulin DAPI
B.
HBEC3KT
α-tubulin
siControl
α-tubulin
siKIF2A
HBEC3KTRL53
α-tubulin
siControl
α-tubulin
siKIF2A
C.
+ FLAG KIF2A T78A
α-tubulin
FLAG α-tubulin DAPI
+ FLAG KIF2A T78E
α-tubulin
FLAG α-tubulin DAPI
D.
KIF2A T78E + +
KIF2A T78A + +
KIF2A + +
FLAG
Cleaved PARP
GAPDH

Figure 2.4. KIF2A regulates interphase microtubules. (A). FLAG-KIF2A was expressed in HeLa (top) or HBEC3KT cells (bottom). By immunofluorescence we detected FLAG-KIF2A (red), α-tubulin (green) and DAPI (blue). (B) Immunostaining of α-tubulin after 96 hour transfection with control (left) or KIF2A siRNA (right) in HBEC3KT (top) or HBEC3KTRL53 (bottom). (C) FLAG-KIF2A T78A (top) or FLAG-KIF2A T78E (bottom) were expressed in HeLa cells. By immunofluorescence we detected FLAG (red), α-tubulin (green) and DAPI (blue). (D) We expressed FLAG-KIF2A, FLAG-KIF2A T78A and FLAG-KIF2A T78E in HBEC3KT cells, Immunoblotting of the indicated proteins is shown.

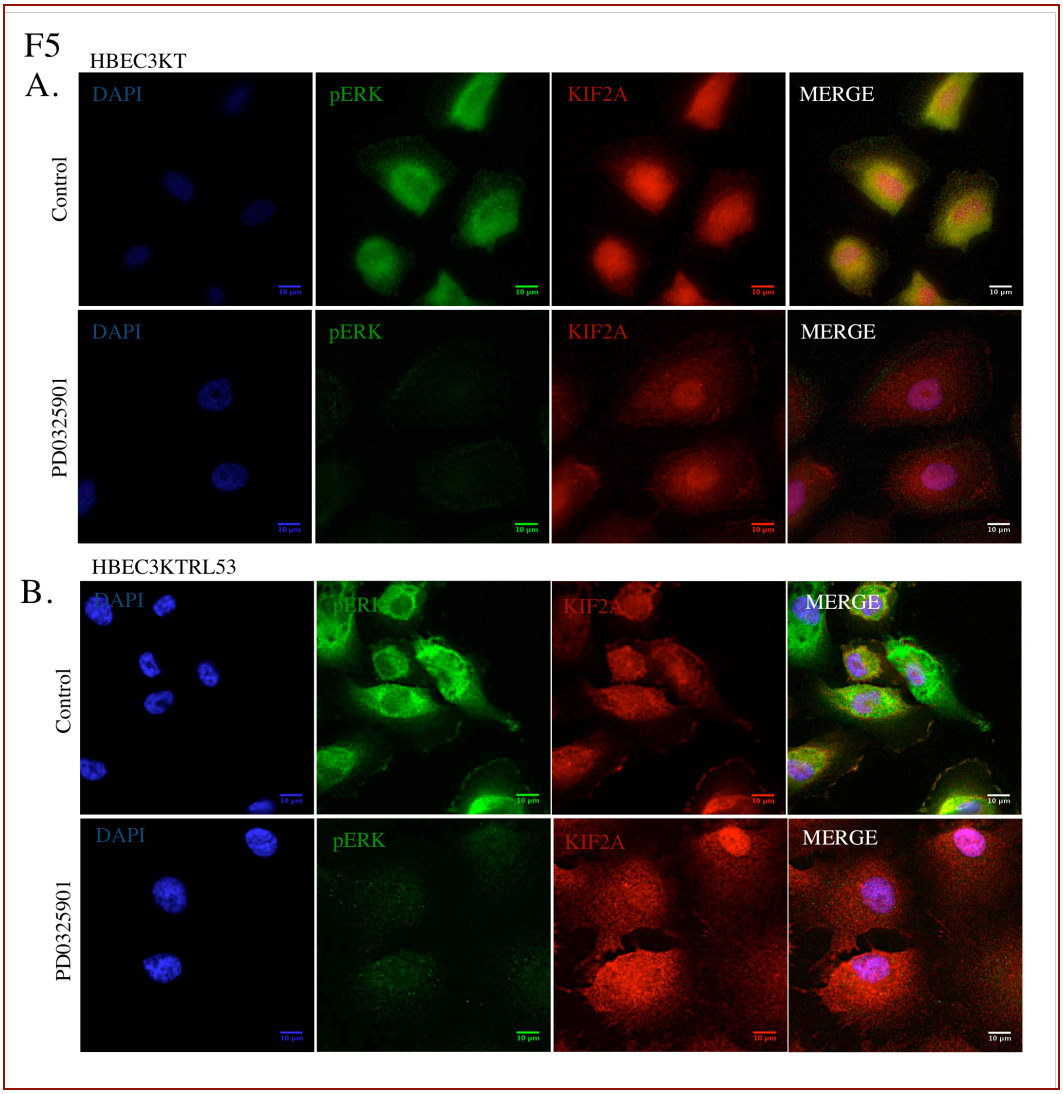

Figure 2.5. Prolonged ERK1/2 inhibition affects KIF2A localization in interphase cells. (A) Immunofluorescence of HBEC3KT cells or (B) HBEC3KTRL53 cells treated with 10 nM PD0325901 for 2 days show a diffuse pattern of KIF2A localization (red) as compared to the control cells in which KIF2A is enriched in the perinuclear region. pERK1/2 (green); DAPI (blue).

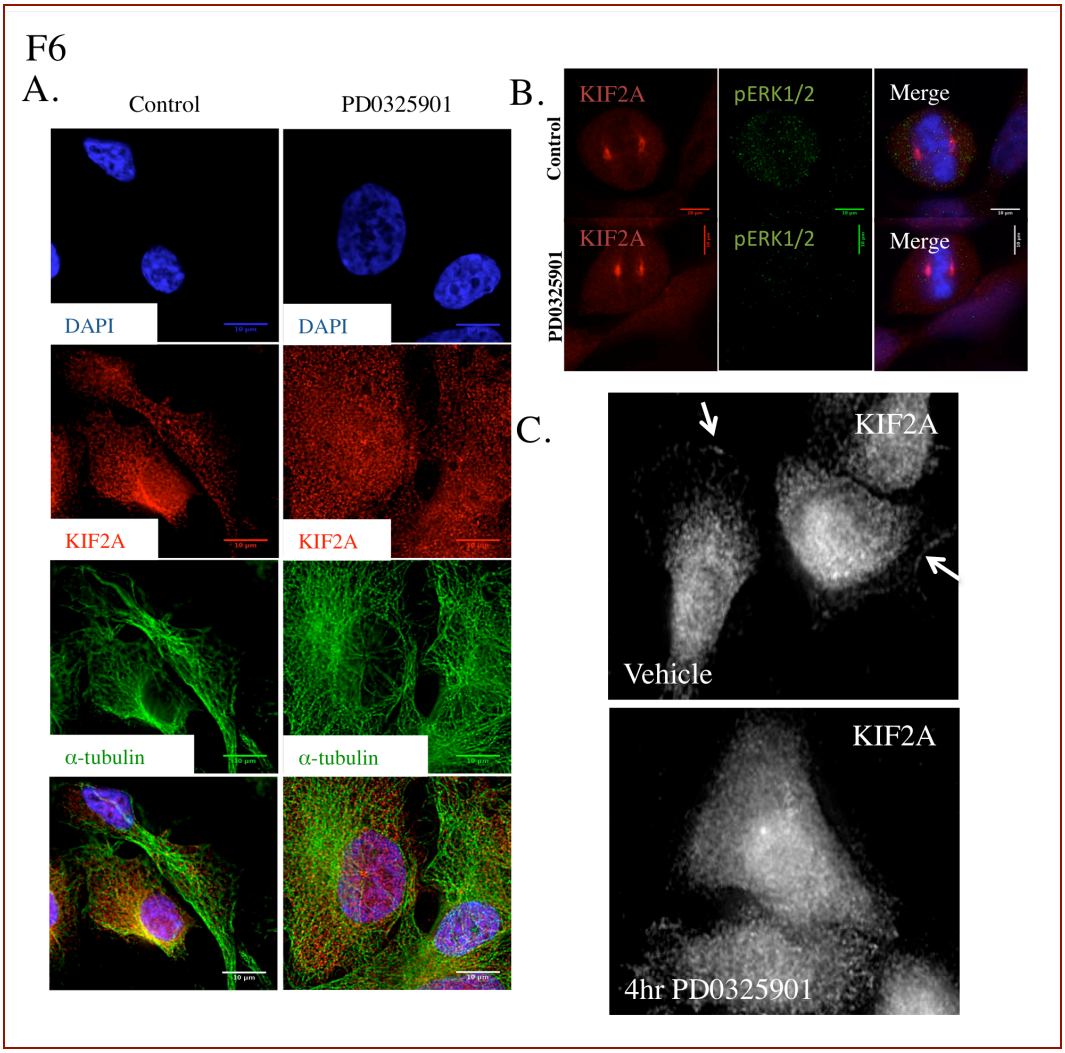

Figure 2.6. pERK1/2 regulate KIF2A localization in interphase but not mitosis. (A) HBEC3KTRL53 cells were treated with 10 nM PD0325901 for 2 days and immunostained with KIF2A (red) and α-tubulin (green) DAPI (blue). (B) HeLa cells were treated with 100 nM PD0325901 for 24 hr and immunostained with KIF2A (red) and pERK1/2 (green). (C) HBEC30KT cells with treated with 100 nM PD0325901 for 4 hr and immunostained with α-KIF2A.

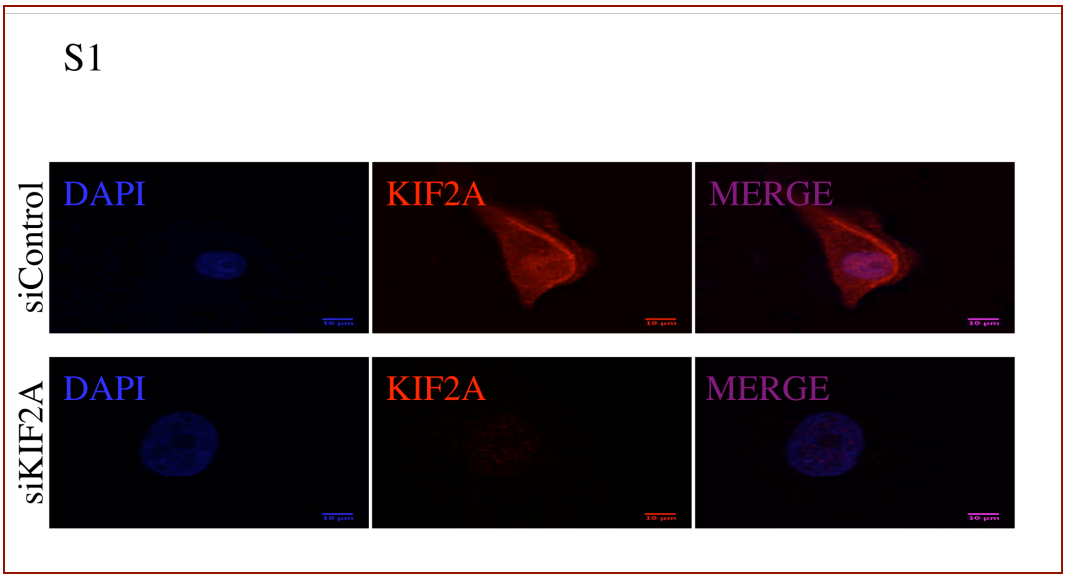

Figure 2.S1. Specificity of the KIF2A antibody for immunofluorescence. Knockdown of KIF2A or non-targeting control by siRNA in HBEC3KT. Immunostaining with antibodies to KIF2A (red) and DAPI (blue).

Figure S2. Annotated spectra of KIF2A phosphorylation residues identified by MS

Annotated Spectrum (Click for details)	Modification Assigment	PTM Score	ModLS Score
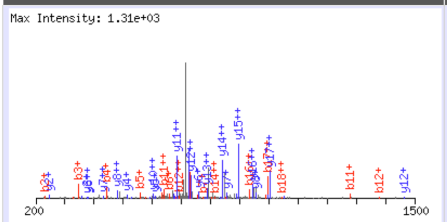	DLDVITIPSKDVVMVHEPK 1 x Oxidation (M) 1 x Phospho (ST) **Search Engine Result**	130	32
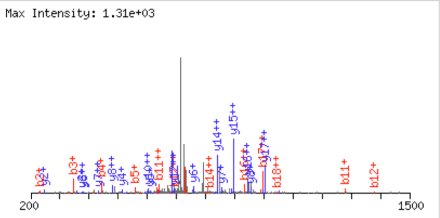	DLDVITIPSKDVVMVHEPK 1 x Oxidation (M) 1 x Phospho (ST)	98	-32

Figure S2. Annotated spectra of KIF2A phosphorylation residues identified by MS

Annotated Spectrum (Click for details)	Modification Assigment	PTM Score	ModLS Score
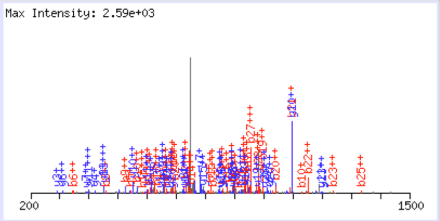	ARPSQFPEQSSSAQQNGSVSDIS<u>P</u>VQAAK 1 x Phospho (ST) **Search Engine Result**	156	72
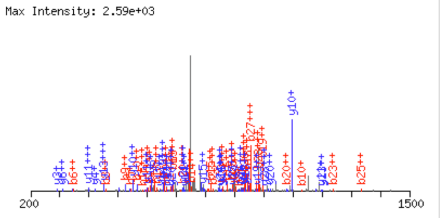	ARPSQFPEQSSSAQQNGSVS<u>D</u>ISPVQAAK 1 x Phospho (ST)	84	-72
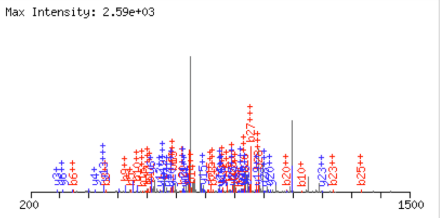	ARPSQFPEQSSSAQQNGS<u>V</u>SDISPVQAAK 1 x Phospho (ST)	41	-115
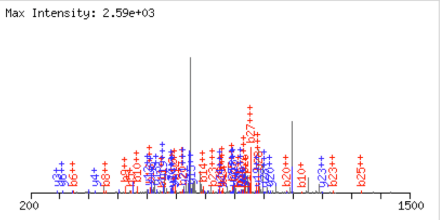	ARPSQFPEQS<u>S</u>SAQQNGSVSDISPVQAAK 1 x Phospho (ST)	31	-125

Figure S2. Annotated spectra of KIF2A phosphorylation residues identified by MS

Annotated Spectrum (Click for details)	Modification Assigment	PTM Score	ModLS Score
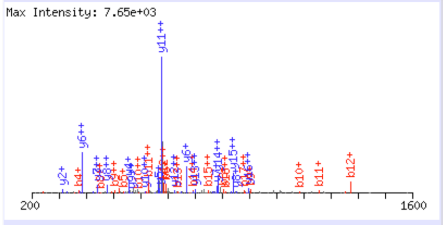	GSLDYRPLTTADPIDEHR 1 x Phospho (ST) **Search Engine Result**	187	36
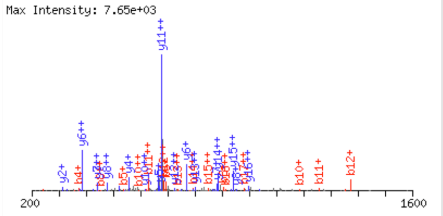	GSLDYRPLTTADPIDEHR 1 x Phospho (ST)	151	-36
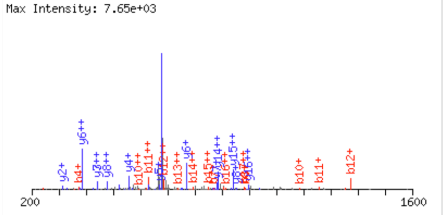	GSLDYRPLTTADPIDEHR 1 x Phospho (Y)	115	-72
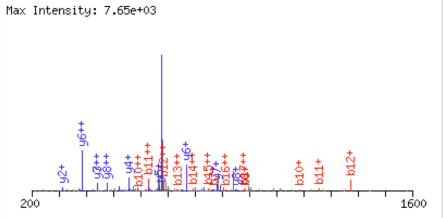	GSLDYRPLTTADPIDEHR 1 x Phospho (ST)	70	-117

Figure 2.S2. Mass spectrometry for KIF2A residues phosphorylated by ERK2 *in vitro*. Using mass spectrometry, we identified 3 peptides that were phosphorylated on KIF2A by pERK2: DLDVITIPS(ph)KDVVMVHEPK, ARPSQFPEQSSSAQQNGSVSDIS(ph)PVQAAK and GSLDYRPLTT(ph)ADPIDEHR. In each case the localization of the phosphorylation site was confirmed by the ModLS algorithm in CPFP and manual inspection, based on an unbroken series of b or y fragment ions across the phosphorylation site.

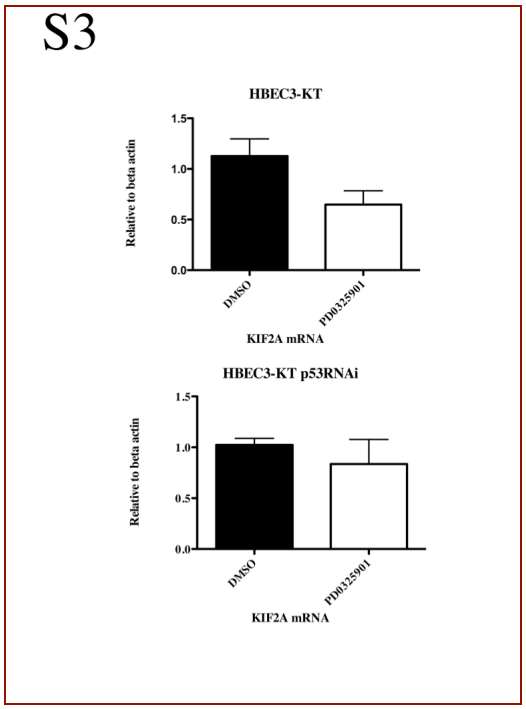

Figure 2.S3. Effect of ERK1/2 inhibition on Kif2A mRNA. RNA was isolated from HBEC3KT and HBEC3KT53 cells and Kif2A gene expression by measured by qPCR after treatment with 1 μM PD0325901 for 48 hrs; data from three independent experiments. Statistical analysis was performed by t-test of control versus treatment; p-value 0.0533 in HBEC3KT and 0.4795 in HBEC3KT53 in an unpaired t test.

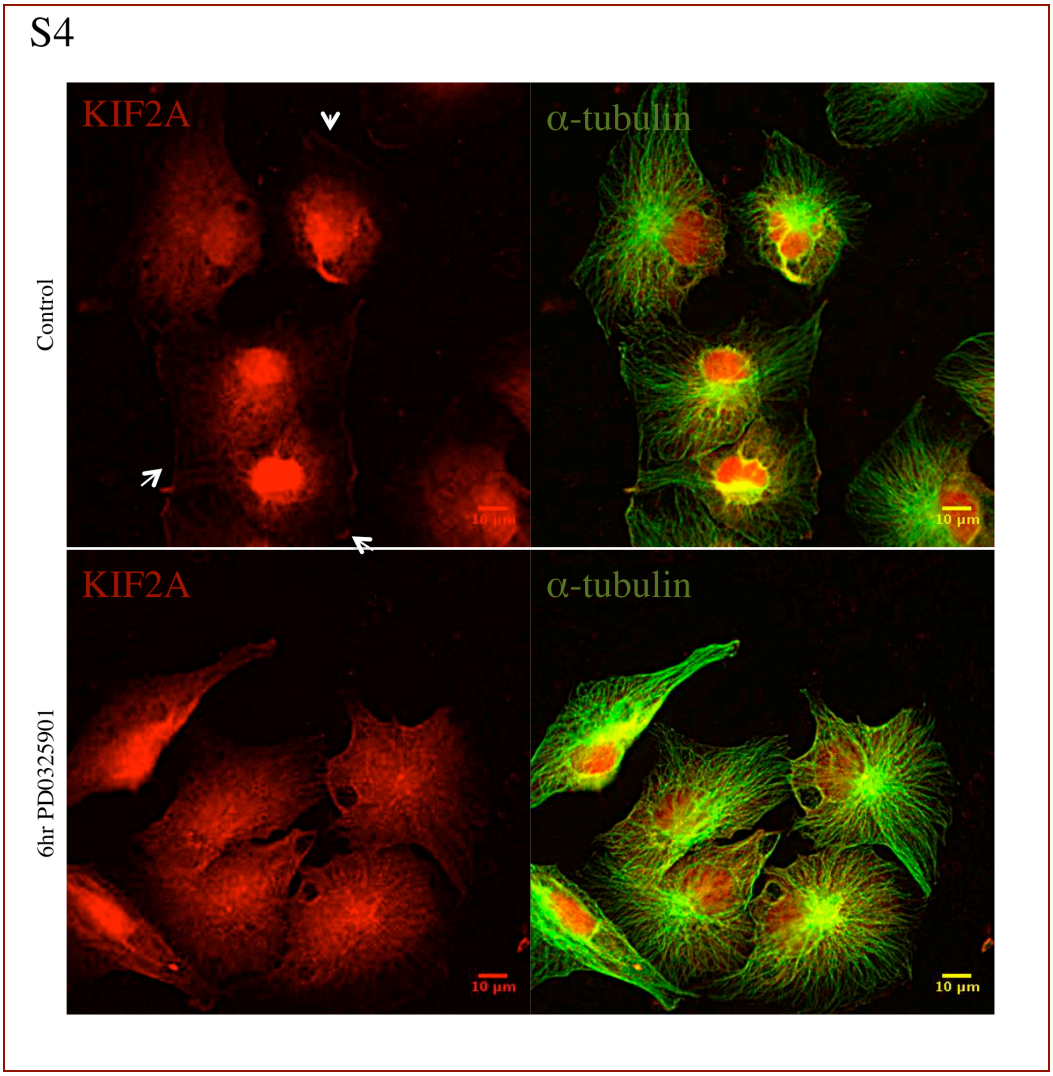

Figure 2.S4. Short term inhibition of ERK1/2 affects KIF2A localization. HeLa cells were treated with 100nM PD0325901 for 6 hrs. Immunostaining with KIF2A (red) and α-tubulin (green).

References

1 Kessner Det al. (2008) ProteoWizard: open source software for rapid proteomics tools development. *Bioinformatics* 24:2534-2536.

2 Trudgian DCet al. (2010) CPFP: a central proteomics facilities pipeline. *Bioinformatics* 26:11311132.

3 Craig R Beavis RC (2004) TANDEM: matching proteins with tandem mass spectra. *Bioinformatics* 20:1466-1467.

4 Geer LYet al. (2004) Open mass spectrometry search algorithm. *J Proteome Res* 3:958-964.

5 Magrane M Consortium U (2011) UniProt Knowledgebase: a hub of integrated protein data. *Database (Oxford)* 2011:bar009

6 Elias JE Gygi SP (2007) Target-decoy search strategy for increased confidence in large-scale protein identifications by mass spectrometry. *Nat Methods* 4:207-214.

7 Keller Aet al. (2005) A uniform proteomics MS/MS analysis platform utilizing open XML file formats. *Mol Syst Biol* 1:2005

8 Olsen JV Mann M (2004) Improved peptide identification in proteomics by two consecutive stages of mass spectrometric fragmentation. *Proc Natl Acad Sci U S A* 101:13417-13422.

9 Olsen JVet al. (2010) Quantitative phosphoproteomics reveals widespread full phosphorylation site occupancy during mitosis. *Sci Signal* 3:ra3

CHAPTER THREE

Ras regulates kinesin 13 family members to promote cancer migration

Abstract

We show that expression of the microtubule depolymerizing kinesin KIF2C is induced by transformation of immortalized human bronchial epithelial cells by expression of K-Ras^{G12V} and knockdown of p53. Further investigation demonstrates that this is due to the K-Ras/ERK1/2 MAPK pathway, as loss of p53 had little effect on KIF2C expression. In addition to KIF2C, we also found that the related kinesin KIF2A is modestly upregulated in this model system; both proteins are expressed more highly in many lung cancer cell lines compared to normal tissue. As a consequence of their depolymerizing activity, these kinesins increase dynamic instability of microtubules. Depletion of either of these kinesins impairs the ability of cells transformed with mutant K-Ras to migrate and invade matrigel. However, depletion of these kinesins does not reverse the epithelial-mesenchymal transition caused by mutant K-Ras. Our studies indicate that increased expression of microtubule destabilizing factors can occur during oncogenesis to support enhanced migration and invasion of tumor cells.

Introduction

The Ras family of small GTP binding proteins are essential signaling components that transfer information received from the extracellular environment to elicit

responses in the cell with the potential to promote differentiation, proliferation, and survival. Ras proteins cycle between the GDP-bound (inactive) and GTP-bound (active) states. Oncogenic Ras mutations such as V12 are resistant to down-regulation by GTPase activating proteins (GAPs), and as a result, remain constitutively in the active state, causing persistent activation of Ras-dependent, downstream effector pathways.

Activating mutations in Ras proteins are present in about 20% of human cancers, with mutations in K-Ras accounting for nearly 85% of the total (Downward, J., 2003). In non-small cell lung cancers (NSCLC), K-Ras is mutated in 15-20% of cases, with highest mutation frequency in lung adenocarcinoma (20%-30%) (Sekido, Y., Fong, K. M., & Minna, J. D., 2003). Epithelial cells expressing mutant K-Ras undergo dramatic morphological changes; they often lose typical epithelial morphology and contact inhibition and become irregularly shaped, consistent with epithelial to mesenchymal transition (EMT). Supporting this idea, morphological changes in certain cell lines can be reverted by blocking pathways downstream of Ras, for example, with farnesyltransferase inhibitors, Anthrax lethal factor, or combinations of kinase inhibitors (Suzuki, N., Del, Villar K., & Tamanoi, F., 1998; Perucho, M. et al., 1981; Duesbery, N. S. et al., 2001; Fukazawa, H. & Uehara, Y., 2000), flattening cells and restoring contact inhibition.

KIF2C, the mitotic centromere-associated kinesin (MCAK), is a kinesin-13 family member which depolymerizes microtubules in an ATP-dependent manner. KIF2C has multiple roles in mitosis from spindle assembly at the centrosome to microtubule turnover at kinetochores (Rogers, G. C. et al., 2004). The related kinesin, KIF2A, is important for formation of bipolar spindles during cell division as well as for suppression

of collateral branch extension in neurons; both functions are mediated through microtubule depolymerization catalyzed by KIF2A (Homma, N. et al., 2003; Ganem, N. J. & Compton, D. A., 2004). Because of their depolymerizing activity, these kinesins increase dynamic instability of microtubules. Few roles have been ascribed to either protein outside of mitosis. Although KIF2C is thought to be degraded after cell division, it has been implicated in microtubule dynamics during interphase and associates with plus end tips of microtubules (Moore, A. T. et al., 2005; Helenius, J., Brouhard, G., Kalaidzidis, Y., Diez, S., & Howard, J., 2006). KIF2A has also been implicated in organelle localization (Korolchuk, V. I. et al., 2011).

In this study, we find that oncogenic K-Ras-induced transformation of human bronchial epithelial cells (HBEC) lacking p53 is accompanied by changes in morphology affecting both microtubule and actin cytoskeletons. Therefore, we hypothesized that regulators of the cytoskeleton may in some way be altered in transformed cells. We find that the kinesin family proteins KIF2A and KIF2C, both destabilizing microtubules, are upregulated in cells that have been transformed with K-Ras^{G12V} and in a fraction of human cancer cell lines. Knocking down either KIF2A or KIF2C reduces the ability of K-Ras^{G12V}-expressing cells to migrate, suggesting that aberrant expression of these proteins during transformation can contribute to the migratory potential of cancer cells.

Materials and Methods

Cell Culture - Immortalized HBEC3KT, HBEC30KT and HBEC3KT53 cells were cultured in Keratinocyte serum free medium (KSFM) (Invitrogen) supplemented with 5

ng/mL epidermal growth factor and 50 μg/mL bovine pituitary extract according to manufacturer's recommendations. HBEC3KTR$_L$53 were cultured in RPMI-1640 medium supplemented with 5% heat-inactivated fetal bovine serum (vol/vol) and 2 mM L-glutamine. Cells were grown at 37°C in a humidified atmosphere of 5% CO_2. MDA-MB-231, HCC38, HCC1143, Htb126, and MCF7 cells were provided by M.A. White (Dept Cell Biology) and T47D and HCC1428 cells were provided by G.W. Pearson (Simmons Comprehensive Cancer Center, Dept Pharmacology). SUM149PT and SUM190PT cells were purchased from Asterand (Detroit, MI) and grown according to provider culture conditions. HCC1937 cells were a gift of A. Gazdar (Hamon Cancer Center, Dept Pathology). HME50 cells were derived from the non-cancerous breast tissue of a female diagnosed with Li-Fraumeni syndrome as previously described (Shay, J. W., Tomlinson, G., Piatyszek, M. A., & Gollahon, L. S., 1995). The missense p53 mutation (M133T) in HME50 was sequence verified. Breast cancer cell lines were cultured in Dulbecco's modified Eagle's medium or RPMI-1640 with 10% fetal calf serum. HME50 was cultured in serum-free conditions as described elsewhere (Shay, J. W., Van Der Haegen, B. A., Ying, Y., & Wright, W. E., 1993).

Microarray - Our cell line panel consists of 118 NSCLCs, 29 SCLCs, 30 HBECs (immortalized human bronchial epithelial cells), and 29 HSAECs (immortalized human small airway epithelial cells). All cell lines were DNA-fingerprinted and mycoplasma-tested. Total RNA (500 ng) was prepared using the RNeasy Midi kit (Qiagen, Valencia, CA) and checked for quality and concentration using the Bio-Rad Experion Bioanalyzer (Hercules, CA). cRNA labeling was done with Ambion Illumina TotalPrep RNA Amplification kit (IL1791). Amplified and labeled cRNA probes (1.5 ug) were

hybridized to Illumina HumanWG-6 V3 Expression BeadChip (BD-101-0203) overnight at 58 degree C, then washed, blocked and detected by streptavidin-Cy3 per manufacturer's protocol. After drying, the chips were scanned by Illumina iScan system. Bead-level data were obtained, and pre-processed using the R package mbcb for background correction and probe summarization (Ding, L. H., Xie, Y., Park, S., Xiao, G., & Story, M. D., 2008). Pre-processed data were then quantile-normalized and log-transformed. All array data are deposited on GEO (GSE32036).

siRNA - Cells were transfected for from 48 to 96 hr as indicated with dsRNA oligonucleotides using Lipofectamine RNAiMax according to manufacturer's protocol (Invitrogen). The following target sequences for KIF2A were used: GAAAACGACCACUCAAUAA (Thermo Scientific) and GACCCTCCTTCAAGAGATA (Thermo Scientific); KIF2C: GCAAGCAACAGGUGCAAGU (Thermo Scientific) and GGCAUAAGCUCCUGUGAAU (Thermo Scientific); Ras: GGAGGGCUUUCUUUGUGUA (Thermo Scientific); p53: GGAGAAUAUUUCACCCUUC (Thermo Scientific).

Immunofluorescence - Cells were washed with Tris-buffered saline (TBS); fixed with 4% paraformaldehyde (vol/vol) in TBS for 10 min; and washed twice for 5 min with TBS. Cells were permeabilized with 0.1% Triton X-100 for 5 minutes and washed twice with TBS. After incubation with 10% normal goat serum (vol/vol) at room temperature for one hr, cells were incubated with the indicated antibodies at 4 °C overnight. Cells were washed with TBS, incubated with Alexa fluor-conjugated secondary antibody at room temperature for one hr, washed with TBS, and imaged. Fluorescent Z-stacks (0.2 mm)

were acquired and deconvolved using the Deltavision RT deconvolution microscope. α-tubulin antibodies were from Sigma (T6199).

qRT-PCR - Cells were harvested and RNA was extracted using QuickRNA^{TM} (Zymo Research) according to the manufacturer's protocol. RNA was reverse transcribed using the iScript cDNA synthesis kit (BioRad). PCR reactions were performed with IQ SYBR Green Supermix (BioRad), and fluorescence was measured using a quantitative real-time thermocycler (ABI 7500). The following primer sets were used: KIF2C (sense 5'-CAGAACTCTTACAGCTTCTTCCC-3' and antisense 5'-CAGTGGACATGCGAGTGGA-3'); KIF2A (sense 5'-TGCAAATAGGGTCAAAGAATTG-3'and antisense 5'-TTGTTCACAAAGAAGTTTTAGATCAT-3'); KIF2B (sense 5' CTGAAACCCTTGAAGCCACAT-3' and antisense 5'-AGCAGGAGTATGGTCTCCAGG-3'); beta actin(5'-CATGTACGTTGCTATCCAGGC-3' and antisense 5'-CTCCTTAATGTCACGCACGAT-3'). Relative changes in gene expression were calculated by $2^{-\Delta Ct}$, where ΔCt= Ct(KIF2)-Ct(ActinB).

Cell harvest - Cells were washed twice with TBS and lysed on ice with in 50 mM HEPES, pH 7.5, 150 mM NaCl, 1.5 mM $MgCl_2$, 1 mM EGTA, 0.2 mM Na_3VO_4, 100 mM NaF, 50 mM β-glycerophosphate, 10% glycerol, 1% Triton X-100, 1.6 μg/ml aprotinin, 0.1 mM phenylmethylsulfonyl fluoride, and 10 μg/ml each of N^{α}-p-tosyl-L-lysine chloromethyl ketone, N^{α}-p-tosyl-L-arginine methyl ester, pepstatin A, and leupeptin. Lysates were frozen in N_2 (liquid) and thawed on ice, followed by centrifugation for 15 min at 16,000 × g in a microcentrifuge at 4 °C. Supernatants boiled

in Laemmli sample buffer (2% SDS, 10% glycerol, 5% β-mercaptoethanol, 0.01% bromphenol blue, 50 mM Tris-HCl) and subjected to SDS-PAGE and immunoblotting. Following antibodies were used: KIF2A (Abcam, 37005), KIF2C (Bethyl Laboratories, A300-807A), actin (Fisher Scientific, MAB1501MI), ERK1/2 (Boulton, T. G. & Cobb, M. H., 1991), pERK (Sigma, M8159), p53 (sc-126), Ras (Santa Cruz, sc-166691), E-cadherin (BD Transduction Laboratories, 610181), N-cadherin (BD Transduction Laboratories, 610920), pS6 (Cell Signaling, 5364).

Cell cycle analysis - HBECK3KTR$_L$53 were transfected with siRNA for 96 hr and collected for flow cytometry. Cells were trypsinized and collected by sedimentation at 1,000 x g. Cells were washed in 1X phosphate buffered saline (PBS) and fixed in 70% cold EtOH at -20° C overnight. Cells were washed in 1X PBS and stained with 0.4 ml of propidium iodide/RNase A 1 solution. DNA content was measured by flow cytometry with FACSCalibur (BD Biosciences), and data were analyzed using FlowJo. Cells harvested for immunoblot were washed with 1X PBS and harvested with Laemmli sample buffer. Samples were boiled for 2 min at 95° C, sonicated, and boiled again for 2 min at 95°C. Protein concentration was measured with BCA Protein Assay (Thermo Scientific Prod # 23235). Cell lysate protein (20 μg) were resolved on gels and processed for immunoblotting as above.

Migration Assays - The HBEC3KTR$_L$53 cell line was used for all migration assays. For the transwell migration assays $5x10^4$ cells were seeded 72 hr post-knockdown of indicated proteins, using Transwell permeable supports (Corning #3422). Cells were seeded in the top chamber in 5% FBS and allowed to migrate along a concentration gradient through a polycarbonate membrane with 8 μm pores to the bottom chamber containing medium

with 25% FBS. After 24 hr cells were fixed, stained (with 1% methylene blue, 1% borax solution), and counted. For invasion assays 1.5 x10^5 cells were imbedded in Growth Factor Reduced Matrigel in transwell permeable supports, 72 hr post-knockdown of indicated proteins. Cells were allowed to migrate for 48 hr across membranes with a gradient of 25 % serum in the bottom chamber. Cells were fixed, stained (with 1% methylene blue, 1% borax solution), and counted.

Results

Expression of oncogenic K-Ras^{G12V} increases expression of the microtubule depolymerases KIF2C and KIF2A.

We found that the microtubule depolymerizing kinesins KIF2C and to a lesser extent KIF2A were upregulated in a number of lung and breast cancer cell lines (Fig. 3.1A,E,F, S1A). Lung cell lines A549, Calu-6, H358, HCC515 and H1155 express K-Ras mutations; and we considered the possibility that mutant K-Ras might alter expression of these proteins. Because larger changes in KIF2C expression were noted, we first determined if increased expression of KIF2C can be caused by mutated K-Ras. To do this we used an immortalized human bronchial epithelial cell (HBEC) system that has been previously described (Sato, M. et al., 2006). HBEC from different patients (distinguished by a number) were immortalized by expression of human telomerase reverse transcriptase (hTERT) and CDK4, yielding HBEC3KT, HBEC30KT, etc. These immortalized cells were further altered by stable knockdown of p53 (HBEC3KT53). p53 is commonly mutated or lost in cancers, and loss of wild type p53 is required for HBEC

to bypass Ras-induced senescence (Parada, L. F., Land, H., Weinberg, R. A., Wolf, D., & Rotter, V., 1984; Sekido, Y., Fong, K. M., & Minna, J. D., 2003; Lundberg, A. S., Hahn, W. C., Gupta, P., & Weinberg, R. A., 2000). K-Ras^{G12V} was stably expressed in p53 knockdown cells yielding HBEC3KTR$_L$53. Expression of KIF2C, almost undetectable in HBEC3KT, was greatly increased in HBEC3KTR$_L$53 grown in serum-containing medium (Fig. 3.1B) (Sato, M. et al., 2013). By placing the cells in Earle's balanced salt solution (EBSS) and removing nutrients and growth factors to slow protein synthesis and energy utilization, we tested the stability of KIF2C. Even after 4 hr of starvation, KIF2C expression remained unaffected. An increase in KIF2A protein was also observed in the K-Ras^{G12V}-transformed cells, but of much smaller magnitude. The increase in KIF2C protein was paralleled by greatly increased KIF2C mRNA in HBEC3KTR$_L$53 compared to HBEC3KT (Fig. 3.1C), suggesting that transcription is enhanced by expression of mutant K-Ras. An increase in KIF2A mRNA expression observed in cells harboring oncogenic K-Ras reached only a low level of statistical significance (Fig. 3.1D). To determine if these results with a laboratory generated model system of mutant K-Ras-transformation might be representative of patient samples, we asked if KIF2C and KIF2A were upregulated in patient-derived cancer cell lines. Information was obtained from microarray studies that had been performed on 148 lung cancer lines and 59 normal lung cells. Statistically significant upregulation of KIF2C was noted in cancer lines compared to normal control cells (Fig. 3.1F); a less significant increase was also noted for KIF2A (Fig. 3.1E). No increase or even a small decrease in expression of KIF2B, a related kinesin 13 family member, was observed in the cancer cell lines (Fig. 3.S1B), consistent with the idea that these KIFs have different cellular functions (Manning, A. L. et al.,

2007). To compare effects of K-Ras mutants, we examined KIF2C expression in HBEC cells that harbor G12C, G12D or G12V K-Ras mutations in a p53 knockdown background. We found that cells expressing G12C or G12D are morphologically similar to HBEC3KT (Fig. 3.S2A,B). In contrast to cells expressing the G12V mutant, a comparable increase in expression of KIF2C was not detected (Fig. 3.2A). This may be due to the significantly lower expression of these K-Ras mutants relative to K-Ras^{G12V}. To determine if loss of K-Ras^{G12V} in HBEC3KTR$_L$53 was sufficient to decrease expression of KIF2C, K-Ras was depleted by siRNA. We found that KIF2C expression decreased to a level similar to that in HBEC3KT, indicating that constant expression of oncogenic K-Ras, even after morphological transformation has occurred, maintains elevated KIF2C expression (Fig. 3.2B). To evaluate the possibility that p53 also affected expression of KIF2C or KIF2A, p53 was transiently knocked down or overexpressed in the HBEC model cell lines. We observed a relatively small effect on expression of either KIF2 protein (Fig. 3.2C-E).

Expression of oncogenic K-Ras^{G12V} causes morphological changes that alter microtubule and actin cytoskeletons. Cells transformed with oncogenic K-Ras in the context of loss or mutation of p53 and grown in serum are morphologically altered from isogenic cells lacking mutant K-Ras. To examine the effect of oncogenic K-Ras transformation on the microtubule and actin cytoskeleton of HBECs, we compared the morphology of HBEC3KT, HBEC30KT (Fig. 3.S3), HBEC3KT53 and HBEC3KTR$_L$53 by immunofluorescence staining for actin and α-tubulin (Fig. 3.3A,B). HBEC3KT, HBEC30KT, and HBEC3KT53 appear larger and flatter than HBEC3KTR$_L$53. Ras-induced transformation caused inhibition of stress fiber formation (Sahai, E., Olson, M.

F., & Marshall, C. J., 2001); actin appeared less organized, consistent with the irregular cell morphology. HBEC3KTR$_L$53 had fewer microtubule polymers compared to HBEC3KT53, suggesting that microtubules may be more dynamic in cells expressing mutant K-Ras, as would be expected with elevated expression of microtubule depolymerizing kinesins. These changes are also consistent with EMT (see also Fig. 3.7D,E). Knocking down K-Ras from HBEC3KTR$_L$53 was sufficient to reverse much of the morphological change, restoring microtubule polymerization and organized actin stress fibers (Fig. 3.3C).

Signaling pathways downstream of Ras regulate morphological changes. Because ERK1/2 are known to regulate microtubule and actin dynamics and are activated downstream of Ras (Harrison, R. E. & Turley, E. A., 2001; Leinweber, B. D., Leavis, P. C., Grabarek, Z., Wang, C. L., & Morgan, K. G., 1999; Olsen, M. K., Reszka, A. A., & Abraham, I., 1998), we hypothesized that inhibition of the ERK1/2 pathway could also revert these phenotypes in HBEC3KTR$_L$53. Indeed, treatment of HBEC3KTR$_L$53 for 48 hr with 100 nM PD0325901, a MEK1/2-specific inhibitor, resulted in longer microtubules and reappearance of stress fibers (Fig. 3.4A), similar to effects of K-Ras knockdown. To demonstrate that prolonged exposure to this MEK inhibitor is not toxic to the cells, cells treated with PD0325901 for 48 hr were placed in fresh serum-containing medium for 30 min which activated ERK1/2 (Fig. 3.4B). Phosphatidylinositol 3-kinase (PI3K) is another important Ras effector that promotes cytoskeleton transformation changes in part through the small Rho family GTPase Rac (Kolsch, V., Charest, P. G., & Firtel, R. A., 2008). To determine if this Ras-activated, growth-promoting pathway is also required for these cytoskeletal changes, we inhibited the PI3K pathway with 10 μM

LY2094002. This PI3K inhibitor did not cause microtubule spreading or flattening of cells, but did elicit some shape changes such as further elongation (Fig. 3.4A). These data suggest the relative importance of the ERK1/2 pathway in influencing actin and microtubule cytoskeleton organization in this oncogenic Ras-transformed system. Because the cytoskeletal changes in the transformed system seemed to be mediated by ERK1/2, we evaluated the importance of this pathway for elevated KIF2C expression. Inhibition of ERK1/2 by exposure of cells to PD0325901 for 48 hr, but not with comparable treatment with a PI3K inhibitor, LY294002, decreased KIF2C protein in HBEC3KTR$_L$53 (Fig. 3.4C). Similar to inhibiting PI3K, inhibiting mTOR, another growth-promoting pathway, with the small molecule rapamycin did not affect KIF2C expression to the same extent as inhibition of ERK1/2 (Fig. 3.4D,E). Inhibition of ERK1/2 for 72 hr also reduced KIF2A protein by approximately 30% (Fig. 3.4F). Inhibition of MEK1/2 with PD0325901 significantly reduced KIF2C mRNA, not only in HBEC3KTR$_L$53 but also in cells that do not express mutant K-Ras, HBEC3KT and HBEC3KT53 (Fig. 3.5A-C). As was the case with KIF2A protein, KIF2A mRNA also decreased with reduced ERK1/2 activity (Fig. 3.5D-F); however, the reduction upon treatment with PD0325901 did not reach statistical significance in all cell lines as it did in HBEC3KTR$_L$53. Interestingly, inhibition of PI3K in HBEC3KT53 results in a significant upregulation of KIF2C mRNA (Fig. 3.5G-I). In contrast, a closely related kinesin 13 family protein, KIF2B was upregulated by MEK inhibition under the same circumstances, suggesting that functions of specific kinesin molecules are differentially sensitive to regulation through this pathway (Fig. 3.S4). KIF2B is also not upregulated in cancer lines (Fig. 3.S1B).

Changes in expression of KIF2C or KIF2A do not alter cell cycle progression in HBEC3KTR$_L$53. KIF2A and KIF2C have well defined but distinct roles in mitosis (Manning, A. L. et al., 2007). Because KIF2C and KIF2A were upregulated in cancer, we wondered if their functions in regulating the cell cycle were disturbed. Therefore, we examined the cell cycle profiles following individual knockdown of KIF2A or KIF2C (Fig. 3.6 A,B). DNA content was measured following depletion of kinesins for 96 hr to analyze cell cycle profiles. There appeared to be no difference in the number of cells in G2/M phase when cells were depleted of KIF2A or KIF2C. Unlike an earlier study suggesting a difference in mitotic index in U2OS cells (Ganem, N. J. & Compton, D. A., 2004), we did not observe mitotic accumulation of HBEC3KTR$_L$53 following knockdown of KIF2A or KIF2C. Under these conditions, residual KIF2A and KIF2C or other compensating proteins are apparently sufficient to prevent abnormalities.

KIF2A and KIF2C facilitate migration of transformed cells.

Microtubule dynamics have long been implicated in the migratory ability of cells (Vasiliev, J. M. et al., 1970; Liao, G., Nagasaki, T., & Gundersen, G. G., 1995). Therefore, we hypothesized that knockdown of KIF2A or KIF2C could have an effect on cell migration by disturbing microtubule dynamics. In HBEC3KTR$_L$53 we knocked down KIF2A, KIF2C or both using siRNA (Fig. 3.7C). We found that knockdown of either or both KIF2A and KIF2C reduced migration of HBEC3KTR$_L$53 through membranes compared to control cells (Fig. 3.7A). Knock down of these kinesins also reduced the ability of HBEC3KTR$_L$53 to invade through matrigel (Fig. 3.7B). HBEC3KT53 express E-cadherin exclusively. On the other hand, HBEC3KTR$_L$53 have lost E-cadherin and instead express N-cadherin. Depletion of either KIF2C or KIF2A

does not alter this pattern of cadherin expression. Thus, KIF2A or 2C knockdown did not reverse EMT caused by mutant K-Ras (Fig. 3.7D,E). Instead, loss of either or both KIF2A and KIF2C reduces the migration and invasiveness of cells transformed with oncogenic K-Ras.

Discussion

We find that KIF2C and to a lesser extent KIF2A, two related microtubule-depolymerizing kinesins, are upregulated in lung cancer cells and contribute to the ability of cells transformed with mutant K-Ras to migrate. A number of kinesins including KIF2A have been implicated in cancers either from cell-based studies or through cancer genome analysis, most in the context of their mitotic roles (Groth-Pedersen, L. et al., 2012; Tanuma, N. et al., 2009; Ahmed, S. M. et al., 2012; Yamashita, J. et al., 2012; Wang, C. Q. et al., 2010). Nearly four dozen human kinesins are known (Miki, H., Setou, M., Kaneshiro, K., & Hirokawa, N., 2001), making the delineation of their individual functions difficult at best. Some transport cargo on microtubules in a plus-end direction, and others transport cargo in a minus-end direction, while a smaller number, including KIF2C, KIF2A, and KIF2B, depolymerize microtubules increasing dynamic instability (Miki, H., Okada, Y., & Hirokawa, N., 2005). Why two of these related kinesins are recruited by K-Ras and the extent to which the actions of these depolymerases in K-Ras-transformed cells reflect on their physiological actions in normal cells are questions that remain to be answered.

The full transforming potential and tumor formation caused by mutant K-Ras depend on its activation of interacting downstream effector pathways. Activated K-Ras contributes to many properties of successful cancers; these include enhanced proliferation under suboptimal conditions, evasion of cell death, escape from the primary tumor and invasion and metastasis to distant sites. A variety of observations have suggested that Ras-transformation increases microtubule dynamics (Fotiadou, P. P., Takahashi, C., Rajabi, H. N., & Ewen, M. E., 2007). Changes in microtubule dynamics may have multiple consequences, but among them is modulating migratory capacity of cells. For example, H-Ras transformed MCF10a cells exhibit fewer acetylated microtubules; a reduction in this post-translational modification indicates a decrease in microtubule stability (Harrison, R. E. & Turley, E. A., 2001). Mechanistic studies have focused largely on microtubule stabilizing factors, such as discs large 1 (Dlg1), RASSF1A and adenomatous polyposis coli (APC) which control cell motility and are frequently lost in human cancers (Humbert, P. O. et al., 2008; van Es, J. H., Giles, R. H., & Clevers, H. C., 2001; Donninger, H., Vos, M. D., & Clark, G. J., 2007). Our studies indicate that increased expression of microtubule destabilizing factors can also occur during oncogenesis to support enhanced cell migration and invasion.

The Raf/ERK1/2 and PI3K pathways are major effectors of Ras transformation and have powerful actions on the cytoskeleton. ERK1/2 were first described as microtubule-associated protein kinases and regulate aspects of both microtubule and actin lattices (Ray, L. B. & Sturgill, T. W., 1987; Gotoh, Y. et al., 1991; Drechsel, D. N., Hyman, A. A., Cobb, M. H., & Kirschner, M. W., 1992; Reszka, A. A., Seger, R., Diltz, C. D., Krebs, E. G., & Fischer, E. H., 1995; Leinweber, B. D., Leavis, P. C., Grabarek,

Z., Wang, C. L., & Morgan, K. G., 1999; Olsen, M. K., Reszka, A. A., & Abraham, I., 1998). In Ras-transformed Swiss-3T3 fibroblasts, sustained ERK-MAPK signaling prevents actin stress fiber formation and promotes migration by downregulating Rho-kinase and ROCK1 (Sahai, E., Olson, M. F., & Marshall, C. J., 2001; Pollock, C. B., Shirasawa, S., Sasazuki, T., Kolch, W., & Dhillon, A. S., 2005). In agreement with this finding, inhibition of pERK1/2 by PD0325901 restored actin stress fibers in our system and restored microtubule polymers as well. Ras-induction of KIF2C was suppressed through inhibition of pERK1/2, resulting in expression of KIF2C comparable to its amount in normal immortalized HBEC. A less dramatic change was also noted in KIF2A. We conclude that the ERK1/2 pathway is a major Ras effector controlling expression of these kinesins.

Mutation of K-Ras induces changes in gene expression and morphology of cancer cells that have been evaluated in a number of ways, leading to the conclusion that changes in many genes downstream of Ras contribute to cancer phenotypes (Sekido, Y., Fong, K. M., & Minna, J. D., 2003; Zuber, J. et al., 2000; Bodemann, B. O. & White, M. A., 2008; Karnoub, A. E. & Weinberg, R. A., 2008; Singh, A. et al., 2009; Sunaga, N. et al., 2011). Among prominent examples, Zeb1 participates in the induction of EMT by suppressing expression of E-cadherin (Singh, A. et al., 2009; Larsen, J. E. & Minna, J. D., 2011). Knockdown of K-Ras in cancer cells has revealed genes whose expression is reversible upon loss of mutant K-Ras and those that have become Ras independent, such as Zeb1 (Singh, A. et al., 2009). In the transformed model we studied, knockdown of K-Ras or inhibition of ERK1/2 activation did reduce KIF2C and KIF2A expression, suggesting that these genes retain Ras dependence for expression.

PI3K influences the actin cytoskeleton to confer a migratory advantage on cancer cells. The mechanism includes the stimulation of Rac through regulation of T-lymphoma invasion and metastasis gene 1 (Tiam), which functions as a specific guanine nucleotide exchange factor (GEF) for Rac1 (Sander, E. E. et al., 1998). Additionally, the regulatory subunit of PI3K, p85α, can activate Cdc42 and subsequently regulate actin dynamics and migration (Jimenez, C. et al., 2000). Though we hypothesized that some of the changes in the actin cytoskeleton as a consequence of K-RasG12V transformation would be reversed with the inhibition of PI3K pathway, we found that in our system this pathway had a smaller than expected effect on the actin phenotype. Prolonged inhibition of this pathway also had a minor effect on microtubule organization and only a small effect on KIF2C expression. Thus, in this model of non-small cell lung cancer, ERK1/2 are dominant regulators of morphology and of kinesins involved in microtubule dynamics.

Finally, we determined that KIF2C and KIF2A are not only upregulated in our laboratory-generated system of K-Ras oncogenic transformation but in many cancer lines isolated from lung cancer patients. Knockdown of KIF2C and KIF2A decreased the ability of HBEC3KTRL53 (and certain cancer cell lines) to migrate and invade, suggesting the utility of targeting Ras-mediated pathways that promote different aspects of cancer biology for therapeutic advantage.

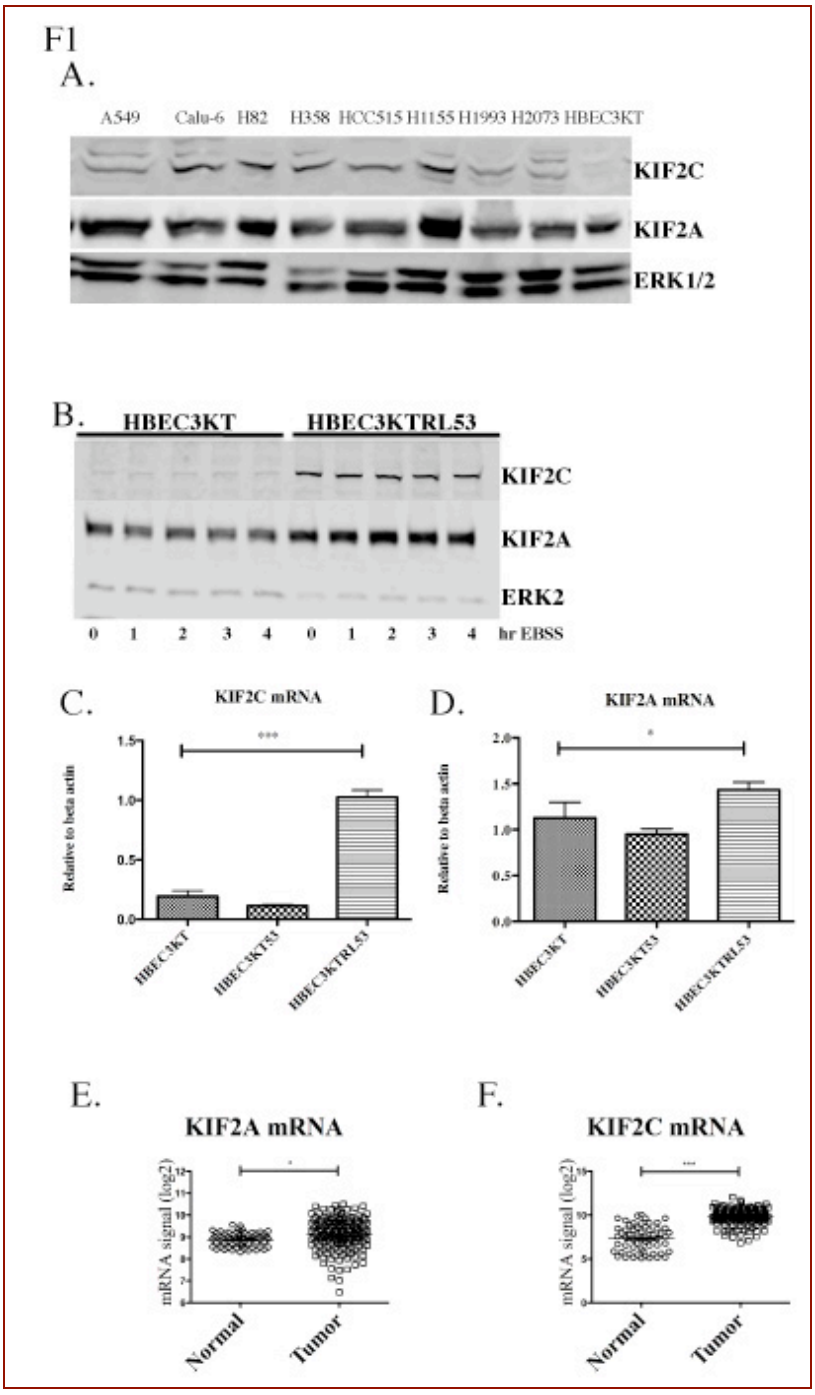
F1
A.
A549
Calu-6
H82
H358
HCC515
H1155
H1993
H2073
HBEC3KT
KIF2C
KIF2A
ERK1/2
B.
HBEC3KT
HBEC3KTRL53
KIF2C
KIF2A
ERK2
0 1 2 3 4 0 1 2 3 4 hr EBSS
C.
KIF2C mRNA
Relative to beta actin
HBEC3KT
HBEC3KT53
HBEC3KTRL53
D.
KIF2A mRNA
Relative to beta actin
HBEC3KT
HBEC3KT53
HBEC3KTRL53
E.
KIF2A mRNA
mRNA signal (log2)
Normal
Tumor
F.
KIF2C mRNA
mRNA signal (log2)
Normal
Tumor

Figure 3.1. Expression of kinesin 13 family proteins in cancer cell lines. (A) KIF2A and KIF2C were detected by immunoblotting of lysate proteins from A549, Calu-6, H82, H358, HCC515, H1155, H1993, H2073, HBEC3KT analyzed on denaturing gels as in *Methods*. (B) HBEC3KT and HBEC3KTR$_L$53 cells were starved in Earl's Balanced Salt Solution (EBSS) for the specified times. Lysate proteins were resolved on a gel followed by immunoblotting with the indicated antibodies. (C) RNA was isolated from HBEC3KT, HBEC3KT53 and HBEC3KTR$_L$53. KIF2C gene expression was measured by qPCR. $p < 0.0001$ by ANOVA (one-way analysis of variance). (D) KIF2A gene expression with $p = 0.045$ by ANOVA. Microarray profile of tumor and normal cell lines for (E) KIF2A; $p = 0.0022$ by two-tailed t test. (F) KIF2C; $p < 0.0001$ by two-tailed t test.

F2

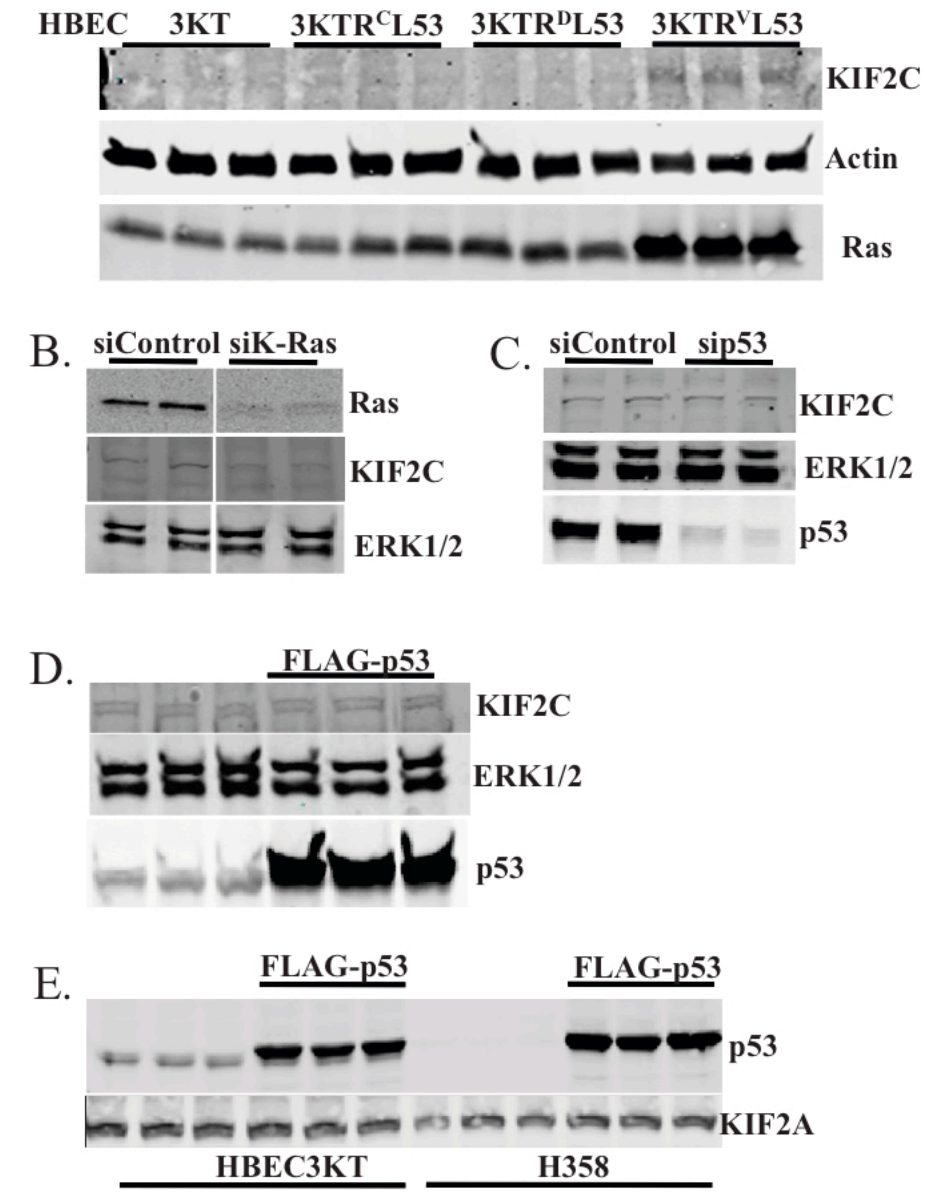
A.
HBEC
3KT
3KTR^CL53
3KTR^DL53
3KTR^VL53
KIF2C
Actin
Ras
B.
siControl
siK-Ras
Ras
KIF2C
ERK1/2
C.
siControl
sip53
KIF2C
ERK1/2
p53
D.
FLAG-p53
KIF2C
ERK1/2
p53
E.
FLAG-p53
FLAG-p53
p53
KIF2A
HBEC3KT
H358

Figure 3.2. K-Ras^{G12V} transformation affects KIF2C expression more than loss of p53. (A) KIF2C was immunoblotted in lysates from HBEC3KT, HBEC3KTR$^{C}_{L}$53, HBEC3KTR$^{D}_{L}$53, HBEC3KTR$^{V}_{L}$53. Immunoreactivity was detected with the LI-COR Odyssey infrared system. (B) KIF2C was immunoblotted in HBEC3KTR$_{L}$53 following depletion of K-Ras with siRNA compared to a non-targeting control siRNA. (C) KIF2C was immunoblotted in HBEC30KT following depletion of p53 with siRNA compared to non-targeting control siRNA. (D) KIF2C was immunoblotted in lysates ofHBEC3KTR$_{L}$53 or (E) KIF2A was immunoblotted in HBEC3KT and H358 in each case following re-expression of p53.

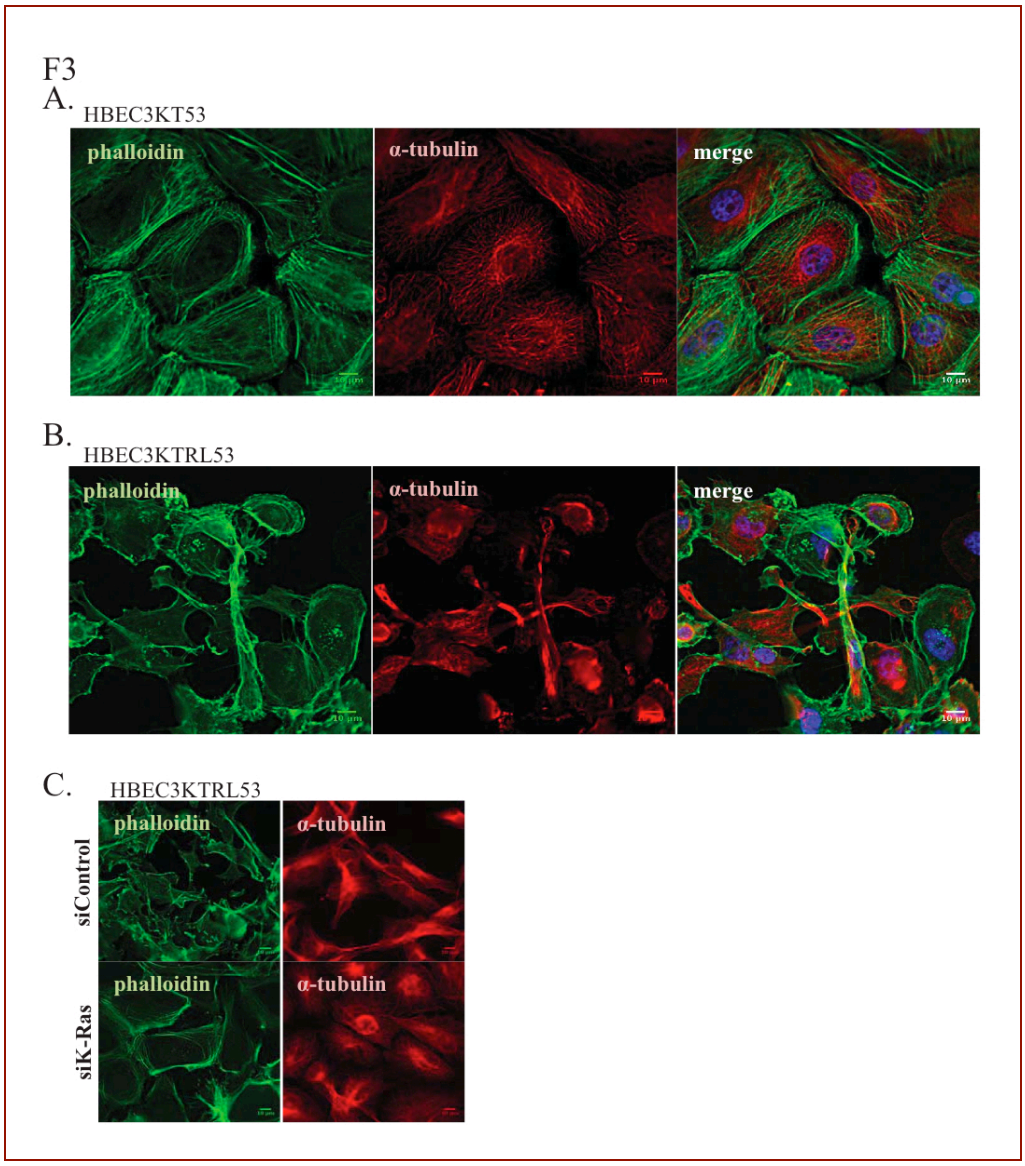

Figure 3.3. Cells transformed with K-Ras^{G12V} display changes in microtubule and actin cytoskeletons. Actin was detected using phalloidin (green) and α-tubulin (red) was detected by immunostaining in (A) HBEC3KT53, (B) HBEC3KTR$_L$53, and (C) HBEC3KTR$_L$53. In (C) staining was performed 72 hr after transfection with control (top) or K-Ras siRNA (bottom).

F4

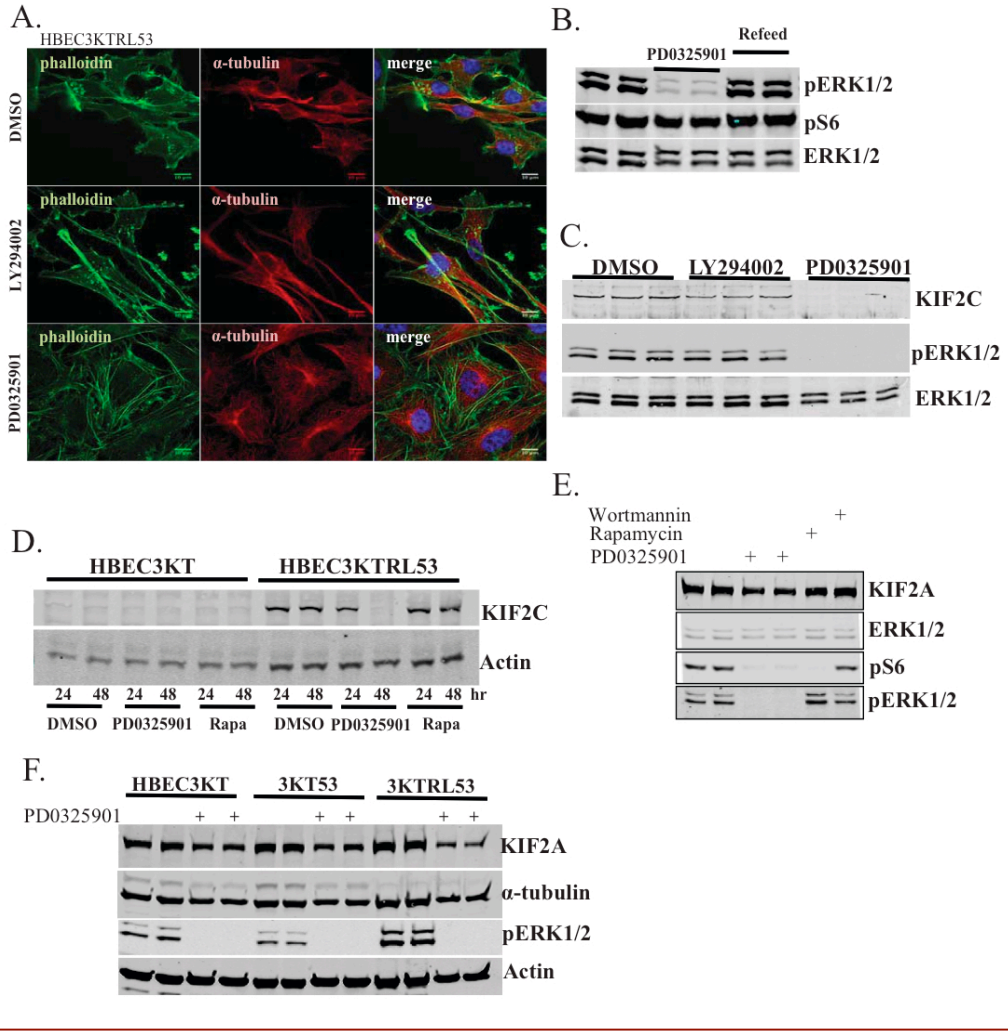
A.
HBEC3KTRL53
phalloidin
α-tubulin
merge
DMSO
LY294002
PD0325901
B.
Refeed
PD0325901
pERK1/2
pS6
ERK1/2
C.
DMSO
LY294002
PD0325901
KIF2C
pERK1/2
ERK1/2
D.
HBEC3KT
HBEC3KTRL53
KIF2C
Actin
24 48 24 48 24 48 24 48 24 48 24 48 hr
DMSO PD0325901 Rapa DMSO PD0325901 Rapa
E.
Wortmannin +
Rapamycin +
PD0325901 + +
KIF2A
ERK1/2
pS6
pERK1/2
F.
HBEC3KT
3KT53
3KTRL53
PD0325901 + + + + + +
KIF2A
α-tubulin
pERK1/2
Actin

Figure 3.4. ERK1/2 activity affects cellular morphology and KIF2C expression. (A) HBEC3KTR$_L$53 were treated with 100 nM PD0325901 or 10 μM LY294002 for 48 hr followed by immunofluorescence with the indicated antibodies. (B) Activation of ERK1/2 was detected by immunoblotting of lysates of HBEC3KTR$_L$53 treated with PD0325901 for 48 hr and stimulated with fresh medium after several washes with PBS to remove the inhibitor. (C) KIF2C was immunoblotted in HBEC3KTR$_L$53 that had been treated for 48 hr with 10 μM LY294002 or 100 nM PD0325901. (D) KIF2C was immunoblotted in HBEC3KT and HBEC3KT53 treated for 24 or 48 hr with 5 μM PD0325901 or 100 nM rapamycin. (E) KIF2A was immunoblotted in HBEC3KT treated with 100 nM rapamycin, 50 nM wortmannin or 1 μM PD0325901 for 72 hr. (F) KIF2A was immunoblotted in lysates of HBEC3KT, HBEC3KT53 and HBEC3KTR$_L$53 treated for 72 hr with 1 μM PD0325901.

F5

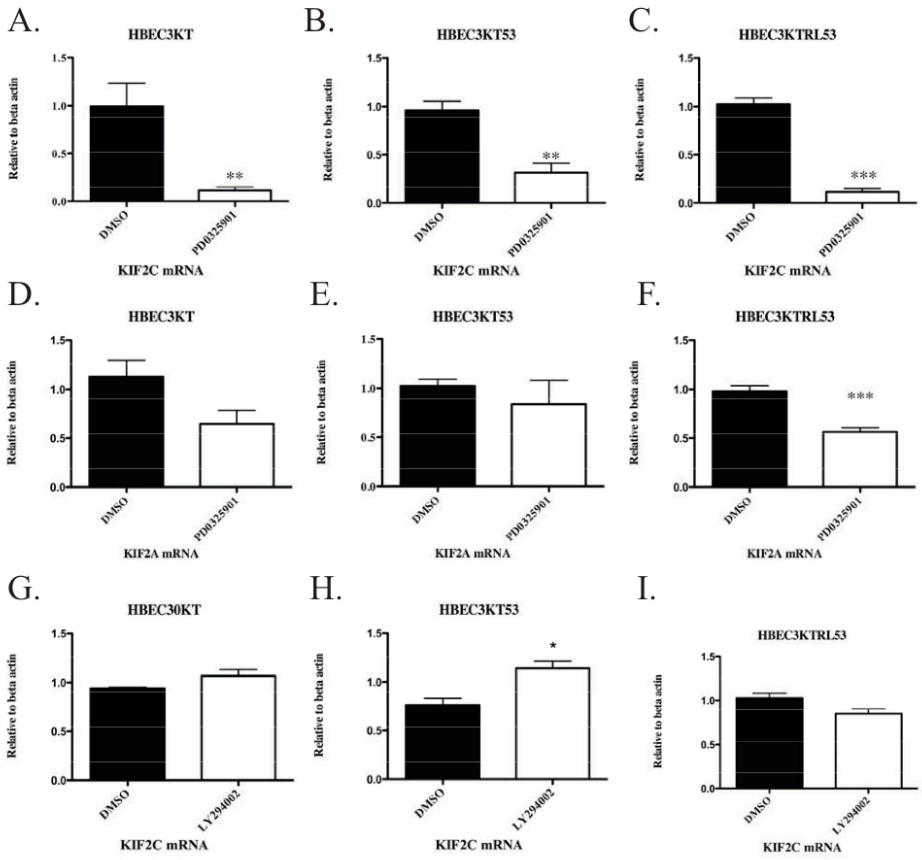
A.
HBEC3KT
Relative to beta actin
1.5
1.0
0.5
0.0
**
DMSO
PD0325901
KIF2C mRNA
B.
HBEC3KT53
Relative to beta actin
1.5
1.0
0.5
0.0
**
DMSO
PD0325901
KIF2C mRNA
C.
HBEC3KTRL53
Relative to beta actin
1.5
1.0
0.5
0.0
***
DMSO
PD0325901
KIF2C mRNA
D.
HBEC3KT
Relative to beta actin
1.5
1.0
0.5
0.0
DMSO
PD0325901
KIF2A mRNA
E.
HBEC3KT53
Relative to beta actin
1.5
1.0
0.5
0.0
DMSO
PD0325901
KIF2A mRNA
F.
HBEC3KTRL53
Relative to beta actin
1.5
1.0
0.5
0.0
***
DMSO
PD0325901
KIF2A mRNA
G.
HBEC30KT
Relative to beta actin
1.5
1.0
0.5
0.0
DMSO
LY294002
KIF2C mRNA
H.
HBEC3KT53
Relative to beta actin
1.5
1.0
0.5
0.0
*
DMSO
LY294002
KIF2C mRNA
I.
HBEC3KTRL53
Relative to beta actin
1.5
1.0
0.5
0.0
DMSO
LY294002
KIF2C mRNA

Figure 3.5. Inhibiting the ERK1/2 pathway affects KIF2C gene expression more than KIF2A.

RNA was isolated from (A) HBEC3KT, (B) HBEC3KT53 and (C) HBEC3KTR_L53 treated for 48 hr with 1 μM PD0325901 followed by qPCR measure of KIF2C gene expression. Three different experiments were analyzed by an unpaired t-test resulting in p-value (A) 0.0045 (B) 0.0028 (C) < 0.0001. RNA was isolated from (D) HBEC3KT, (E) HBEC3KT53, or (F) HBEC3KTR_L53 and KIF2A gene expression was measured by qPCR after 48 hrs of treatment with PD0325901. Data from three experiments was graphed. Statistical analysis was performed by t-test of control versus treatment: p-value (D) 0.0533, (E) 0.4795 and (F) 0.0301. Treatment of (G) HBEC3KT, (H) HBEC3KT53 and (I) HBEC3KTR_L53 with 10 μM LY294002 followed by qPCR for KIF2C gene expression as above. Statistical analysis was performed by t-test of control versus treatment: p-value (G) 0.1464, (H) 0.0192 and (I) 0.0628.

F6

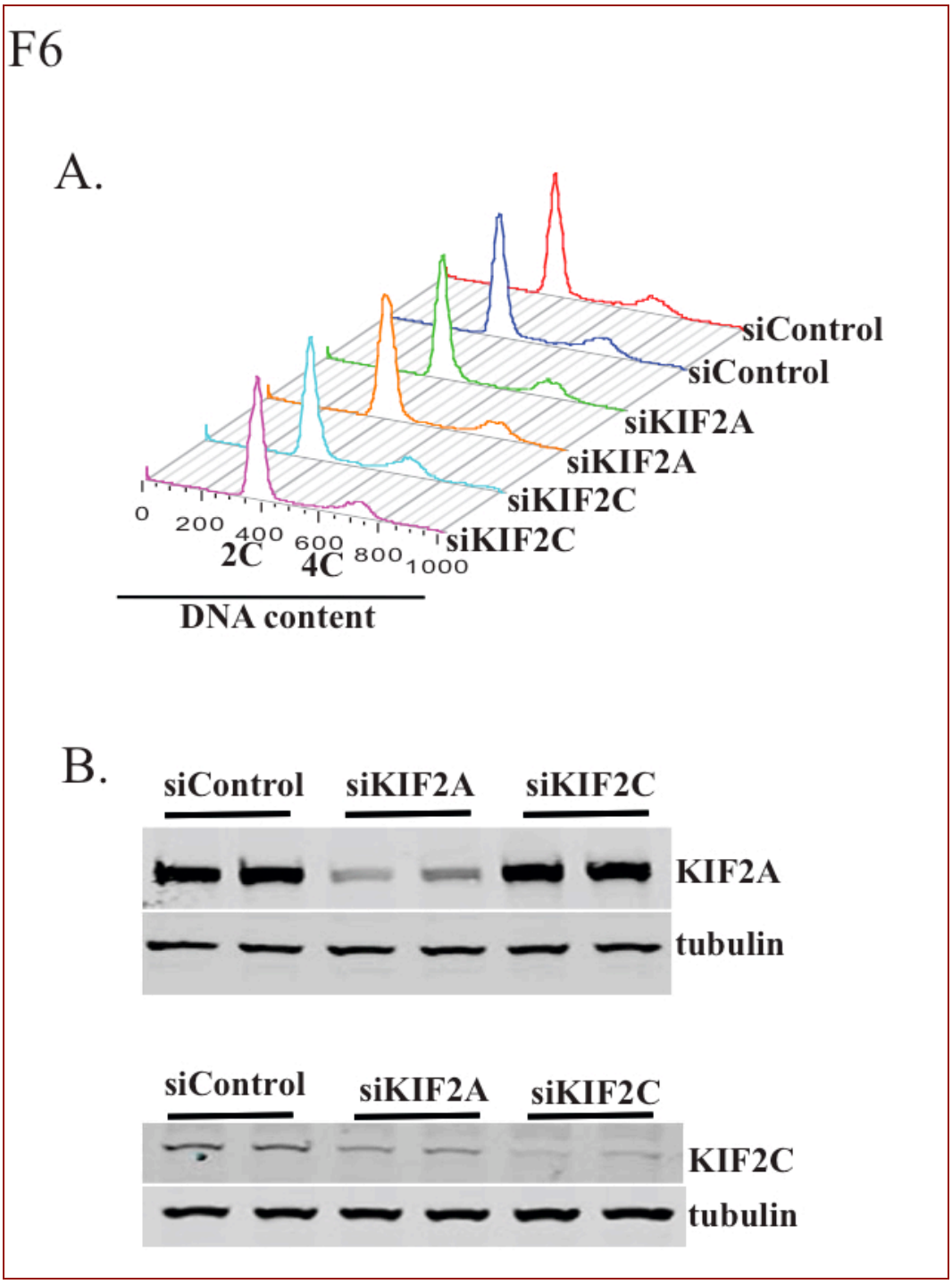
A.
siControl
siControl
siKIF2A
siKIF2A
siKIF2C
siKIF2C
0
200
400
600
800
1000
2C
4C
DNA content
B.
siControl
siKIF2A
siKIF2C
KIF2A
tubulin
siControl
siKIF2A
siKIF2C
KIF2C
tubulin

Figure 3.6. Depletion of either KIF2A or KIF2C does not change the cell cycle profile in HBEC3KTR$_L$53. HBEC3KTR$_L$53 were harvested for flow cytometry and immunblotting following depletion for 96 hr of KIF2A and KIF2C alone or together. (A) Cells were stained with propidium iodide (PI) and DNA content was measured by flow cytometry with FACSCalibur (BD Biosciences). Data were analyzed using FlowJo. (B) Lysate proteins (20 μg) were resolved on gels and immunoblotted to detect the indicated proteins.

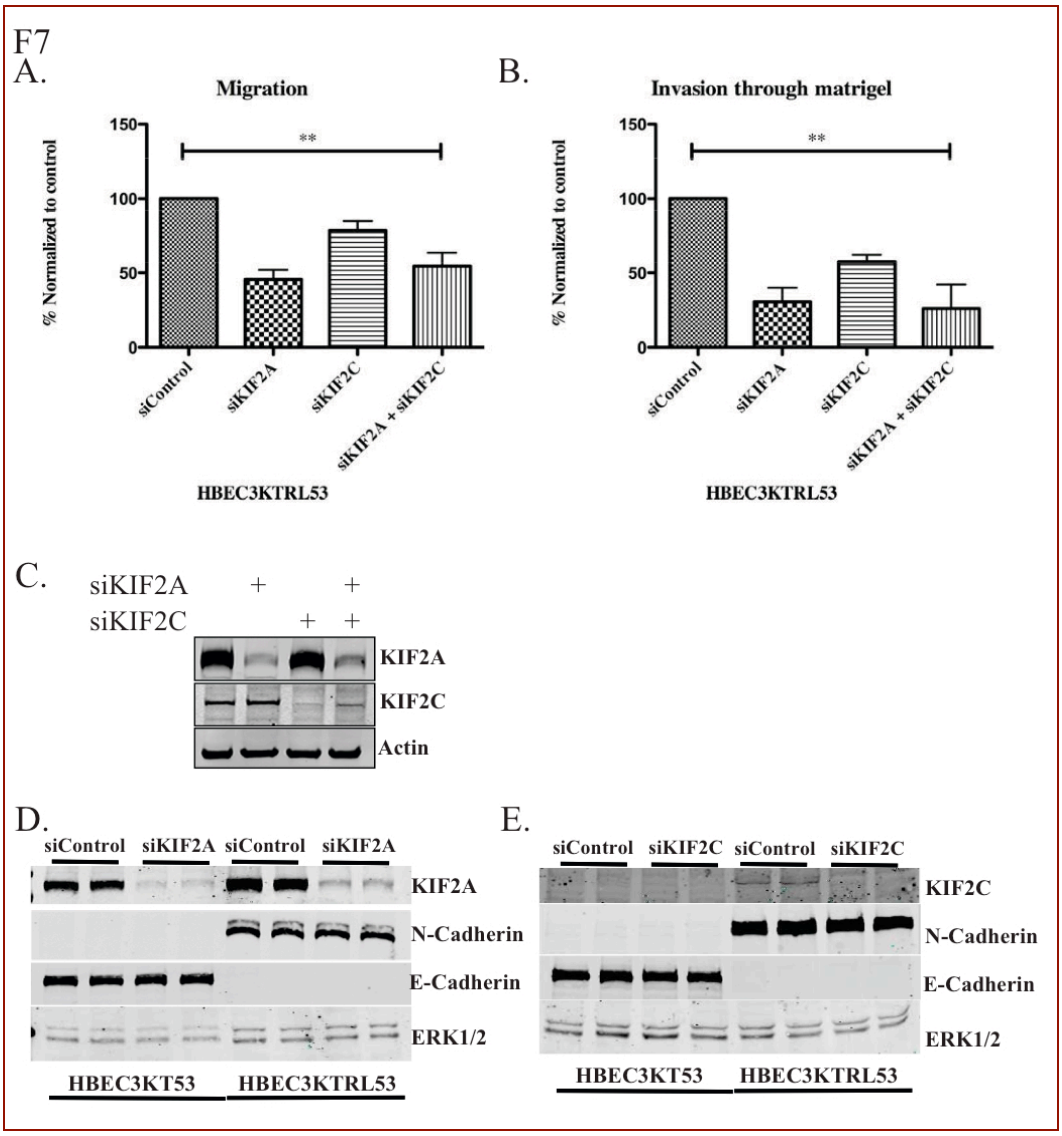

Figure 3.7. KIF2A and KIF2 facilitate cell migration. Cell migration was measured in HBEC3KTR$_L$53 after depletion of KIF2A or KIF2C: (A) transwell migration assay (B) invasion assay through Matrigel. (C) Panel shows efficient knockdown of kinesins for panels (A) and (B). Knockdown of (D) KIF2A or (E) KIF2C followed by immunoblotting of the indicated proteins in HBEC3KT53 and HBEC3KTR$_L$53.

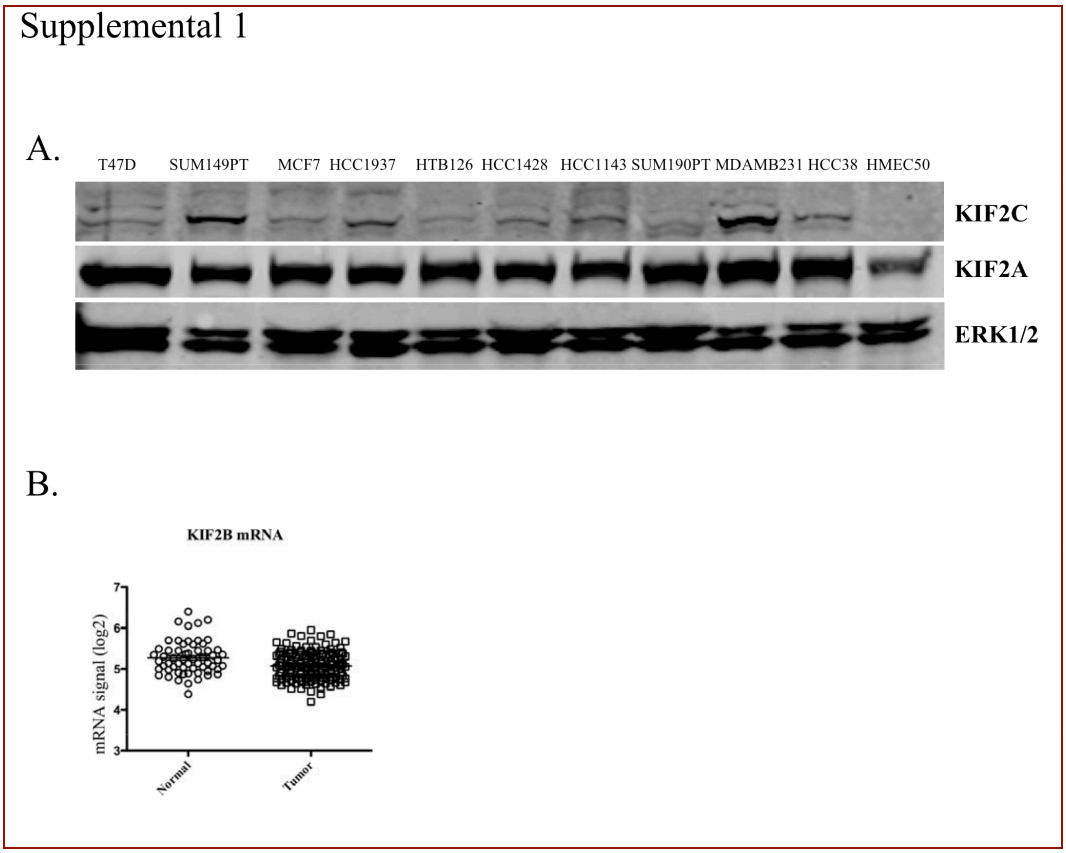

Figure 3.S1. Expression of kinesin 13 family proteins in cancer. (A) KIF2A and KIF2C expression in breast cells T47D, SUM149PT, MCF7, HCC1937, HTB126, HCC1428, HCC1143, SUM190PT, MDA-MB-231, HCC38, HMEC50. (B) . Microarray profile of tumor and normal panel cell lines for KIF2B with p value of 0.0006 by two-tailed t test. The signals with KIF2B probes are near the limit of detection. The mean difference is in the range of 10%. In spite of the small p-value, the difference may not be significant.

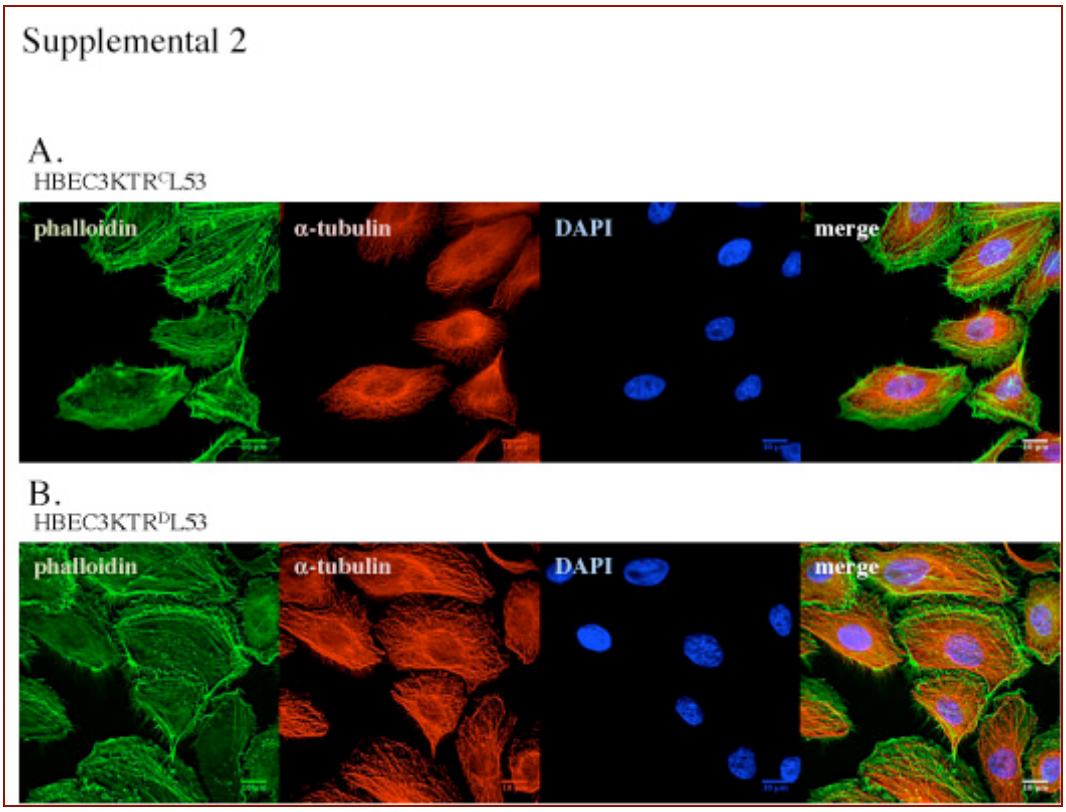

Figure 3.S2. Cell morphology. (A) HBEC3KTR^{C}L53 (B) HBEC3KTR^{D}L53 were immunostained with phalloidin (green), α-tubulin (red) and DAPI (blue) and processed in ImageJ.

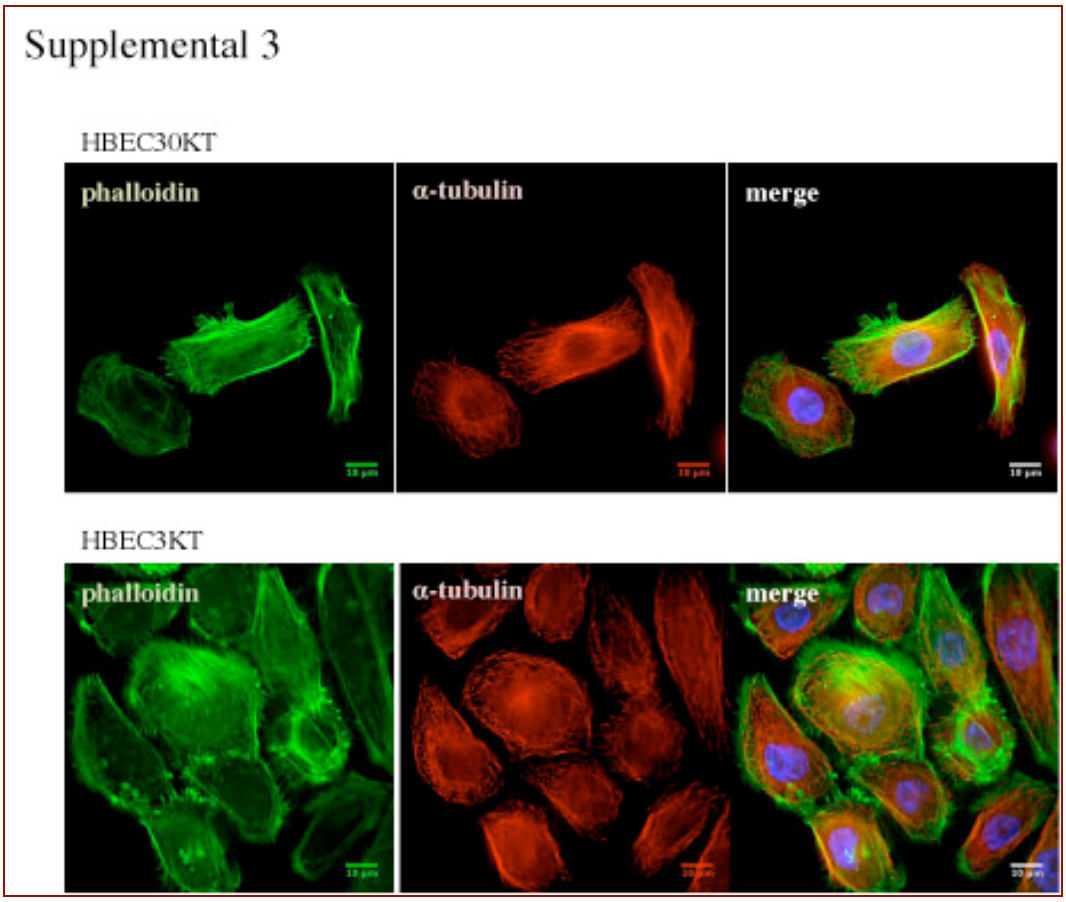

Figure 3.S3. Cell morphology. (A) HBEC30KT (B) HBEC3KT were immunostained with phalloidin (green), α-tubulin (red) and DAPI (blue) and processed in ImageJ.

Supplemental 4

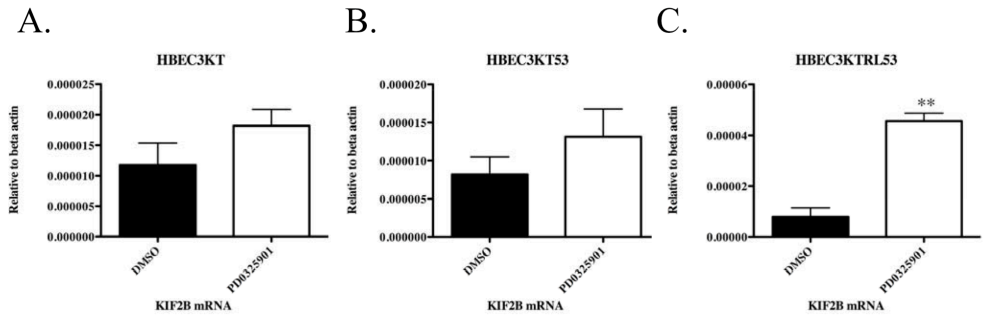

Figure 3.S4. KIF2B gene expression after MEK-ERK pathway inhibition. RNA was isolated out of (A) HBEC3KT, (B) HBEC3KT53 and (C) HBEC3KTRL53 cells were treated for 48 hours with 1 μM PD0325901 followed by qPCR measure of KIF2B gene expression. Three different experiments were analyzed by an unpaired t-test resulting in p-value (A) 0.2029 (B) 0.2914 (C) 0.0013.

CHAPTER FOUR

KIF2A and KIF2C are required for lysosomal organization and impact signaling

Abstract

KIF2A, a microtubule depolymerizing kinesin, has been suggested as a required component of mTORC1 signaling as it promotes its localization on lysosomes. We find that both KIF2A, and a closely related kinesin, KIF2C are both required for mTORC1 localization on lysosomes and its activity in response to amino acids in normal but not in lung cancer model cells. In contrast, neither KIF2A nor KIF2C are necessary for mTORC1 activation by combination of serum and amino acids. We find that our lung cancer model that has been transformed by expression of K-Ras^{G12V} and knockdown of p53 is also resistant to mTORC1 suppression after energy stress and after ERK1/2 inhibition. Here, we describe a number of mechanisms that oncogenic signaling is able to overcome to insure mTORC1 activation and survival.

Introduction

Complex signaling pathways are engaged in order to coordinate cellular growth and proliferation in response to positive stimulatory signals such as nutrients and growth factors or inhibitory signals such as intracellular or extracellular stresses. The loss of coordination of signaling events is often observed in pathologies such as cancer. Mechanistic target of rapamycin (mTOR), a serine/threonine kinase in a

phosphatidylinositol 3-kinase (PI3K)-related family, is a central regulator of events leading to cell growth and proliferation in response to nutrient availability. It carries out this role primarily as part of a complex (mTORC1). Positive regulatory signals to mTORC1 can originate from a known proto-oncoprotein the small GTPase Ras and its interaction with two important signaling cascades: the extracellular signal-regulated kinase ERK (Ras-ERK) and the phosphatidylinositol 3-kinase (Ras-PI3K) (Efeyan, Zoncu, & Sabatini, 2012). Low energy states that increase AMP and ADP relative to ATP provide an inhibitory signal to mTORC1 through the activation of AMP-activated protein kinase (AMPK). AMPK activates a small GTPase tuberous sclerosis complex protein 2 (TSC2) and also phosphorylates raptor, a component of mTORC1 (Gwinn et al, 2008(Inoki, Zhu, & Guan, 2003; Shaw et al., 2004), and consequently inhibits mTORC1. AMPK can also induce p53 activation in response to stress which can further induce metabolic re-programming. Cell cycle arrest or senescence may be induced depending on duration of stress (Jones et al., 2005). The AMPK-p53 link is reciprocal, as p53 can promote AMPK activation to shut off mTORC1 in response to genotoxic stress (Feng, Zhang, Levine, & Jin, 2005).

Some cancers utilize activating oncogenic mutations of Ras to promote their survival and invasion. Oncogenic Ras can be a positive regulator of autophagy; however, the effect of autophagy on cancer survival is largely context specific, inducing death in one system and promoting tumorigenicity in another (Elgendy, Sheridan, Brumatti, & Martin, 2011; Guo et al., 2011). Autophagy was first recognized as a cellular process required for maintenance of homeostasis because it removes damaged or unnecessary cellular components by promoting degradation in lysosomes. Thus, autophagy is critical

for development, differentiation as well as overall health of a cell. Cancer, among other disorders, has been noted to exhibit disregulated autophagy, which makes the question of how autophagy is regulated of great biomedical importance. One mechanism of inhibiting autophagy is through mTORC1, which phosphorylates and therefore suppresses proteins that are necessary for autophagosome membrane formation. mTOR particularly inhibits autophagy under conditions in which nutrients such as glucose and amino acids or growth factors are abundant. Because cancers utilize mTOR to optimize cellular functions to promote growth and survival, it is important to characterize how mTOR coordination of nutrient sensing and autophagy differ in cancer cells compared to normal, non-transformed cells.

KIF2A, a microtubule depolymerizing kinesin has been found to regulate lysosomal positioning which appears to be important for mTOR activation (Korolchuk, Sabatini). Because we identified KIF2A and a related family protein KIF2C, as molecules regulated by the Ras pathway (Zaganjor, E in review), we examined the roles of KIF2A and KIF2C depletion in Ras-propagated autophagy and regulation of mTOR. Although KIF2A and KIF2C are required for mTORC1 activation *potential* by amino acids after starvation, we find that they are dispensable for re-activation with serum and amino acids, suggesting that serum factors override amino acid-regulated mechanisms that enhance mTORC1 activation under nutrient-rich conditions. We hypothesize that the ability of normal cells to reactivate mTORC1 with the addition of serum and amino acids, even when molecules that regulate mTORC1 localization in response to amino acids are depleted, parallels the transformation phenotype in which mTORC1 activity is little

affected by nutrient limitation, potentially because the growth factor pathways compensate in a constitutive manner.

Materials and Methods

Antibodies- Following antibodies were used: KIF2A (Abcam, Cat. # ab37005; Novus Biologicals, Cat# NB500), α-tubulin (Sigma, Cat. # T6199), Actin (Millipore, Cat. # MAB1501MI), FLAG (Sigma, Cat. # F3165), pS6 (Cell Signaling Technology, Cat. # 5364), pERK (Sigma, Cat. # M8159 and Cell Signaling, Cat. #4377), LC3 (MBL, Cat. #PM036), p62 (Santa Cruz Biotechnology, Cat. #SC28359), LAMP2 (Abcam, Cat. #ab25631), pAKT (Cell Signaling, Cat. #4060), KIF2C (Bethyl Labs, Cat. # A300-807A), mTOR (Cell Signaling, Cat. #2983), Ras (Santa Cruz, sc-166691) ERK1/2 (Y691 previously described (Boulton & Cobb, 1991)).

Cell Culture - Immortalized HBEC3KT, HBEC30KT and HBEC3KT53 cells were cultured in keratinocyte serum free medium (KSFM) (Invitrogen) supplemented with 5 ng/mL epidermal growth factor and 50 μg/mL bovine pituitary extract according to manufacturer's recommendations. HBEC3KTRL53, HCT116 and H358 were cultured in RPMI-1640 medium supplemented with 5% heat-inactivated fetal bovine serum (vol/vol) and 2 mM L-glutamine. Cells were grown at 37º C in a humidified atmosphere of 5% CO_2.

Immunofluorescence – Cells were fixed with 4% paraformaldehyde (vol/vol) in Tris-

buffered saline TBS for 10 min, and permeabilized with 0.1% Triton X-100 for 5 minutes. After blocking with 10% normal goat serum (vol/vol) at room temperature for one hour, cells were incubated with the indicated antibodies at 4º C overnight. Cells were incubated with Alexa fluor-conjugated secondary antibody at room temperature for one hour, mounted and imaged. Fluorescent Z-stacks (0.2 mm) were acquired and deconvolved using the Deltavision RT deconvolution microscope.

siRNA - Cells were transfected for from 48 to 96 hours as indicated with dsRNA oligonucleotides using Lipofectamine RNAiMax according to manufacturer's protocol (Invitrogen). The following target sequences for KIF2A were used: GAAAACGACCACUCAAUAA (Thermo Scientific) and GACCCTCCTTCAAGAGATA (Thermo Scientific); KIF2C: GCAAGCAACAGGUGCAAGU (Thermo Scientific) and GGCAUAAGCUCCUGUGAAU (Thermo Scientific); Ras: GGAGGGCUUUCUUUGUGUA (Thermo Scientific); p53: GGAGAAUAUUUCACCCUUC (Thermo Scientific).

Cell harvest- Cells were lysed on ice in 50 mM HEPES, pH 7.5, 150 mM NaCl, 1.5 mM $MgCl_2$, 1 mM EGTA, 0.2 mM Na_3VO_4, 100 mM NaF, 50 mM β-glycerophosphate, 10% glycerol, 0.1% Triton X-100, 1.6 μg/ml aprotinin, 0.1 mM phenylmethylsulfonyl fluoride, and 10 μg/ml each of N^{α}-p-tosyl-L-lysine chloromethyl ketone, N^{α}-p-tosyl-L-arginine methyl ester, pepstatin A, and leupeptin. Lysates were frozen in N_2 (liquid) and

thawed on ice, followed by centrifugation for 15 minutes at 16,000 × g in a microcentrifuge at 4 °C. Lysates were subsequently boiled in Laemmli sample buffer (2% SDS, 10% glycerol, 5% β-mercaptoethanol, 0.01% bromphenol blue, 50 mM Tris-HCl) and subjected to polyacrylamide gel electrophoresis in sodium dodecyl sulfate.

Results

Cancer cell transformation unlinks growth factor signaling.

Fast growth and limited vascularization are just some of the environmental hurdles that provide a challenge to cancer cell survival. Signaling in cancer cells must be altered compared to normal cells to adjust to the high demand on nutrients and low oxygen availability. To assess signaling differences between normal and cancer cells that occur upon starvation, we placed immortalized human bronchial epithelial cells (HBEC3KT) and colorectal cancer cells (HCT116) in Earl's Balanced Salt Solution (EBSS), which lacks both serum and amino acids. We observed that in HBEC3KT cells the MAPK pathway is turned off as quickly as 15 minutes after starvation, and mTOR activity is reduced within 45 minutes after starvation. These growth pathways are resistant to starvation in HCT116 cells, however, even after 1 hour in EBSS (Fig. 4.1A). Because mTORC1 is, at least in part, activated through interaction with Rag small GTPases and the Ragulator complex on lysosomes, we were interested in how removal of amino acids and serum affects mTOR localization in HBEC3KT and HCT116 cells. We found that starvation causes a dispersal of mTOR from the lysosomes in HBEC3KT cells but not in HCT116 where mTOR remained concentrated in the proximity of the lysosomal marker

LAMP1 (Fig. 4.1B). This result suggested that perhaps the inability of mTOR to dissociate from the lysosomes keeps it activated in cancer cells in nutrient-poor conditions.

Inhibition of ERK1/2 or activation of AMPK inhibits mTORC1 in normal cells but not those transformed with K-Ras and loss of p53.

In our initial experiments we used colon cancer cells that harbor an oncogenic Ras mutation. To further study how nutrient signaling pathways are altered in cancers, we compared HBEC to a laboratory-generated non-small cell lung cancer (NSCLC) system. Beginning with HBEC3KT, which had been immortalized by expression of cyclin-dependent kinase 4 (CDK4) and telomerase (hTERT), cells were further altered by knockdown of p53, commonly lost or mutated in cancer, and stable expression of K-Ras^{G12V}, yielding HBEC3KTRL53. In our previous publication, we observed that ERK1/2 are activated by amino acids and in part involved in mTORC1 activation by amino acids in beta cells and cardiac cells (Wauson et al., 2012). Therefore, we inhibited ERK1/2 activity with a MEK1 inhibitor, PD0325901, for two days, mimicking chronic treatment during chemotherapy administration. In HBEC3KT, ERK1/2 inhibition almost completely inhibited pS6 phosphorylation, a measure of mTORC1 activity. Similar observations were made in HBEC30KT, a normal lung cell line from a different patient; inhibition of ERK1/2 resulted in mTORC1 inhibition (Fig. 4.S1A). Although PD0325901 inhibited pERK1/2, it had no effect on S6 phosphorylation in HBEC3KTRL53 (Fig. 4.2A). In H358, which, like HBEC3KTRL53, have an oncogenic K-Ras mutation and have lost p53, we observed that inhibition of ERK1/2 had no effect on mTORC1 activity

(Fig. 4.S1B). These data suggested that ERK1/2 and mTORC1 pathways are coordinated in normal cells whereas mTORC1 is less sensitive to ERK1/2 inhibition in the cancer model. Consistent with the results of amino acid and serum starvation, mTORC1 activity was not affected by inhibition of ERK1/2 for 30 minutes in HBEC3KT. Prolonged inhibition of ERK1/2 also had significant effects on both mTOR and LAMP2 association, causing dispersal of both and inactivation of mTORC1, as assessed by S6 phosphorylation, in HBEC3KT (Fig. 4.2B, 4.2A). In the absence of perturbation, HBEC3KTRL53 exhibited a more dispersed lysosomal phenotype which was not substantially altered by prolonged inhibition of ERK1/2, suggesting that oncogenic transformation overrides the changes in organelle compartments that occur in normal cells after growth pathway inhibition. Next, we wanted to determine if the growth pathway dependence that occurs in normal lung cells is limited to ERK-mTORC1 cross-talk or if other molecules contribute to coordination of these events. Therefore, we activated the AMPK with AICAR (5-aminoimidazole-4-carboxamide-1-β-D-ribofuranoside), a small molecule which mimics AMP. AMPK activation has previously been observed to inhibit mTORC1 and induce autophagy (Gwinn et al., 2008). Indeed, this inhibition of mTOR by AMPK activation occurs in HBEC3KT as early as 6 hours after treatment with AICAR (Fig. 4.3A). Metformin, another activator of AMPK, which acts through inhibition of Complex I of the respiratory chain, also inhibits mTORC1 in HBEC3KT, but to a lesser extent in HBEC3KTRL53 (Fig. 4.3B). Exposure to metformin also causes dissociation of mTOR from lysosomes in HBEC3KT but not in HBEC3KTRL53 (Fig. 4.3C). These data suggest that oncogene-induced transformation prevents a comprehensive shut-down of signaling pathways that are coordinated in

normal cells.

KIF2A and KIF2C are required for mTORC1 activation by amino acids.

Given the observation that mTOR was slower to dissociate from lysosomes either through starvation or growth pathway inhibition (Fig. 4.1B, 4.2B) in cancer models, we wondered about the mechanism underlying sustained mTOR-lysosome localization and activity. Recently, KIF2A was identified as a motor protein that is required for mTORC1 positioning on lysosomes (Korolchuk et al., 2011). Additionally, KIF2A and a related family protein KIF2C are upregulated in many cancers and their expression is, at least in part, supported by oncogenic Ras and the MAPK pathway (Zaganjor E, in review). To test the involvement of KIF2A and KIF2C in mTORC re-activation after starvation, we knocked down KIF2A and KIF2C in HBEC3KT and HBEC3KTRL53 and re-stimulated the cells with amino acids (Fig. 4.4A). Loss of either KIF2A or KIF2C reduced mTORC1 activity in HBEC3KT but had no such effect in HBEC3KTRL53, as assessed by pS6 phosphorylation. Because mTORC1 localization to lysosomes is crucial for its activation, we wanted to assess if KIF2A and KIF2C disrupt this localization after amino acid re-stimulation. Indeed in HBEC3KT, addition of amino acids to cells transfected with control oligonucleotide after starvation triggered the movement of mTORC1 to co-localize with the lysosomal membrane marker LAMP2. Amino acid stimulation of HBEC3KT in which either KIF2A or KIF2C had been depleted failed to restore mTORC1 localization to lysosomes; instead mTOR remained diffuse in the presence of amino acids (Fig. 4.4B). In HBEC3KTRL53, loss of KIF2A or KIF2C had no effect on mTORC1 ability to localize to lysosomes after amino acid stimulation (Fig. 4.S2).

KIF2A and KIF2C are not required for mTOR activation by amino acids and serum.

In HBEC3KT, mTORC1 could be inhibited by various means including starvation, inhibition of growth pathways, energy stress and loss of the kinesins KIF2A or KIF2C. Because HBECKTRL53 and HCT116 cells were resistant to mTORC1 inhibition by any of these interventions, we hypothesized that there are overriding mechanisms mediated by oncogenic transformation that contribute to the capacity of these cells to withstand these challenges..Constitutive activation of growth factor pathways may provide the overriding signal that overcomes amino acid depletion to maintain mTORC1 activity. The inability of cancers to sense the environment and suppress mTORC1 activity in response to nutrient depletion caused us to ask whether normal cells would be resistant to mTORC1 downregulation due to loss of kinesins in the presence of abundant nutrients. To test this hypothesis, we knocked down KIF2A or KIF2C in HBEC3KT and, after starvation, re-stimulated the cells with medium containing amino acids and serum. In contrast to the results observed with re-stimulation by amino acids alone, re-stimulation with amino acids plus serum activated mTORC1 even in cells with reduced KIF2A and KIF2C expression (Fig. 4.5A, 4.5C). Predictably, HBEC3KTRL53 were completely insensitive to loss of KIF2A and loss of KIF2C in that mTORC1 remained active in response to re-stimulation with serum and amino acids added after starvation (Fig. 4.5B, 4.5D). Distinct from the inability of amino acids to localize mTORC1 to lysosomes following loss of KIF2A or KIF2C, addition of serum and amino acids caused mTORC1 enrichment on lysosomes in both HBEC3KT and HBEC3KTRL53 (Fig. 4.6A, 4.6B). These results suggest distinct mechanisms at play in Ras-transformed cells.

KIF2C induces autophagy through an mTOR-independent mechanism.

Recently much interest was generated in Ras-propagated autophagy that promotes cancer survival (Elgendy et al., 2011; Guo et al., 2011; Yang et al., 2011). mTORC1 can support tumor growth and suppress autophagy. Paradoxically, autophagy can also be upregulated in cancers, even in the presence of active mTOR. It is thought that autophagy promotes survival in the low-nutrient microenvironment of a tumor. A common methodology to measure autophagy is to assess the conversion of the ubiquitin-like protein LC3-I to its lipidated form, LC3-II, which accumulates in autophagosomes. We find that in HBEC3KTRL53 there is an increase in LC3-II compared to HBEC3KT or the HBEC3KT non-transformed counterparts expressing K-Ras ^{G12C} or K-Ras^{G12D} (Fig. 4.7A). Because a number of Ras functions are executed by the downstream effectors, phosphatidylinositol 3-kinase (PI3K) and ERK1/2, we wanted to know how much these pathways contribute to sustained autophagy. We inhibited both pathways in HBEC3KTRL53 with small molecules: LY294002 which inhibits the PI3K pathway and PD0325901, which inhibits MEK1 and subsequently ERK1/2. Inhibition of either PI3K or ERK1/2 alone inhibited autophagy, suggesting that oncogenic Ras promotes autophagy through either of these effectors (Fig. 4.7B). We hypothesized that knocking down Ras would reverse the autophagy observed in K-Ras transformed cells. Instead, autophagy was further enhanced by K-Ras knockdown, as assessed by loss of p62, a marker of autophagic flux which is sequestered by autophagosomes and degraded in lysosomes when autophagy is induced (Fig. 4.7C). Because loss of KIF2A was suggested to induce autophagy, we tested whether loss of KIF2C also promotes autophagy. Indeed, even in HBEC3KTRL53 where

loss of KIF2C had no effect on mTORC1 activity, we observed an enhancement of autophagy, as assessed by a decrease in p62 (Fig. 4.7D). Because changes in energy states also induce autophagy, we measured ATP content in HBEC3KT and HBEC3KTRL cells and found a decrease in ATP in cells with KIF2A and KIF2C depleted (Fig. 4.7E).

Discussion

Sensing nutrient availability is essential for coordination of growth and proliferation in normal cells. The ability to properly sense the environment and modulate growth is often dysregulated in cancers. Here, we demonstrate that prolonged inhibition of growth factor pathways or a decrease in energy state suppresses mTORC1, a positive regulator of growth in normal lung cells. In contrast, the NSCLC model and various cancer lines such as H358 are completely insensitive to these changes in the environment and do not inactivate mTORC1.

We find that microtubule destabilizing kinesins KIF2A and KIF2C are required for activation of mTORC1 by amino acids but not by serum and amino acids in combination, suggesting a hierarchy in signaling that leads to mTORC1 activation in normal cells. KIF2A and KIF2C are also required for mTORC1 accumulation at lysosomes after amino acid stimulation but are indispensable for mTORC1 localization to lysosomes in the presence of growth factors under nutrient replete conditions. In contrast, cancer models do not require KIF2A and KIF2C for mTORC1 activity or its localization to the lysosome. This may be because growth factor pathways are constitutively turned on, rendering cells insensitive to mTORC1 dissociation. As previously reported for loss

of KIF2A, loss of KIF2C also induces autophagy even in HBEC3KTRL53 where mTORC1 remains activated. This is an unexpected result because drugs that inhibit microtubule dynamics such as nocodazole and taxol prevent starvation-induced autophagy (Geeraert et al., 2010). It will be important to further assess if the induction of autophagy by depletion of KIF2A and KIF2C is independent of the regulation of microtubule dynamics.

Lysosomes are localized at the microtubule organizing center (MTOC) and require microtubule dynamics for lysosomal organization(Matteoni & Kreis, 1987). It would then be expected that cells with different microtubule dynamics, would have different patterns of lysosomal distribution. Cells transformed with oncogenic Ras have been noted to have increased microtubule instability (Harrison & Turley, 2001). This change in microtubule dynamics may explain why in HBEC3KT lysosomes are organized along the nucleus whereas in HBEC3KTRL53 lysosomes are somewhat dispersed throughout the cytoplasm. The increase in microtuble dynamics in cancers may impose an increased need for trafficking (Mosesson, Mills, & Yarden, 2008). Therefore, rather than targeting specific oncoproteins in cancer, targeting molecules that are involved in organelle dynamics may prove to be another option for cancer therapy.

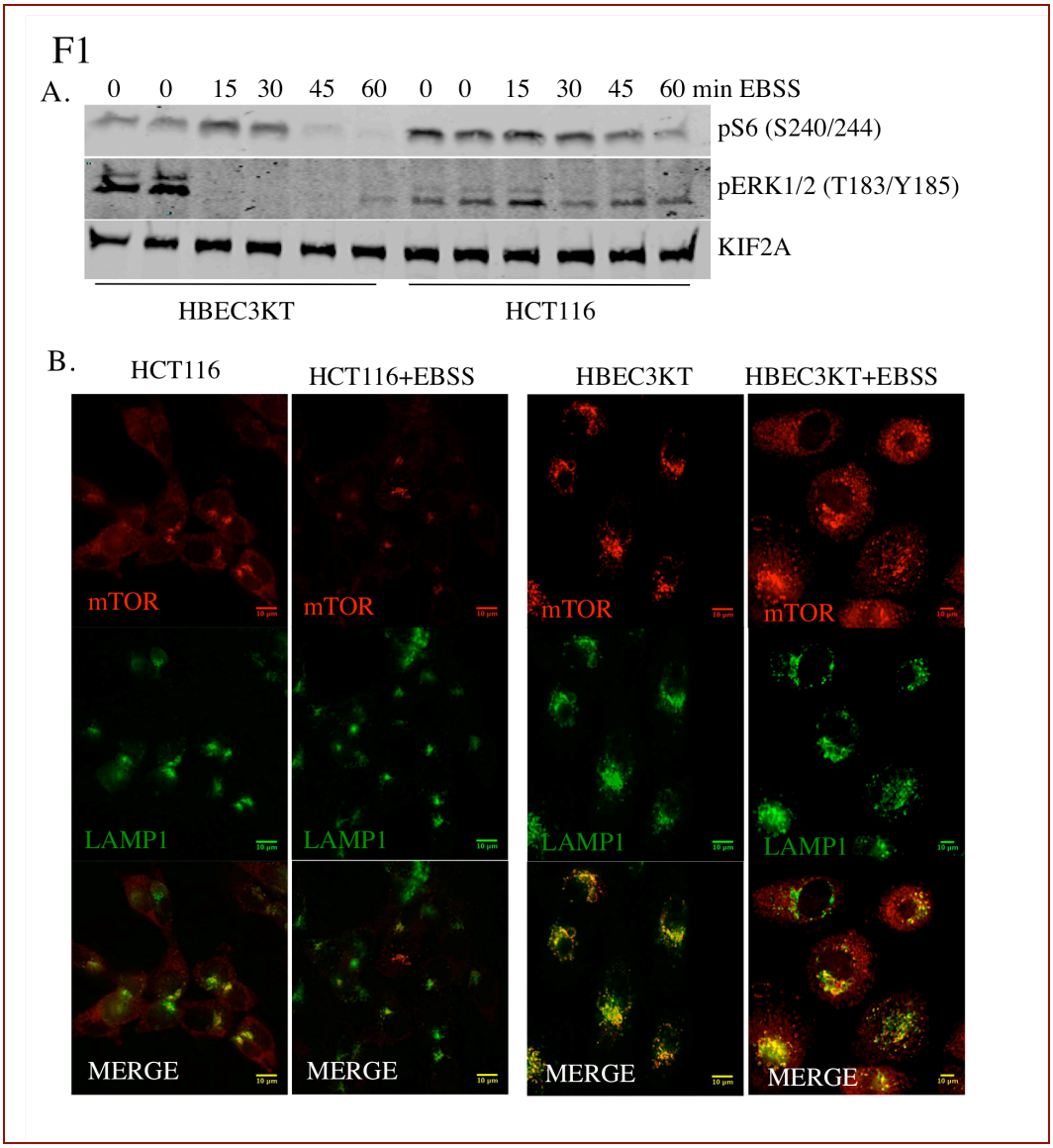

Figure 4.1. Cancer cells with K-Ras mutations are less sensitive to starvation than normal cells. (A) HBEC3KT and HCT116 cells were starved in Earl's Balanced Salt Solution (EBSS) for the specified times. Lysate proteins were resolved on gels followed by immunoblotting with the indicated antibodies. (B) HBEC3KT and HCT116 cells were starved in EBSS for 2 hours and then co-immunostained for endogenous mTOR (red) and

endogenous LAMP1 (green).

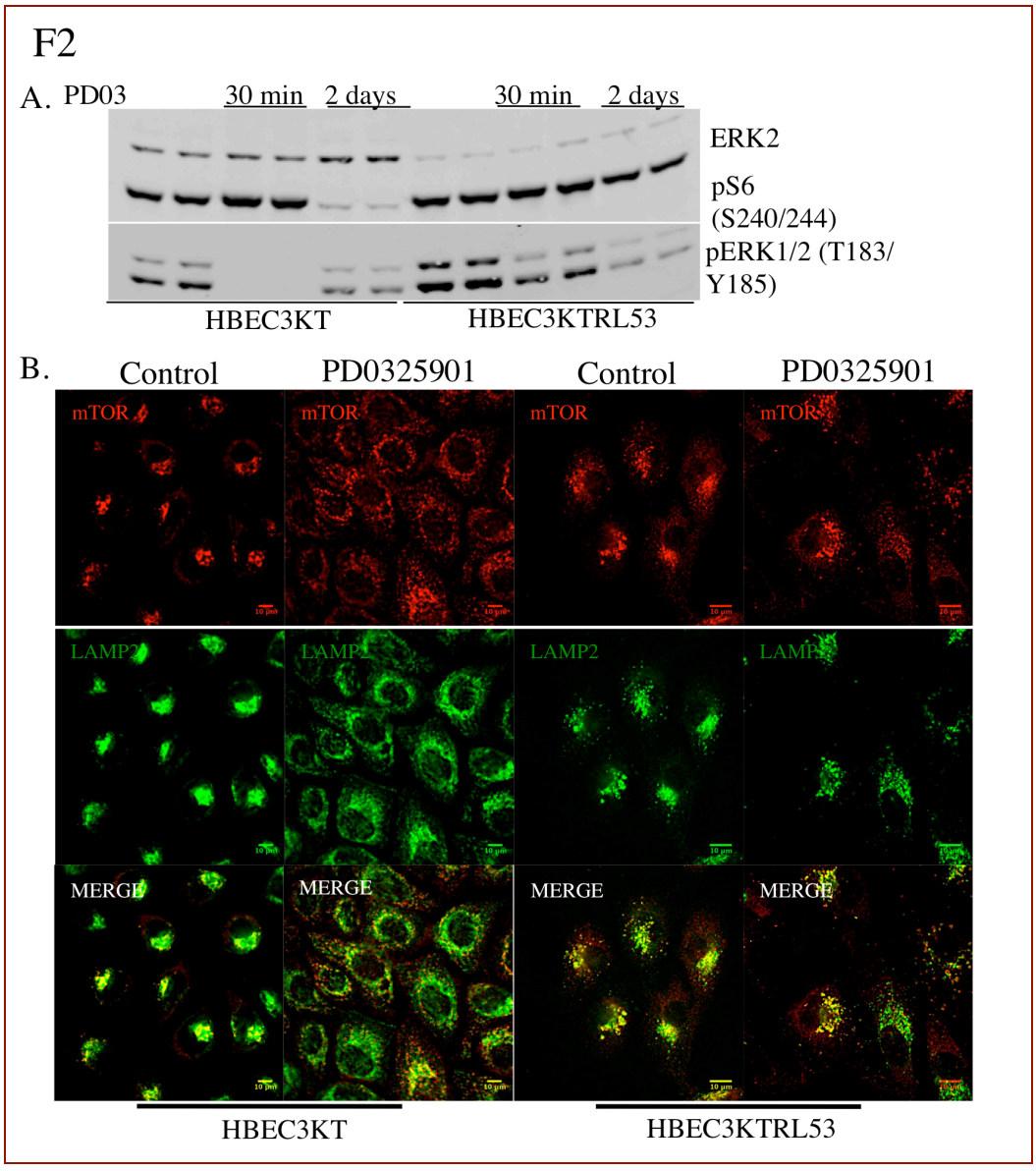

Figure 4.2. Inhibition of ERK1/2, inhibits mTORC1 in normal lung but not in the NSCLC model. (A) HBEC3KT and HBEC3KTRL53 cells were treated for either 30 minutes or 2 days with 10 nM PD0325901. Lysates were resolved on SDS-PAGE gels, immunobloted and the indicated proteins were detected with the LI-COR Odyssey infrared system. (B) Following 2 day of treatment with 100 nM PD0325901, HBEC3KT or HBEC3KTRL53 were immunostained as in Fig.1B.

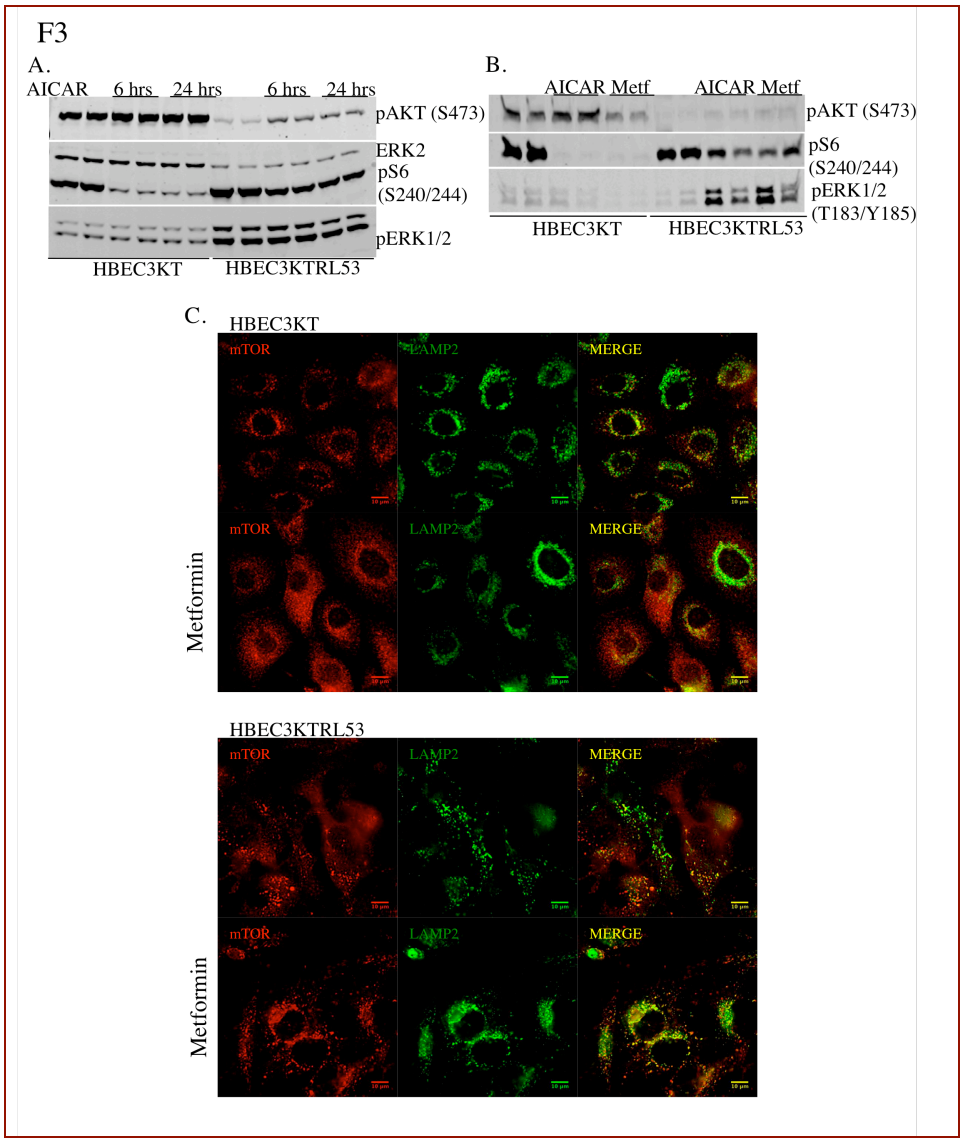

Figure 4.3. Energy stress inhibits mTORC1 in normal lung but not in the NSCLC model. (A) HBEC3KT or HBEC3KTRL53 were treated with 0.5mM AICAR for 6 or 24 hours and proteins were analyzed by immunoblotting. (B) HBEC3KT or HBEC3KTRL53 were treated for 2 days with 0.5 mM AICAR or 2 mM metformin.(C) HBEC3KT and HBEC3KTRL53 were treated for 2 days with 2 mM metformin; cells were immunostained with designated antibodies.

F4

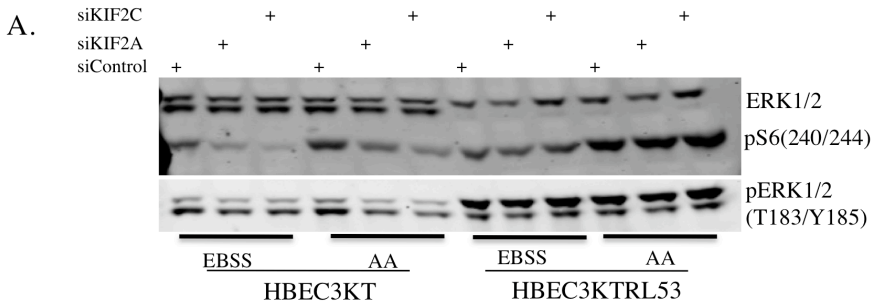
A.
siKIF2C
siKIF2A
siControl
ERK1/2
pS6(240/244)
pERK1/2
(T183/Y185)
EBSS
AA
EBSS
AA
HBEC3KT
HBEC3KTRL53

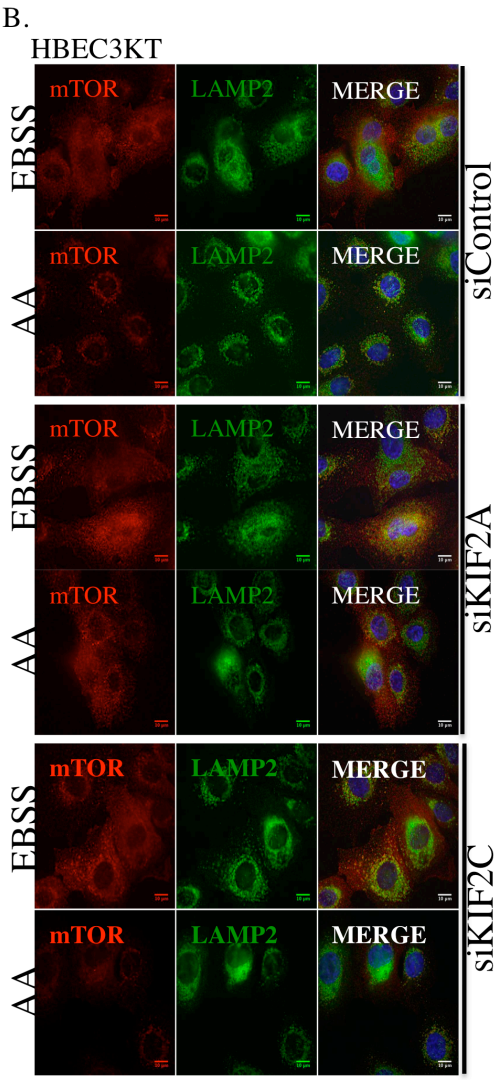
B.
HBEC3KT
mTOR
LAMP2
MERGE
EBSS
AA
siControl
siKIF2A
siKIF2C

Figure 4.4. KIF2A and KIF2C are required for amino acid activation of normal but not cancer model cells. (A) KIF2A and KIF2C were depleted by siRNA in HBEC3KT and HBEC3KTRL cells. Cells were starved for 2 hours and re-stimulated for 30 minutes with amino acids (AA), a combination of each amino acid contained in L-glutamine-free DMEM plus 0.5 mM L-glutamine. (B) Cells were prepared as in Fig. 3A and analyzed by immunofluorescence.

F5

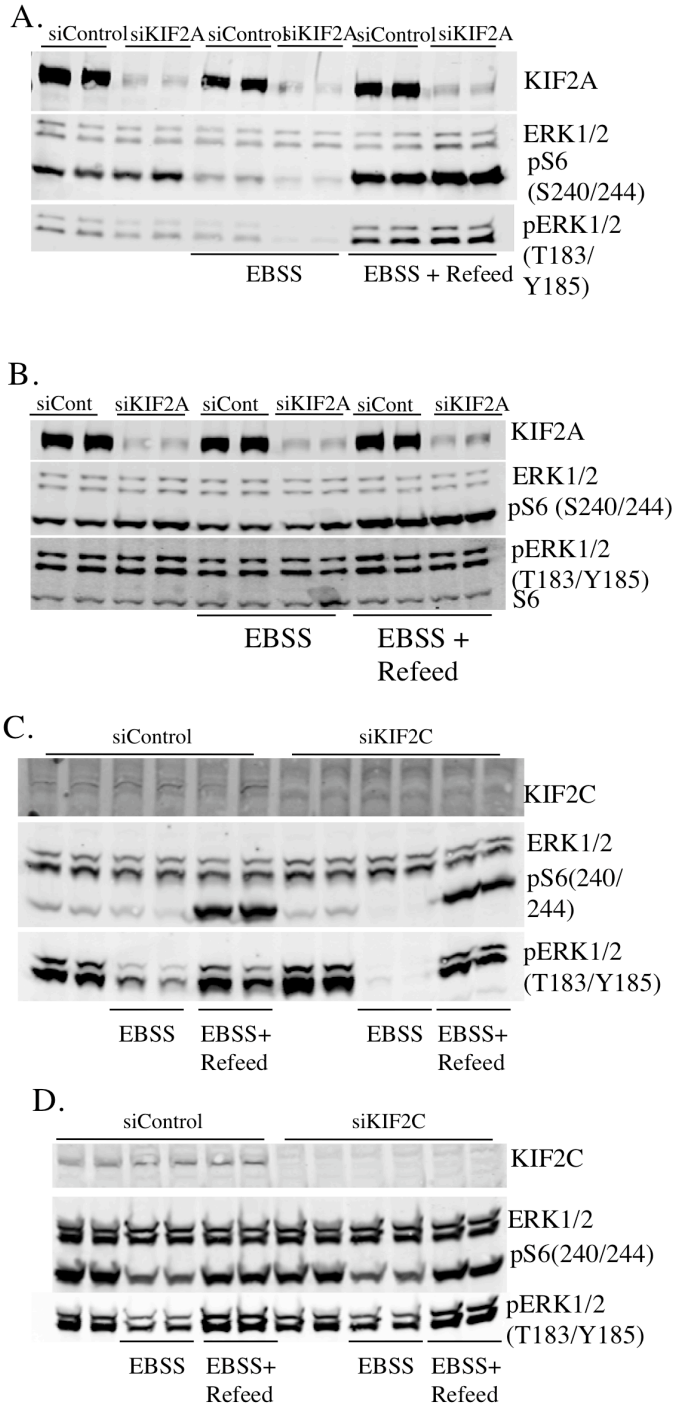
A.
siControl
siKIF2A
siControl
siKIF2A
siControl
siKIF2A
KIF2A
ERK1/2 pS6 (S240/244)
pERK1/2 (T183/ Y185)
EBSS
EBSS + Refeed
B.
siCont
siKIF2A
siCont
siKIF2A
siCont
siKIF2A
KIF2A
ERK1/2 pS6 (S240/244)
pERK1/2 (T183/Y185)
S6
EBSS
EBSS + Refeed
C.
siControl
siKIF2C
KIF2C
ERK1/2 pS6(240/ 244)
pERK1/2 (T183/Y185)
EBSS
EBSS+ Refeed
EBSS
EBSS+ Refeed
D.
siControl
siKIF2C
KIF2C
ERK1/2 pS6(240/244)
pERK1/2 (T183/Y185)
EBSS
EBSS+ Refeed
EBSS
EBSS+ Refeed

Figure 4.5. KIF2A and KIF2C are not required for mTORC1 activation by serum and amino acids in either normal or Ras-transformed cells. (A) KIF2A was depleted by siRNA in HBEC3KT cells. Cells were starved for 2 hours and stimulated for 30 min with fresh medium. (B) KIF2A was depleted by siRNA in HBEC3KTRL53 cells that were starved for 2 hours and stimulated for 30 min with fresh medium. (C) KIF2C was depleted by siRNA in HBEC3KT cells that were starved for 2 hours and stimulated for 30 min with fresh medium. (D) KIF2C was depleted by siRNA in HBEC3KTRL53 cells. Cells were starved for 2 hours and stimulated for 30 min with fresh medium. Lysate proteins were resolved on gels, transferred to membranes and immunoblotted.

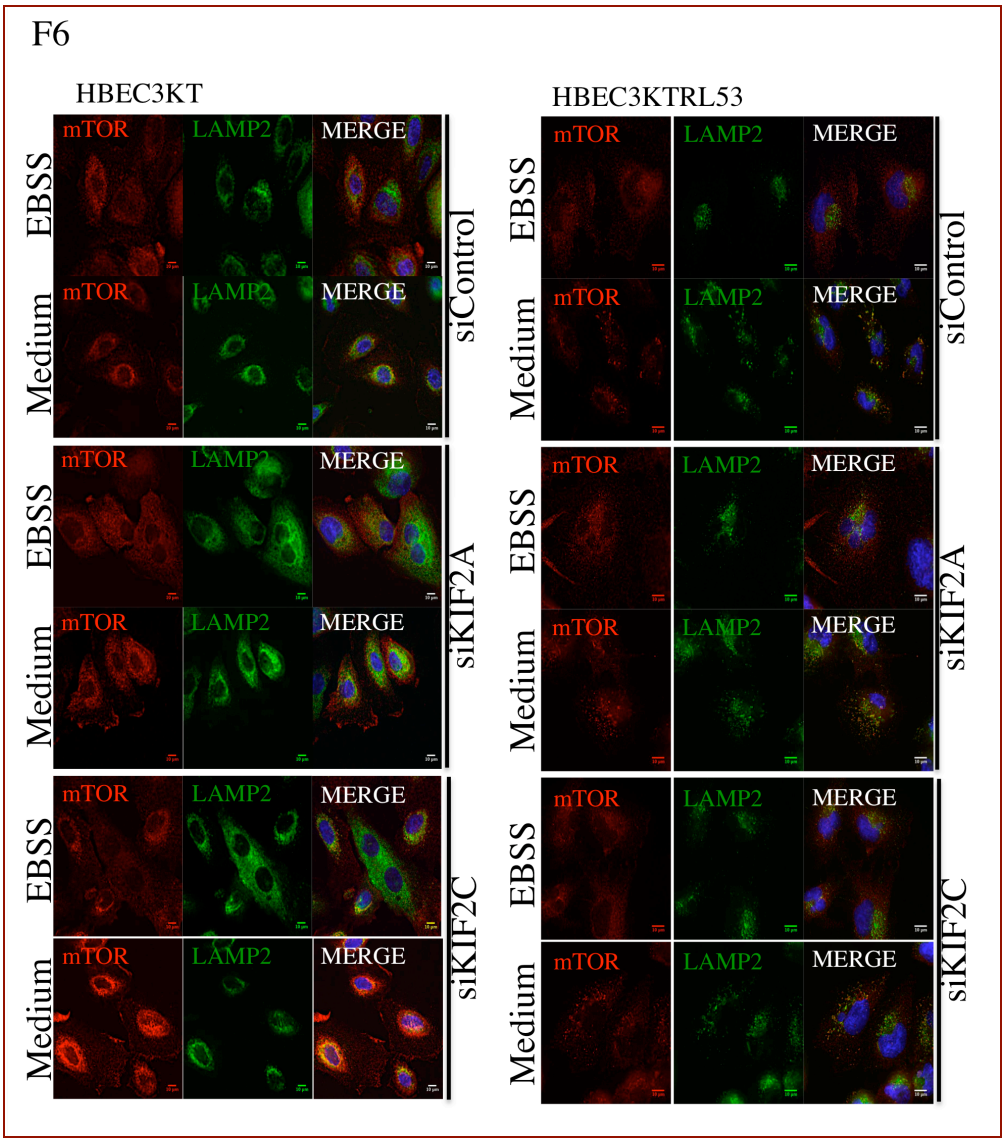

Figure 4.6. KIF2A and KIF2C are not required for mTORC1 localization to lysosomes by serum and amino acids in either normal or Ras-transformed cells. (A) KIF2A and KIF2C were depleted from HBEC3KT. Following starvation, cells were stimulated with serum and amino acids as in Fig. 4. Endogenous mTOR (red) and LAMP2 (green) were observed by immunofluorescence. (B) KIF2A and KIF2C were depleted from HBEC3KTRL53 and representative images were obtained as in Fig. 5A.

F7

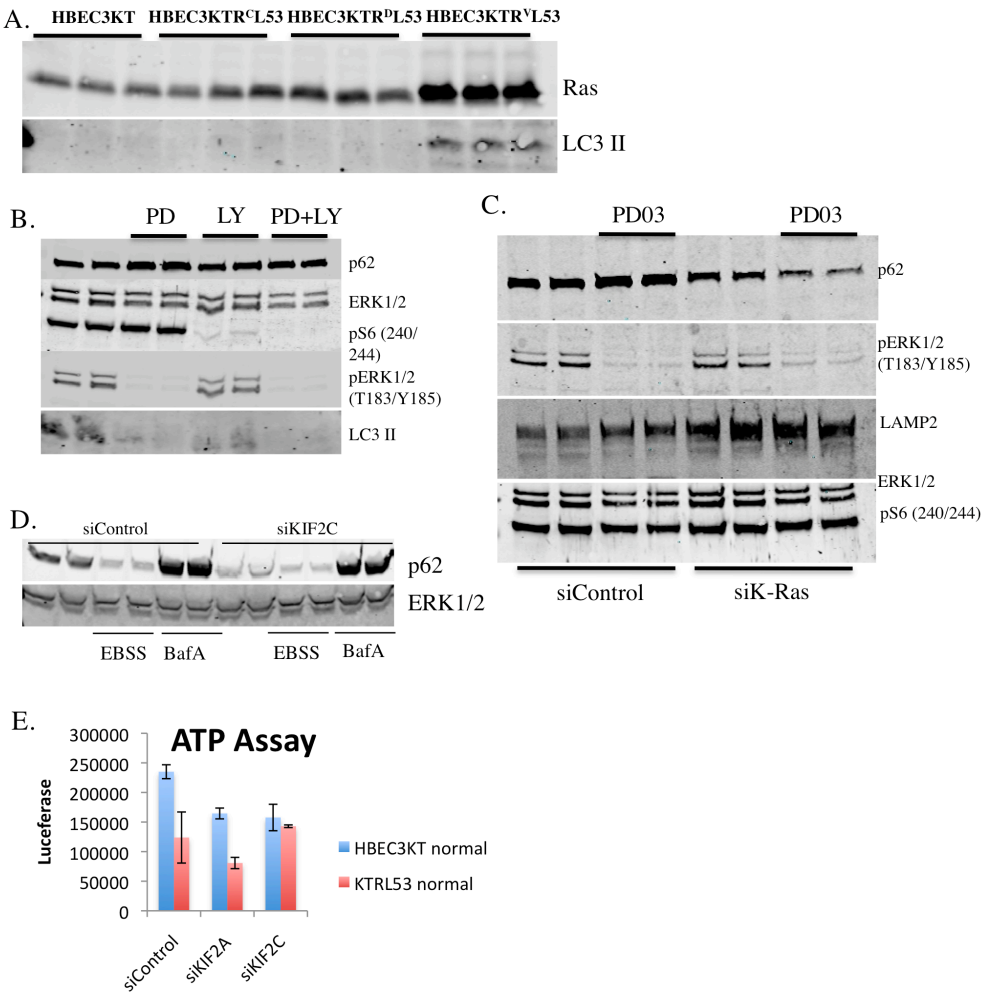
A.
HBEC3KT
HBEC3KTRCL53
HBEC3KTRDL53
HBEC3KTRVL53
Ras
LC3 II
B.
PD
LY
PD+LY
p62
ERK1/2
pS6 (240/244)
pERK1/2 (T183/Y185)
LC3 II
C.
PD03
PD03
p62
pERK1/2 (T183/Y185)
LAMP2
ERK1/2
pS6 (240/244)
siControl
siK-Ras
D.
siControl
siKIF2C
p62
ERK1/2
EBSS
BafA
EBSS
BafA
E.
ATP Assay
Luceferase
300000
250000
200000
150000
100000
50000
0
siControl
siKIF2A
siKIF2C
HBEC3KT normal
KTRL53 normal

Figure 4.7. Loss of KIF2C induces autophagy. LC3-II was immunoblotted in equal amount of protein lysate from HBEC3KT, HBEC3KTR^{C}L53, HBEC3KTR^{D}L53, HBEC3KTR^{V}L53. Immunoreactivity was quantified with the LI-COR Odyssey infrared system. (B) HBEC3KTRL53 cells were treated for 24 hours with 100 nM PD0325901 or 10 μM LY294002 followed by immunoblotting of lysates with indicated antibodies. (C) Ras was depleted with siRNA. HBEC3KTRL53 were treated for 3 days with 100 nM PD0325901 followed by immunoblotting of lysates. (D) KIF2C was depleted with siRNA from HBEC3KTRL53. Cells were starved for 12 hours in EBSS or treated with 10 nM Baflomycin A. (E) ATP was measured using ApoSENSOR^{TM} Cell Viability Assay Kit according to manufacturer's protocol in HBEC3KT or HBEC3KTRL53 in which KIF2A or KIF2C had been depleted with siRNA.

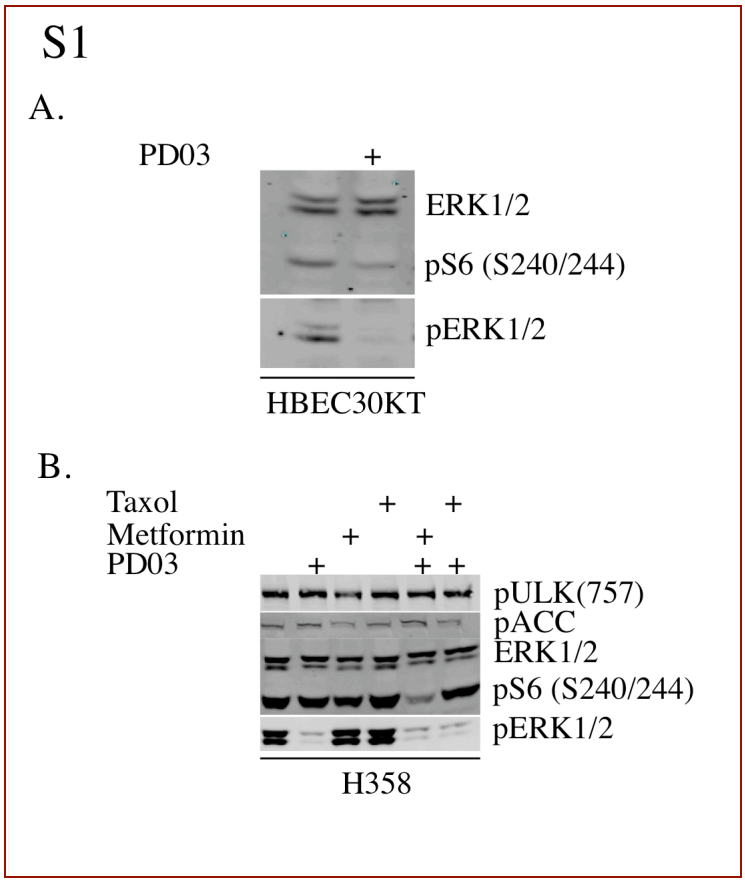

Figure 4.S1. Prolonged inhibition of ERK1/2 inhibits mTORC1 in HBEC30KT but not in H358. (A) HBEC30KT were treated 2 days with 100 nM PD0325901. Lysates were resolved on SDS-PAGE gels, immunobloted and the indicated proteins were detected with the LI-COR Odyssey infrared system. (B) H358 cells were treated with 100 nM PD0325901, 2 mM metformin or 10 nM Taxol for 2 days.

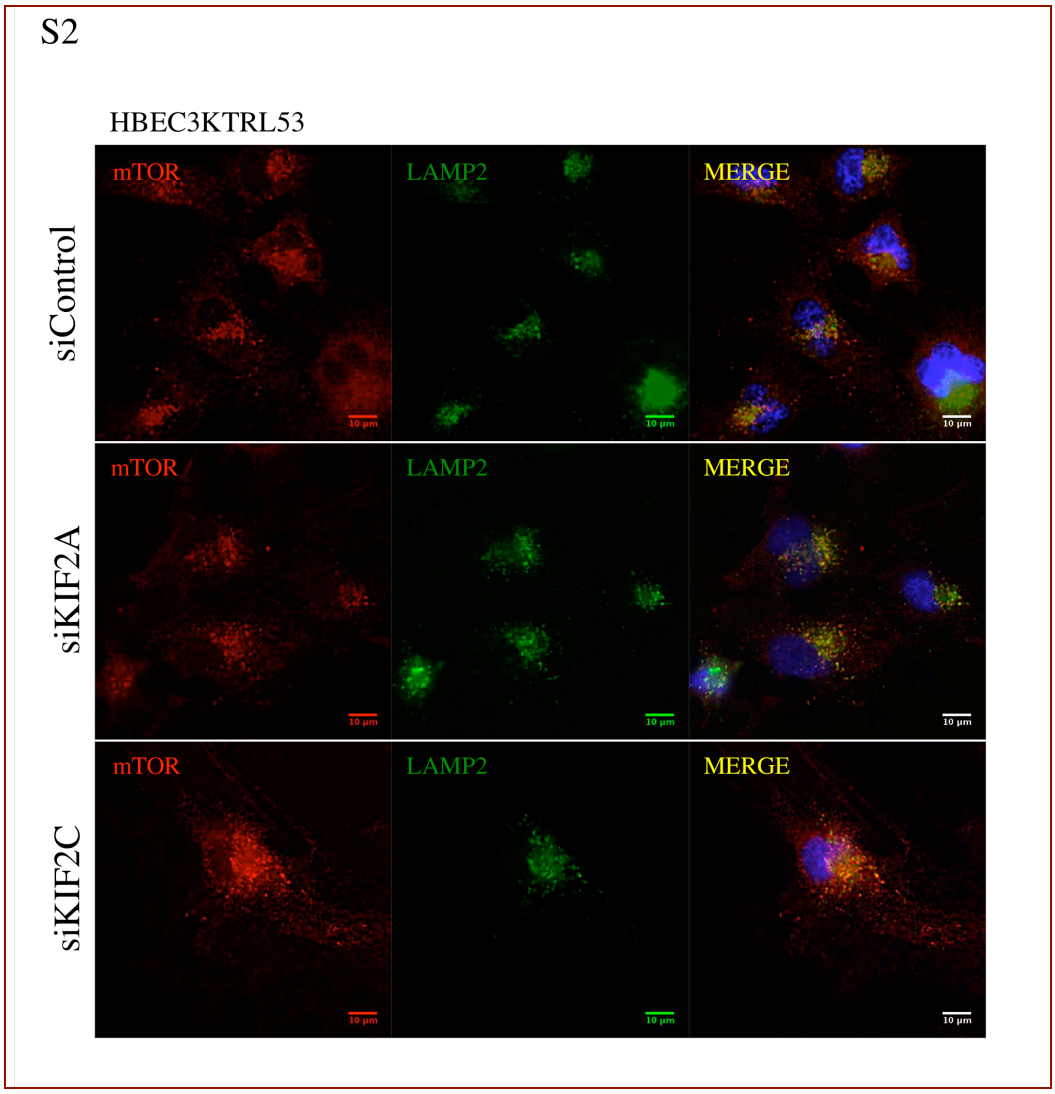

Figure 4.S2. KIF2A and KIF2C are not required for mTORC1 localization to lysosomes by amino acids in Ras-transformed cells. KIF2A and KIF2C were depleted from HBEC3KTRL53. Following 90 minute starvation, cells were stimulated with amino acids for 30 minutes. Endogenous mTOR (red) and LAMP2 (green) were observed by immunofluorescence.

CHAPTER FIVE
Conclusions and Future Directions

ERK REGULATION OF KIF2A & KIF2C

KIF2A Localization

The regulation of transcription factors in the nucleus by ERK1/2 contributes to pathology and has been extensively studied. The importance of regulation of cytosolic substrates by ERK1/2, however, is only now becoming recognized. Of particularly interest to this dissertation is regulation of cytoskeleton components by ERK1/2 that are critical for migration; these components are often aberrantly regulated in pathological states such as cancer and neurodegeneration. One such example of ERK1/2 regulation of cytoskeleton and migration is its phosphorylation and subsequent activation of the WAVE2 regulatory complex (WRC) that leads to its association with Arp2/3 to promote actin polymerization and leading edge advancement (Mendoza et al., 2011). Additionally, ERK1/2 can regulate cytosolic components involved in organelle dynamics, in both cytoskeleton-dependent and independent manners. For example, ERK can directly phosphorylate a structural Golgi protein GRASP65; an event which is critical for Golgi remodeling and therefore establishment of cell polarity and migration (Bisel et al., 2008).

In the first chapter of this thesis we show that ERK1/2 regulate KIF2A through phosphorylation and that ERK1/2 activity is important for the subcellular distribution of KIF2A. Preliminary data suggest that HBEC3KTRL53 cells accumulate more cytosolic KIF2A than the normal, control cell line HBEC3KT (data not shown). This observation opens up a number of important questions. Does cytosolic KIF2A localization contribute to dynamic instability of microtubules in cancer models to promote migration? Because

HBEC3KTRL53 cells have increased ERK1/2 activity, might the change in KIF2A localization be regulated by this activity? If so, what is the mechanism? Post-translational modifications have often been found to restrict cellular localization of proteins, making it possible that ERK1/2 phosphorylation of KIF2A directly dictates its accumulation in the cell.

Alternatively, we and others have found ERK1/2 regulation of nucleoporin-mediated nuclear transport (Kosako et al., 2009). Therefore, we cannot exclude the possibility that a more general effect of ERK1/2 regulation of other proteins involved in nucleo-cytoplasmic shuttling indirectly leads to changes in KIF2A localization. We analyzed the primary sequence of KIF2A to determine if it contained one or more nuclear localization sequences (NLS) or nuclear export sequences (NES) in order to assess how its localization may be regulated. KIF2A has a bipartite classical NLS sequence: 154-RRKS-157 and 169 –KREKRR-174 (Nguyen Ba, Pogoutse, Provart, & Moses, 2009). Additionally, another conserved, monopartite NLS 144-RRKGK-148 was confirmed to be necessary for the nuclear import of recombinant KIF2A in interphase *Xenopus* eggs (Wilbur & Heald, 2013). Proteins containing canonical NLSs are imported into the nucleus by interacting with karyopherin α (importin α) family members. Karyopherin α proteins are adaptor proteins that recognize the NLS but require association with karyopherin β transport factors and their interaction with the nuclear pore complex to mediate nuclear translocation in a GTP dependent manner (Marfori et al., 2011). Therefore, we hypothesized that karyopherin β may be required for import of KIF2A in the nucleus. To test this, karyopherin β1 was knocked down in HeLa cells and following cytosolic-nuclear cellular fractionation, KIF2A localization was assessed (Figure 5.1).

Indeed, there is an increase in cytosolic KIF2A in karyopherin β1 knockdown cells, suggesting the involvement of this import factor in nuclear translocation of KIF2A. In vitro binding assays with purified proteins and co-immunoprecipitation experiments would help resolve the question of how direct this interaction is and if it occurs in cells. Another interesting question is why there are multiple different NLSs and do they regulate KIF2A import in a distinct, context-specific manner?

Translocation of proteins from the nucleus to the cytosol is accomplished through exportins. CRM1/Exportin1 has the most identified substrates, in part due to the fact that there is a natural inhibitor Leptomycin B that has allowed for many discoveries (Kutay & Guttinger, 2005). The recognition sequence for CRM1 is the leucine-rich nuclear export sequence (NES) (la Cour et al., 2004; Xu, Grishin, & Chook, 2012). We identified a number of possible NESs on KIF2A: 659-YATQLEAILEQKIDI-673, 603-VSPQLFTFHEAVSQM-617, 606-QLFTFHEAVSQMVEM-620 (hydrophobic residues are colored red). Therefore, we hypothesized that CRM1 may be a regulator of KIF2A nuclear export. To test this hypothesis, we treated HBEC3KT and HBEC3KTRL53 cells with Leptomycin B for 24 hours and assessed KIF2A localization by both immunofluorescence and cellular fractionation. Indeed, we find that inhibition of CRM1 with Leptomycin B, causes enrichment of KIF2A in the nucleus (Figure 5.2). Particularly, we noted a greater nuclear accumulation of KIF2A in HBEC3KT than in HBEC3KTRL53 cells. This difference, may suggest that KIF2A shuttles in and out of nucleus less in HBEC3KTRL53 cells. As with nuclear import, further biochemical and cell biological experiments are required to establish how CRM1 contributes to KIF2A shuttling.

KIF2A Function Discovery Through Interacting Partners

In order to gain more insight into KIF2A function, we performed immunoprecipitation experiments in HBEC3KTRL53 cells with multiple KIF2A antibodies. We detected a number of significant proteins of interest found only in KIF2A immunoprecipitates but not in the control and were less abundant in KIF2A knockdown cells including: OPA1, WDHD1, CPSF5 and PNPT1 (Table 5.1).

OPA1 (Optic atrophy 1) is a dynamin-like GTPase that resides in the inner mitochondrial membrane and controls mitochondrial fusion and cristae remodeling (Delettre et al., 2000; Ishihara, Fujita, Oka, & Mihara, 2006; Olichon et al., 2002). KIF2A has not been shown to localize with mitochondria, but we have detected it in membrane fractions, which likely contain mitochondria. Additionally, KIF2A knockdown results in a reduction in cellular ATP, which could reflect some mitochondrial function of this protein.

WDHD1 contains an N-terminal WD40-domain and a C-terminal high mobility group (HMG) domain containing protein (Kohler, Schmidt-Zachmann, & Franke, 1997). WDHD1 has been described to associate with DNA and is involved in DNA replication (Bermudez, Farina, Tappin, & Hurwitz, 2010). WDHD1 also associates with centromeric heterochromatin in mitosis where it alters epigenetic marks leading to gene silencing (Hsieh et al., 2011). From the mass spectrometry data we noted that both KIF2A and KIF2C were enriched in immunoprecipitates. It is likely that the antibodies used for immunoprecipitation cross-react with both proteins, which is supported by ummunoblotting of recombinant KIF2C with antibodies against KIF2A, but we cannot exclude the possibility that these two proteins interact. Therefore, it will be important to

distinguish with which kinesin WDHD1 interacts. Numerous publications have reported KIF2C localization on centromeres, but it is not clear if KIF2A can also localize to centromeres (Knowlton, Vorozhko, Lan, Gorbsky, & Stukenberg, 2009; Manning et al., 2007). However, though KIF2C and WDHD1 can both be placed at centromeres, WDHD1 could still be a KIF2A specific interactor as we detected less WDHD1 by mass spectrometry once we specifically depleted KIF2A. In either instance, potential interaction of kinesins with WDHD1 and a possible function in mitotic gene silencing would be a novel property for this family of proteins that remains to be explored.

CPSF5 is a cleavage and polyadenylation specific factor, which regulates 3' mRNA processing. Not much is known about the specific functions of this protein, therefore, this may be a lower priority to pursue as a potential KIF2A partner.

The PNPT1 gene encodes a polynucleotide phosphorylase (PNPASE), a component of the RNA import pathway localized to the intermembrane mitochondrial space (IMS) (Leszczyniecka et al., 2002; Piwowarski et al., 2003). PNPASE is essential for proper mitochondrial function and reduced levels also result in lactate accumulation, lower ATP production and reduced cellular proliferation (Chen et al., 2006). A potential interaction of KIF2A with another mitochondrial protein requires a further interrogation of the KIF2A requirement for mitochondrial function.

Regulation of KIF2A Function by ERK1/2

In previous chapters I showed phenotypes associated with inhibition of ERK and of KIF2A function on cytoskeleton and organelle organization. It appears that ERK inhibition and KIF2A knockdown result in similar phenotypes. For example, both KIF2A knockdown and prolonged ERK1/2 inhibition lead to cell flattening and extended

microtubule polymers. Similarly, KIF2A knockdown and ERK inhibition cause loss of polarity in the cell resulting in lysosomes that are dispersed rather than accumulated in a perinuclear region. It will be important to assess the extent to which these phenotypes are linked. ERK1/2 do affect KIF2A expression modestly as well as phosphorylated it. Does ERK regulate much of cellular organization through KIF2A? We have started to assess the answer to this question through use of the phospho-mutant T78A. Nevertheless, we do know that ERK, at least *in vitro*, can phosphorylate additional sites. It is possible that all these residues need to be mutated in order to observe clear phenotypes that are a result of loss of ERK phosphorylation on KIF2A.

Regulation of KIF2C Function by ERK1/2

We have some preliminary data showing that ERK1/2 can bind to KIF2C and phosphorylate it *in vitro* (Figure 5.3). Also, in Chapter 3 of this thesis, I showed that ERK activity more strongly increases KIF2C than KIF2A expression. Further experiments are necessary to determine if in cells ERK1/2 associates with KIF2C in a functionally productive manner. For example, since KIF2C is overexpressed in lung cancers and phosphorylated by ERK, we could test if the KIF2C phoshpo-mutants are less able to promote migration. We could also test the relevance of these phosphorylation sites on the ability of KIF2C to destabilize microtubules.

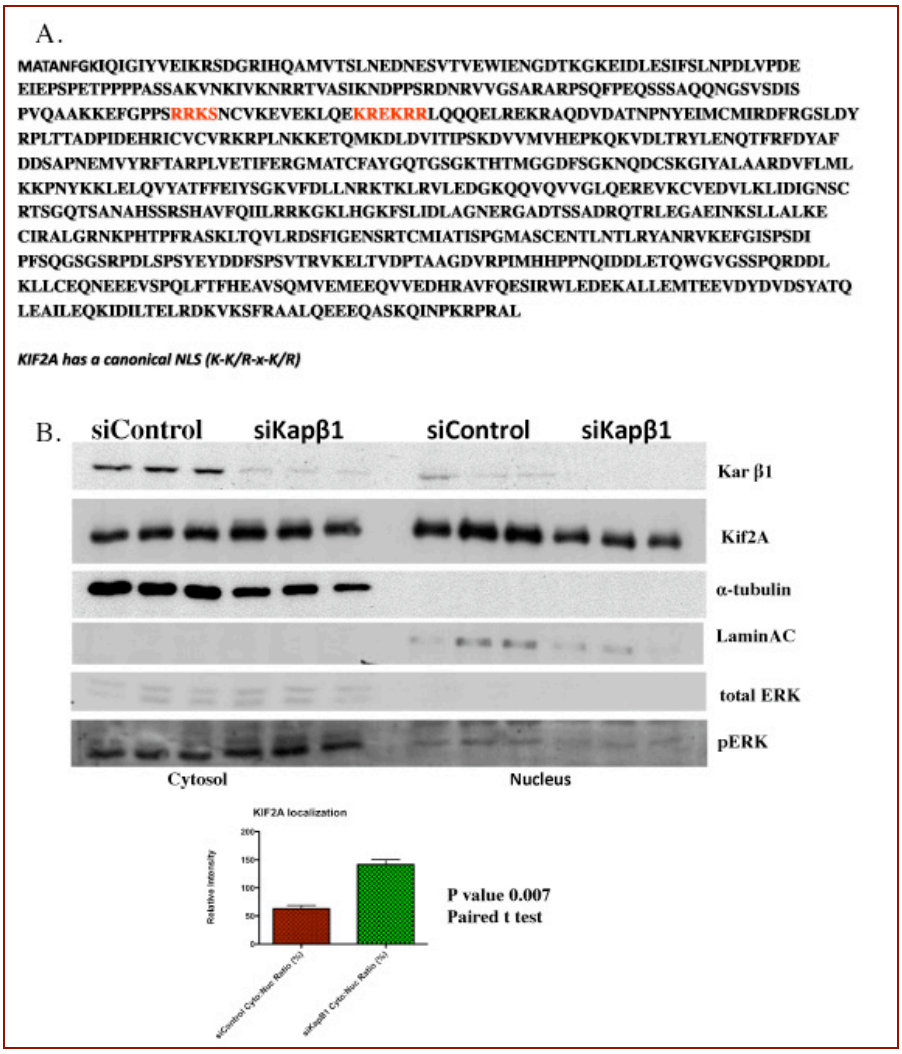

Figure 5.1. KIF2A has a bipartite classical NLS. (A) Human KIF2A sequence with the NLS indicated in red. (B) Immunoblot data showing the effect of Karyopherin beta 1 knockdown on KIF2A localization by fractionation.

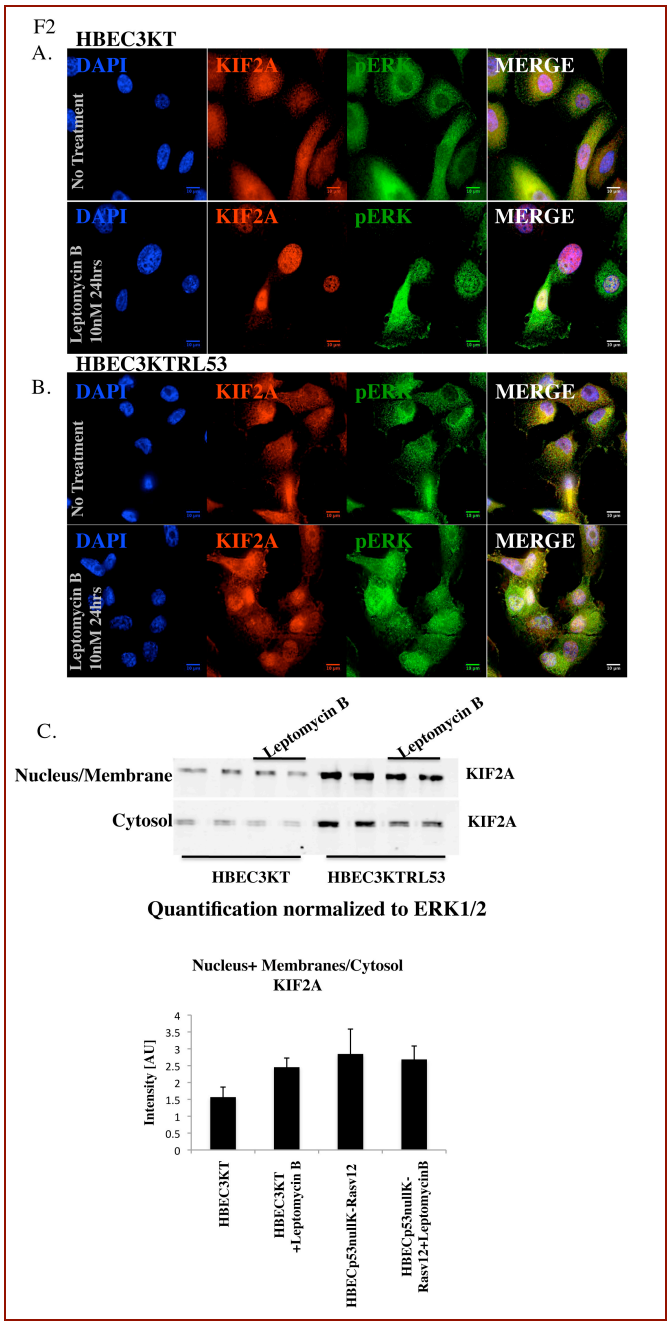
F2
A.
HBEC3KT
DAPI
KIF2A
pERK
MERGE
No Treatment
DAPI
KIF2A
pERK
MERGE
Leptomycin B 10nM 24hrs
B.
HBEC3KTRL53
DAPI
KIF2A
pERK
MERGE
No Treatment
DAPI
KIF2A
pERK
MERGE
Leptomycin B 10nM 24hrs
C.
Leptomycin B
Leptomycin B
Nucleus/Membrane
KIF2A
Cytosol
KIF2A
HBEC3KT
HBEC3KTRL53
Quantification normalized to ERK1/2
Nucleus+ Membranes/Cytosol
KIF2A
Intensity [AU]
4
3.5
3
2.5
2
1.5
1
0.5
0
HBEC3KT
HBEC3KT +Leptomycin B
HBECp53nullK-Rasv12
HBECp53nullK-Rasv12+LeptomycinB

Figure 5.2. KIF2A localization after treatment with Leptomycin B, a CRM1 inhibitor treatment. HBEC3KT or HBEC3KTRL53 cells were treated for 24 hours with 10 nM Leptomycin B and processed for (A) immunofluorescence or (B) fractionation, followed by immunoblotting.

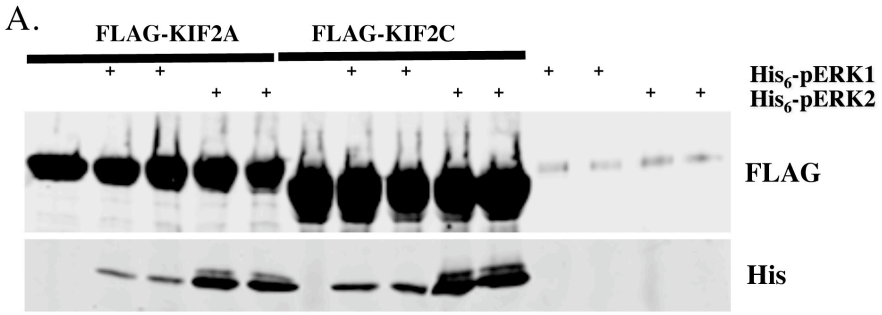

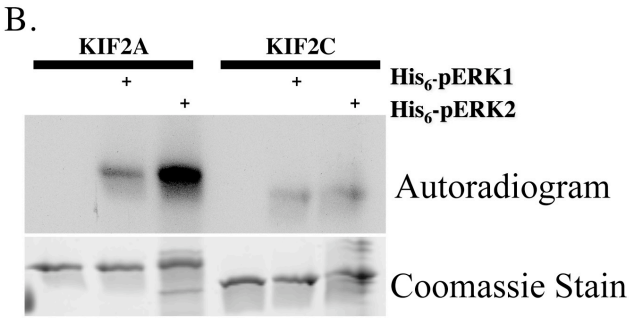

C. Mass Spectrometry Results

pERK1 + KIF2C	***Peptide 1: KQFSVPPAPTRPSCPAVAEIPLR*** ***Peptide 2: TCMIATISPGISSCEYTLNTLR***
pERK2 + KIF2C	*Peptide 1: KQFSVPPAPTRPSCPAVAEIPLR* *Peptide 2: TCMIATISPGISSCEYTLNTLR* *Peptide 3: GSSSANPVNSVR* *Peptide 4: VLEDGKQQVQVVGLQEHLVNSADDVI*

Figure 5.3. pERK1/2 interact with and phosphorylated KIF2C *in vitro*. (A) *In vitro* pull down assay with bacterially expressed and purified FLAG-KIF2A and FLAG-KIF2C and His_6-pERK1 and His_6-pERK2. (B) *In vitro* kinase assay with purified proteins. (C) Mass spectrometry followed experiment in B.

					SPECTRAL COUNTS								
					CONTROL			LS-B251			NB500		
Protein	Description	Peptide Spectrum Matches	Peptide Sequences	% Sequence Coverage	DMSO	PD0325901	siKIF2A	DMSO	PD032590	siKIF2A	DMSO	PD032590	siKIF2A
O00139-2	KIF2A_HU	76	30	44.2				7.5	7		9.5	8	0.5
Q99661	KIF2C_HU	178	27	46.1				22.68	18.73	13.78	35.47	19.69	25.61
O75717	WDHD1_HU	52	21	21.3				7.93	7.94	1.99	9.92	4.96	1.99
O43809	CPSF5_HU	27	7	35.2					1		6	6	6
O60313-2	OPA1_HU	137	34	40.1				6.94	11.89	5.95	27.73	27.74	18.82
Q8TCS8	PNPT1_HU	83	29	40.7				1	3	1	21	18	14

Table 5.1. Novel KIF2A interactors identified by mass spectrometry. Two different antibodies (LS-B251 and NB500) were used to immunoprecipitate KIF2A from HBEC3KTRL53 cells that were either treated with DMSO, PD0325901 or KIF2A knockdown.

BIBLIOGRAPHY

Ahmed, S. M., Theriault, B. L., Uppalapati, M., Chiu, C. W., Gallie, B. L., Sidhu, S. S., & Angers, S. (2012). KIF14 negatively regulates Rap1a-Radil signaling during breast cancer progression. *Journal of Cell Biology, 199,* 951-967.

Bodemann, B. O. & White, M. A. (2008). Ral GTPases and cancer: linchpin support of the tumorigenic platform. *Nat.Rev.Cancer, 8,* 133-140.

Boulton, T. G. & Cobb, M. H. (1991). Identification of multiple extracellular signal-regulated kinases (ERKs) with antipeptide antibodies. *Cell Regulation, 2,* 357-371.

Desai, A., Verma, S., Mitchison, T. J., & Walczak, C. E. (1999). Kin I kinesins are microtubule-destabilizing enzymes. *Cell, 96,* 69-78.

Di, P. G., Antonsson, B., Kassel, D., Riederer, B. M., & Grenningloh, G. (1997). Phosphorylation regulates the microtubule-destabilizing activity of stathmin and its interaction with tubulin. *FEBS Letters, 416,* 149-152.

Ding, L. H., Xie, Y., Park, S., Xiao, G., & Story, M. D. (2008). Enhanced identification and biological validation of differential gene expression via Illumina whole-genome expression arrays through the use of the model-based background correction methodology. *Nucleic Acids Res., 36,* e58.

Donninger, H., Vos, M. D., & Clark, G. J. (2007). The RASSF1A tumor suppressor. *Journal of Cell Science, 120,* 3163-3172.

Downward, J. (2003). Targeting RAS signalling pathways in cancer therapy. *Nat.Rev.Cancer., 3,* 11-22.

Drechsel, D. N., Hyman, A. A., Cobb, M. H., & Kirschner, M. W. (1992). Modulation of the dynamic instability of tubulin assembly by the microtubule-associated

protein tau. *Molecular Biology of the Cell, 3,* 1141-1154.

Duesbery, N. S., Resau, J., Webb, C. P., Koochekpour, S., Koo, H. M., Leppla, S. H., & Vande Woude, G. F. (2001). Suppression of ras-mediated transformation and inhibition of tumor growth and angiogenesis by anthrax lethal factor, a proteolytic inhibitor of multiple MEK pathways. *Proc.Natl.Acad.Sci.U.S.A, 98,* 4089-4094.

Efeyan, A., Zoncu, R., & Sabatini, D. M. (2012). Amino acids and mTORC1: from lysosomes to disease. Trends Mol Med, 18(9), 524-533.

Elgendy, M., Sheridan, C., Brumatti, G., & Martin, S. J. (2011). Oncogenic Ras-induced expression of Noxa and Beclin-1 promotes autophagic cell death and limits clonogenic survival. Mol Cell, 42(1), 23-35.

Ems-McClung, S. C. & Walczak, C. E. (2010). Kinesin-13s in mitosis: Key players in the spatial and temporal organization of spindle microtubules. *Semin.Cell Dev.Biol., 21,* 276-282.

Feng, Z., Zhang, H., Levine, A. J., & Jin, S. (2005). The coordinate regulation of the p53 and mTOR pathways in cells. Proc Natl Acad Sci U S A, 102(23), 8204-8209.

Fotiadou, P. P., Takahashi, C., Rajabi, H. N., & Ewen, M. E. (2007). Wild-type NRas and KRas perform distinct functions during transformation. *Molecular & Cellular Biology, 27,* 6742-6755.

Fukazawa, H. & Uehara, Y. (2000). U0126 reverses Ki-ras-mediated transformation by blocking both mitogen-activated protein kinase and p70 S6 kinase pathways. *Cancer Research, 60,* 2104-2107.

Ganem, N. J. & Compton, D. A. (2004). The KinI kinesin Kif2a is required for bipolar spindle assembly through a functional relationship with MCAK. *J Cell Biol., 166,* 473-478.

Geeraert, C., Ratier, A., Pfisterer, S. G., Perdiz, D., Cantaloube, I., Rouault, A., et al. (2010). Starvation-induced hyperacetylation of tubulin is required for the stimulation of autophagy by nutrient deprivation. J Biol Chem, 285(31), 24184-24194.

Gotoh, Y., Moriyama, K., Matsuda, S., Okumura, E., Kishimoto, T., Kawasaki, H., Suzuki, K., Yahara, I., Sakai, H., & Nishida, E. (1991a). *Xenopus* M Phase MAP Kinase: Isolation of Its cDNA and Activation by MPF. *The EMBO Journal, 10,* 2661-2668.

Gotoh, Y., Nishida, E., Matsuda, S., Shiina, N., Kosako, H., Shiokawa, K., Akiyama, T., Ohta, K., & Sakai, H. (1991). *In vitro* effects on microtubule dynamics of purified *Xenopus* M phase-activated MAP kinase. *Nature, 349,* 251-254.

Groth-Pedersen, L., Aits, S., Corcelle-Termeau, E., Petersen, N. H., Nylandsted, J., & Jaattela, M. (2012). Identification of cytoskeleton-associated proteins essential for lysosomal stability and survival of human cancer cells. *PLoS.ONE., 7,* e45381.

Guo, J. Y., Chen, H. Y., Mathew, R., Fan, J., Strohecker, A. M., Karsli-Uzunbas, G., et al. (2011). Activated Ras requires autophagy to maintain oxidative metabolism and tumorigenesis. Genes Dev, 25(5), 460-470.

Gwinn, D. M., Shackelford, D. B., Egan, D. F., Mihaylova, M. M., Mery, A., Vasquez, D. S., et al. (2008). AMPK phosphorylation of raptor mediates a metabolic checkpoint. Mol Cell, 30(2), 214-226.

Harrison, R. E. & Turley, E. A. (2001). Active erk regulates microtubule stability in H-ras-transformed cells. *Neoplasia., 3,* 385-394.

Helenius, J., Brouhard, G., Kalaidzidis, Y., Diez, S., & Howard, J. (2006). The depolymerizing kinesin MCAK uses lattice diffusion to rapidly target microtubule ends. *Nature., 441,* 115-119.

Homma, N., Takei, Y., Tanaka, Y., Nakata, T., Terada, S., Kikkawa, M., Noda, Y., & Hirokawa, N. (2003). Kinesin superfamily protein 2A (KIF2A) functions in suppression of collateral branch extension. *Cell, 114,* 229-239.

Hornbeck, P. V., Kornhauser, J. M., Tkachev, S., Zhang, B., Skrzypek, E., Murray, B., Latham, V., & Sullivan, M. (2012). PhosphoSitePlus: a comprehensive resource for investigating the structure and function of experimentally determined post-translational modifications in man and mouse. *Nucleic Acids Res., 40,* D261-D270.

Hoshi, M., Ohta, K., Gotoh, Y., Mori, A., Murofushi, H., Sakai, H., & Nishida, E. (1992). Mitogen-activated-protein-kinase-catalyzed phosphorylation of microtubule-associated proteins, microtubule-associated protein 2 and microtubule-associated protein 4, induces an alteration in their function. *Eur.J Biochem., 203,* 43-52.

Humbert, P. O., Grzeschik, N. A., Brumby, A. M., Galea, R., Elsum, I., & Richardson, H. E. (2008). Control of tumourigenesis by the Scribble/Dlg/Lgl polarity module. *Oncogene., 27,* 6888-6907.

Inoki, K., Zhu, T., & Guan, K. L. (2003). TSC2 mediates cellular energy response to control cell growth and survival. Cell, 115(5), 577-590.

Jang, C. Y., Coppinger, J. A., Seki, A., Yates, J. R., III, & Fang, G. (2009). Plk1 and Aurora A regulate the depolymerase activity and the cellular localization of Kif2a. *Journal of Cell Science, 122,* 1334-1341.

Jimenez, C., Portela, R. A., Mellado, M., Rodriguez-Frade, J. M., Collard, J., Serrano, A., Martinez, A., Avila, J., & Carrera, A. C. (2000). Role of the PI3K regulatory subunit in the control of actin organization and cell migration. *Journal of Cell Biology, 151,* 249-262.

Jivan, A., Earnest, S., Juang, Y. C., & Cobb, M. H. (2009). Radial spoke protein 3 is a mammalian protein kinase A-anchoring protein that binds ERK1/2. *J Biol Chem., 284,* 29437-29445.

Jones, R. G., Plas, D. R., Kubek, S., Buzzai, M., Mu, J., Xu, Y., et al. (2005). AMP-activated protein kinase induces a p53-dependent metabolic checkpoint. Mol Cell, 18(3), 283-293.

Kardon, J. R. & Vale, R. D. (2009). Regulators of the cytoplasmic dynein motor. *Nat.Rev.Mol.Cell Biol, 10,* 854-865.

Karnoub, A. E. & Weinberg, R. A. (2008). Ras oncogenes: split personalities. *Nat.Rev.Mol.Cell Biol, 9,* 517-531.

Knowlton, A. L., Vorozhko, V. V., Lan, W., Gorbsky, G. J., & Stukenberg, P. T. (2009). ICIS and Aurora B coregulate the microtubule depolymerase Kif2a. *Curr.Biol, 19,* 758-763.

Kobayashi, T., Tsang, W. Y., Li, J., Lane, W., & Dynlacht, B. D. (2011). Centriolar kinesin Kif24 interacts with CP110 to remodel microtubules and regulate ciliogenesis. *Cell, 145,* 914-925.

Kolsch, V., Charest, P. G., & Firtel, R. A. (2008). The regulation of cell motility and chemotaxis by phospholipid signaling. *Journal of Cell Science, 121,* 551-559.

Korolchuk, V. I., Saiki, S., Lichtenberg, M., Siddiqi, F. H., Roberts, E. A., Imarisio, S., Jahreiss, L., Sarkar, S., Futter, M., Menzies, F. M., O'Kane, C. J., Deretic, V., & Rubinsztein, D. C. (2011). Lysosomal positioning coordinates cellular nutrient responses. *Nat.Cell Biol., 13,* 453-460.

Larsen, J. E. & Minna, J. D. (2011). Molecular biology of lung cancer: clinical implications. *Clin.Chest Med., 32,* 703-740.

Lawrence, C. J., Dawe, R. K., Christie, K. R., Cleveland, D. W., Dawson, S. C., Endow, S. A., Goldstein, L. S., Goodson, H. V., Hirokawa, N., Howard, J., Malmberg, R. L., McIntosh, J.

R., Miki, H., Mitchison, T. J., Okada, Y., Reddy, A. S., Saxton, W. M., Schliwa, M., Scholey, J. M., Vale, R. D., Walczak, C. E., & Wordeman, L. (2004). A standardized kinesin nomenclature. *J Cell Biol, 167,* 19-22.

Leinweber, B. D., Leavis, P. C., Grabarek, Z., Wang, C. L., & Morgan, K. G. (1999). Extracellular regulated kinase (ERK) interaction with actin and the calponin homology (CH) domain of actin-binding proteins. *Biochemical Journal, 344,* 117-123.

Liao, G., Nagasaki, T., & Gundersen, G. G. (1995). Low concentrations of nocodazole interfere with fibroblast locomotion without significantly affecting microtubule level: implications for the role of dynamic microtubules in cell locomotion. *Journal of Cell Science, 108,* 3473-3483.

Lundberg, A. S., Hahn, W. C., Gupta, P., & Weinberg, R. A. (2000). Genes involved in senescence and immortalization. *Curr.Opin.Cell Biol, 12,* 705-709.

Manning, A. L., Ganem, N. J., Bakhoum, S. F., Wagenbach, M., Wordeman, L., & Compton, D. A. (2007). The kinesin-13 proteins Kif2a, Kif2b, and Kif2c/MCAK have distinct roles during mitosis in human cells. *Mol.Biol Cell, 18,* 2970-2979.

Marklund, U., Brattsand, G., Shingler, V., & Gullberg, M. (1993). Serine 25 of oncoprotein 18 is a major cytosolic target for the mitogen-activated protein kinase. *Journal of Biological Chemistry, 268,* 15039-15049.

Matteoni, R., & Kreis, T. E. (1987). Translocation and clustering of endosomes and lysosomes depends on microtubules. J Cell Biol, 105(3), 1253-1265.

Mendoza, M. C., Er, E. E., Zhang, W., Ballif, B. A., Elliott, H. L., Danuser, G., & Blenis, J. (2011). ERK-MAPK drives lamellipodia protrusion by activating the WAVE2 regulatory complex. *Mol.Cell, 41,* 661-671.

Mennella, V., Rogers, G. C., Rogers, S. L., Buster, D. W., Vale, R. D., & Sharp, D. J. (2005). Functionally distinct kinesin-13 family members cooperate to regulate microtubule dynamics during interphase. *Nat.Cell Biol., 7,* 235-245.

Miki, H., Okada, Y., & Hirokawa, N. (2005). Analysis of the kinesin superfamily: insights into structure and function. *Trends in Cell Biology, 15,* 467-476.

Miki, H., Setou, M., Kaneshiro, K., & Hirokawa, N. (2001). All kinesin superfamily protein, KIF, genes in mouse and human. *Proc.Natl.Acad.Sci.U.S.A, 98,* 7004-7011.

Moore, A. T., Rankin, K. E., von, D. G., Peris, L., Wagenbach, M., Ovechkina, Y., Andrieux, A., Job, D., & Wordeman, L. (2005). MCAK associates with the tips of polymerizing microtubules. *Journal of Cell Biology, 169,* 391-397.

Mosesson, Y., Mills, G. B., & Yarden, Y. (2008). Derailed endocytosis: an emerging feature of cancer. Nat Rev Cancer, 8(11), 835-850.

Noda, Y., Niwa, S., Homma, N., Fukuda, H., Imajo-Ohmi, S., & Hirokawa, N. (2012). Phosphatidylinositol 4-phosphate 5-kinase alpha (PIPKalpha) regulates neuronal microtubule depolymerase kinesin, KIF2A and suppresses elongation of axon branches. *Proc.Natl.Acad.Sci.U.S.A, 109,* 1725-1730.

Obenauer, J. C., Cantley, L. C., & Yaffe, M. B. (2003). Scansite 2.0: Proteome-wide prediction of cell signaling interactions using short sequence motifs. *Nucleic Acids Res., 31,* 3635-3641.

Olsen, M. K., Reszka, A. A., & Abraham, I. (1998). KT5720 and U-98017 inhibit MAPK and alter the cytoskeleton and cell morphology. *Journal of Cell Physiology, 176,* 525-536.

Parada, L. F., Land, H., Weinberg, R. A., Wolf, D., & Rotter, V. (1984).

Cooperation between gene encoding p53 tumour antigen and ras in cellular transformation. *Nature, 312,* 649-651.

Perucho, M., Goldfarb, M., Shimizu, K., Lama, C., Fogh, J., & Wigler, M. (1981). Human-tumor-derived cell lines contain common and different transforming genes. *Cell, 27,* 467-476.

Pollock, C. B., Shirasawa, S., Sasazuki, T., Kolch, W., & Dhillon, A. S. (2005). Oncogenic K-RAS is required to maintain changes in cytoskeletal organization, adhesion, and motility in colon cancer cells. *Cancer Research, 65,* 1244-1250.

Pullikuth, A. K. & Catling, A. D. (2007). Scaffold mediated regulation of MAPK signaling and cytoskeletal dynamics: a perspective. *Cell Signal., 19,* 1621-1632.

Ramirez, R. D., Sheridan, S., Girard, L., Sato, M., Kim, Y., Pollack, J., Peyton, M., Zou, Y., Kurie, J. M., DiMaio, J. M., Milchgrub, S., Smith, A. L., Souza, R. F., Gilbey, L., Zhang, X., Gandia, K., Vaughan, M. B., Wright, W. E., Gazdar, A. F., Shay, J. W., & Minna, J. D. (2004). Immortalization of human bronchial epithelial cells in the absence of viral oncoproteins. *Cancer Research, 64,* 9027-9034.

Ray, L. B. & Sturgill, T. W. (1987). Rapid stimulation by insulin of a serine/threonine kinase in 3T3-L1 adipocytes that phosphorylates microtubule-associated protein 2 *in vitro*. *Proceedings of the National Academy of Science U.S.A., 84,* 1502-1506.

Reszka, A. A., Seger, R., Diltz, C. D., Krebs, E. G., & Fischer, E. H. (1995). Association of mitogen-activated protein kinase with the microtubule cytoskeleton. *Proceedings of the National Academy of Science U.S.A., 92,* 8881-8885.

Robbins, D. J., Zhen, E., Owaki, H., Vanderbilt, C., Ebert, D., Geppert, T. D., & Cobb, M. H. (1993). Regulation and properties of extracellular signal-regulated protein kinases 1 and 2 *in vitro*. *Journal of Biological Chemistry, 268,* 5097-5106.

Rogers, G. C., Rogers, S. L., Schwimmer, T. A., Ems-McClung, S. C., Walczak, C. E., Vale, R. D., Scholey, J. M., & Sharp, D. J. (2004). Two mitotic kinesins cooperate to drive sister chromatid separation during anaphase. *Nature, 427,* 364-370.

Sahai, E., Olson, M. F., & Marshall, C. J. (2001). Cross-talk between Ras and Rho signalling pathways in transformation favours proliferation and increased motility. *The EMBO Journal, 20,* 755-766.

Sanchez, C., az-Nido, J., & Avila, J. (2000). Phosphorylation of microtubule-associated protein 2 (MAP2) and its relevance for the regulation of the neuronal cytoskeleton function. *Prog.Neurobiol., 61,* 133-168.

Sander, E. E., van, D. S., ten Klooster, J. P., Reid, T., van der Kammen, R. A., Michiels, F., & Collard, J. G. (1998). Matrix-dependent Tiam1/Rac signaling in epithelial cells promotes either cell-cell adhesion or cell migration and is regulated by phosphatidylinositol 3-kinase. *J Cell Biol., 143,* 1385-1398.

Sato, M., Larsen, J. E., Lee, W., Sun, H., Shames, D. S., Dalvi, M. P., Ramirez, R. D., Tang, H., DiMaio, J. M., Gao, B., Xie, Y., Wistuba, I. I., Gazdar, A. F., Shay, J. W., & Minna, J. D. (2013). Human lung epithelial cells progressed to malignancy through specific oncogenic manipulations. *Submitted*.

Sato, M., Vaughan, M. B., Girard, L., Peyton, M., Lee, W., Shames, D. S., Ramirez, R. D., Sunaga, N., Gazdar, A. F., Shay, J. W., & Minna, J. D. (2006). Multiple oncogenic changes (K-RAS(V12), p53 knockdown, mutant EGFRs, p16 bypass,

telomerase) are not sufficient to confer a full malignant phenotype on human bronchial epithelial cells. *Cancer Research, 66,* 2116-2128.

Sekido, Y., Fong, K. M., & Minna, J. D. (2003). Molecular genetics of lung cancer. *Annu.Rev.Med., 54:73-87. Epub@2001 Dec 3.,* 73-87.

Shaw, R. J., Kosmatka, M., Bardeesy, N., Hurley, R. L., Witters, L. A., DePinho, R. A., et al. (2004). The tumor suppressor LKB1 kinase directly activates AMP-activated kinase and regulates apoptosis in response to energy stress. Proc Natl Acad Sci U S A, 101(10), 3329-3335.

Shay, J. W., Tomlinson, G., Piatyszek, M. A., & Gollahon, L. S. (1995). Spontaneous in vitro immortalization of breast epithelial cells from a patient with Li-Fraumeni syndrome. *Molecular & Cellular Biology, 15,* 425-432.

Shay, J. W., Van Der Haegen, B. A., Ying, Y., & Wright, W. E. (1993). The frequency of immortalization of human fibroblasts and mammary epithelial cells transfected with SV40 large T-antigen. *Experimental Cell Research, 209,* 45-52.

Shinohara-Gotoh, Y., Nishida, E., Hoshi, M., & Sakai, H. (1991). Activation of microtubule-associated protein kinase by microtubule disruption in quiescent rat 3Y1 cells. *Experimental Cell Research, 193,* 161-166.

Singh, A., Greninger, P., Rhodes, D., Koopman, L., Violette, S., Bardeesy, N., & Settleman, J. (2009). A gene expression signature associated with "K-Ras addiction" reveals regulators of EMT and tumor cell survival. *Cancer Cell, 15,* 489-500.

Sunaga, N., Shames, D. S., Girard, L., Peyton, M., Larsen, J. E., Imai, H., Soh, J., Sato, M., Yanagitani, N., Kaira, K., Xie, Y., Gazdar, A. F., Mori, M., & Minna, J. D. (2011). Knockdown of oncogenic KRAS in non-small cell lung cancers suppresses tumor

growth and sensitizes tumor cells to targeted therapy. *Mol.Cancer Ther., 10,* 336-346.

Suzuki, N., Del, V. K., & Tamanoi, F. (1998). Farnesyltransferase inhibitors induce dramatic morphological changes of KNRK cells that are blocked by microtubule interfering agents. *Proceedings of the National Academy of Sciences of the United States of America, 95,* 10499-10504.

Tanuma, N., Nomura, M., Ikeda, M., Kasugai, I., Tsubaki, Y., Takagaki, K., Kawamura, T., Yamashita, Y., Sato, I., Sato, M., Katakura, R., Kikuchi, K., & Shima, H. (2009). Protein phosphatase Dusp26 associates with KIF3 motor and promotes N-cadherin-mediated cell-cell adhesion. *Oncogene, 28,* 752-761.

Tu, S., Bugde, A., Luby-Phelps, K., & Cobb, M. H. (2011). WNK1 is required for mitosis and abscission. *Proc Natl Acad Sci U S A, 108,* 1385-1390.

van Es, J. H., Giles, R. H., & Clevers, H. C. (2001). The many faces of the tumor suppressor gene APC. *Experimental Cell Research, 264,* 126-134.

Vasiliev, J. M., Gelfand, I. M., Domnina, L. V., Ivanova, O. Y., Komm, S. G., & Olshevskaja, L. V. (1970). Effect of colcemid on the locomotory behaviour of fibroblasts. *J.Embryol.Exp.Morphol., 24,* 625-640.

Wang, C. Q., Qu, X., Zhang, X. Y., Zhou, C. J., Liu, G. X., Dong, Z. Q., Wei, F. C., & Sun, S. Z. (2010). Overexpression of Kif2a promotes the progression and metastasis of squamous cell carcinoma of the oral tongue. *Oral Oncol., 46,* 65-69.

Wauson, E. M., Zaganjor, E., Lee, A. Y., Guerra, M. L., Ghosh, A. B., Bookout, A. L., et al. (2012). The G protein-coupled taste receptor T1R1/T1R3 regulates mTORC1 and autophagy. Mol Cell, 47(6), 851-862.

Yamashita, J., Fukushima, S., Jinnin, M., Honda, N., Makino, K., Sakai, K.,

Masuguchi, S., Inoue, Y., & Ihn, H. (2012). Kinesin family member 20A is a novel melanoma-associated antigen. *Acta Derm.Venereol., 92,* 593-597.

Yang, S., Wang, X., Contino, G., Liesa, M., Sahin, E., Ying, H., et al. (2011). Pancreatic cancers require autophagy for tumor growth. Genes Dev, 25(7), 717-729.

Zuber, J., Tchernitsa, O. I., Hinzmann, B., Schmitz, A. C., Grips, M., Hellriegel, M., Sers, C., Rosenthal, A., & Schafer, R. (2000). A genome-wide survey of RAS transformation targets. *Nat.Genet., 24,* 144-152. Ahmed, S. M., Theriault, B. L., Uppalapati, M., Chiu, C. W., Gallie, B. L., Sidhu, S. S., & Angers, S. (2012). KIF14 negatively regulates Rap1a-Radil signaling during breast cancer progression. *Journal of Cell Biology, 199,* 951-967.